Distributed MIMO For Wireless Sensor Networks

Xiaojun Wen

A thesis submitted for the degree of Doctor of Philosophy

The University of Edinburgh

February 2011

Abstract

Over the past decade, wireless sensor networks have gained more research attention for their potential applications in healthcare, defense, environmental monitoring, etc. Due to the strict energy limitation in the sensor node, techniques used for energy saving are necessary for this kind of network. MIMO technology is proven to be an effective method of increasing the channel capacity and supporting higher data rate under a fixed power budget and bit-error-rate requirement. So, wireless sensor networks and MIMO technology are combined and investigated in this thesis.

The key contributions of this thesis are detailed below. Firstly, the extended total energy consumption equations for different transmission modes in cluster-based wireless sensor networks are derived. The transmitting energy consumption and the circuit energy consumption are taken into account in both intra-cluster and inter-cluster phases respectively.

Secondly, a resource allocation framework is proposed for cluster-based cooperative MIMO on consideration of circuit energy. By introducing two adjusting parameters for the transmitting energy and the time slot allocation between intra-cluster and inter-cluster phases, this framework is designed to achieve the maximum data throughput of the whole system whilst maintaining the capacity and outage probability requirement in these two phases respectively.

Thirdly, on comparison of various transmission modes in wireless sensor networks, a relatively energy-efficient mode switching framework is proposed for both single-hop and multi-hop transmissions. Based on the destination and the neighboring nodes' path-loss, the source node can decide which transmission mode, SISO or cooperative MISO, single-hop or multi-hop, should be chosen. Conditions for each mode switching are investigated. The possible existing area of the cooperative nodes and the relaying nodes can be obtained from this framework.

Declaration of Originality

I hereby declare that the research recorded in this thesis and the thesis itself was composed and originated entirely by myself in the School of Engineering and Electronics at The Univesity of Edinburgh.

Xiaojun Wen
December 2010

Acknowledgements

"Do not, for one repulse, give up the purpose that you resolved to effect."
--William Shakespeare, British dramatist

Studying abroad for a PhD degree is doomed to be never easy from the very beginning especially in a country with different language, culture, and customs. Now, looking back from the end of this journey, I am surprised to discover that what I have gained is not only the professional knowledge but also a wonderful adventure in my life. So many people, colleagues and friends, constitute my memorable experience in UK. By this opportunity, I would like to express my deepest gratitude to a number of people who have provided me with invaluable help over the past three years.

First of all, I would like to give my sincere thanks to my supervisor Dr. David Laurenson for his patient guidance over the course of my research and proofreading of this thesis. His wise and convincing suggestions always help me out of the dead end in research work and head to the right destination.

I would like to thank my dear friends and colleagues, Dr. Zheng Wang, Dr. Ran Zhang, Dr. Hongjian Sun, who helped me a lot in both studying and living in UK.

The financial aids I received from the Wolfson Microelectronics Scholarship and the School of Engineering and Electronics Studentship are also appreciated.

Last but most importantly, I will give my thanks to my parents, Lisen Wen and Jingping Liang, my fiancée Jin Zhou, and all the other family members. It was their boundless love and spiritual encourages that made me never be devastated by any difficulties.

Xiaojun Wen
Edinburgh, February 2011

Contents

List of Figures

List of Tables

Acronyms and Abbreviations

AF	Amplify and Forward
AWGN	Additive White Gaussian Noise
ADC	Analog-Digital Converter
BTMA	Busy-Tone Multiple Access
BEB	Binary Exponential Backoff
BER	Bit-Error-Rate
CDMA	Code-Division Multiple Access
Co-MIMO	Cooperative MIMO
Co-MISO	Cooperative MISO
CSI	Channel State Information
CDF	Cumulative Density Function
CSMA	Carrier Sense Multiple Access/Collision Detect
DPC	Dirty Paper Coding
DE-MAC	Distributed Energy-Aware MAC
DD	Directed Diffusion
DVS	Dynamic Voltage Scaling
DAC	Digital-Analog Converter
DF	Decode and Forward
FDMA	Frequency-Division Multiple Access
GSM	Global System for Mobile Communication
GEAR	Geographic and Energy Aware Routing
HSDPA	High Speed Downlink Packet Access
HREEMR	Highly-Resilient Energy-Efficient Multipath Routing
IrDA	Infrared Data Association
ISM	Industrial, Scientific and Medical Radio
IFA	Intermediate Frequency Amplifier,
ITA	Intra-cluster Phase
ITE	Inter-cluster Phase
LO	Local Oscillator
LNA	Low Noise Amplifier

Los	Line-of-Sight
LEACH	Low-Energy Adaptive Clustering Hierarchy
MISO	Multiple-Input Single-Output
MIMO	Multiple-Input Multiple-Output
MU-MIMO	Multi-User MIMO
MMSE	Minimum Mean Square Error
MEMS	Micro-Electro-Mechanism System
MAC	Media Access Control
MSAP	Mini-Slotted Alternating Priorities
MILD	Multiplicative Increase Linear Decrease
MD	Mediation Device
OFDM	Orthogonal Frequency Division Multiplexing
OSI	Open Systems Interconnection
PDF	Probability Density Function
PCF	Point Coordination Function
PEGASIS	Power-Efficient Gathering in Sensor Information system
PA	Power Amplifier
QoS	Quality of Service
RFID	Radio-Frequency Identification
Rx	Receivers
RF	Radio Frequency
RTS-CTS	Request To Send/Clear To Send
SISO	Single-Input Single-Output
SIMO	Single-Input Multiple-Output
SensIT	Sensor Information Technology
SNR	Signal-to-Noise Ratio
SVD	Singular Value Decomposition
STBC	Space-Time Block Coding
SRMA	Split Channel Reservation Multiple Access
SDMA	Space-Division Multiple Access
S-MAC	Sensor-MAC
SPIN	Sensor Protocol for Information via Negotiation
SAR	Sequential Assignment Routing
SMECN	Small Minimum Energy Communication Network

TDMA	Time-Division Multiple Access
Tx	Transmitters
TEEN	Threshold Sensitive Energy-efficient Sensor Network Protocol
UWB	Ultra-Wide Band
WSN	Wireless Sensor Network
Wi-Max	Worldwide Interoperability for Microwave Access
WINS	Wireless Integrated Network Sensors
WLAN	Wireless Local-Area Networks
WWAN	Wireless Wide-Area Networks
WTRP	Wireless Token Ring Protocol
ZF	Zero-Forcing
μAMPS	Micro-Adaptive Multi-Domain Power-Aware Sensors

List of Symbols

$a \sim (0, \sigma_0^2 / 2)$	Gaussian random variables
$b \sim (0, \sigma_0^2 / 2)$	Gaussian random variables
α	parameter for time slot allocation
B	signal bandwidth
β	power allocation
C	channel capacity
$C_{full-CSI}$	channel capacity with full CSI
$C_{statistical-CSI}$	channel capacity with statistical CSI
C_{no-CSI}	channel capacity with no CSI
$\mathbb{C}^{N_t \times N_r}$	$N_t \times N_r$ matrix
$C_{multi-hop}$	multi-hop system channel capacity
C_{1xr}	channel capacity for $1 \times r$ SIMO mode with full CSI
$\hat{C}_{\zeta}(a)$	Capacity Integral
C_{MIMO_STBC}	channel capacity of MIMO communication with STBCs
d	propagation distance
D_s	Doppler spread
d_{ITA}	transmission distance within the cluster
d_{ITE}	transmission distance between two relaying clusters
$E_{bt-SISO}$	total energy consumption per bit in SISO mode
$E_{bt-Co-MIMO}$	total energy consumption per bit in cooperative MIMO mode
$E_{bt-Co-MISO}$	total energy consumption per bit in cooperative MISO mode
$\overline{E}_{b-ITA}$	received energy per bit for a given BER requirement in the ITA slot
$\overline{E}_{b-ITE}$	received energy per bit for a given BER requirement in the ITE slot
$\overline{E}_b$	mean required energy per bit at the receiver for a given BER requirement

$E_{bt-MIMO}$	total energy consumption per bit for a MIMO communication
$E_{bt-multi-SISO}$	total energy consumption per bit for multi-hop SISO transmission
$E_{bt-multi-Co-MISO}$	total energy consumption per bit for multi-hop Co-MISO transmission
$E\{\cdot\}$	expectation
G_t	antenna gain of the transmitter
G_R	antenna gain of the receiver
h	channel impulse response
$\|h\|$	channel amplitude gain
$\|h\|^2$	channel power gain
h_{ji}	channel response between the *j*-th receiving antenna and the *i*-th transmitting element
$\mathbf{H}(\cdot)$	channel impulse response Metrix
$I_0(\cdot)$	modified Bessel function of first kind and zero order
$\mathbf{inf}\{\cdot\}$	infimum
K	Rician Factor
m_f	severity of fading in Nakagami
m	number of hops
N	power of noise
M_l	link margin compensating the hardware process variations and other additive background noise or interference
n_t	number of cooperative transmitters
n_r	number of cooperative receiver
N_t	number of transmitters
N_r	number of receivers
$\mathbf{n}(t)$	noise vector
N_f	receiver noise figure
N_s	power spectral density of the total effective noise at input of the receiver
N_0	power spectral density of the single-sided thermal noise
$p(x)$	probability density function

P_r	signal power at the receiver
P_t	signal power at the transmitter
P_{ct}	circuit power consumption at a transmitter
P_{cr}	circuit power consumption at a receiver
P_{DAC}	power consumed in DAC
P_{mix}	power consumed in Mixer
P_{fil}	power consumed in filter
P_{syn}	power consumed in syncrinizer
P_{LNA}	power consumed in LNA
P_{IFA}	power consumed in IFA
P_{ADC}	power consumed in ADC
P_{PA}	power consumed in the amplifiers
P_c	power consumed in circuit blocks
P_{tran}	transmitting power
P_{out}	outage probability
P_e	bit-error-rate
Ω	average power
R_b	system data rate
R	STBCs code rate
R_{intra}	Code rate for intra-cluster broadcasting
R_{inter}	Code rate for inter-cluster transmission
r	number of receivers in ITA slot
ρ	average SNR per antenna at the Rx
S / N	signal-to-noise ratio
$\Upsilon(\cdot)$	the lower incomplete Gamma function
γ	sub-channel gain
T_c	coherence time
T	duration of a packet transmission
t_1	time slot allocated to the intra-cluster phase
t_2	time slot allocated in the inter-cluster phase
tr(Q)	total power transmitted at Tx
τ	peak amplitude of the dominant path and the power ratio of the dominant path
$\Gamma(\cdot)$	Gamma function

δ	path loss exponent
σ_0	standard deviation
$\mathbf{x}(t)$	transmitting signal vector
$\mathbf{y}(t)$	received signal vector
λ_i	eigenvalue of $\mathbf{H}\mathbf{H}^H$
λ	wavelength of the signal
Φ	maximum symbol rate of a sensor antenna
$\Phi'_{full-duplex}$	data throughput
ξ	the Peak-to-Average Ratio
η	drain efficiency of the RF power amplifier
θ	angle of corporative node to the source
φ	angle of the relaying node to the signal middle point
(l,φ)	polar coordinate of relaying node from the middle point of the sight signal
$[\cdot]^H$	the Hermitian transpose

Chapter 1
Introduction

Since the first wireless telegraph was invented by Guglielmo Marconi in 1901, wireless communication technology has developed for more than one century and become the most active area in communications and networking. From the end-to-end message transmission to multimedia, large volumes of information flow and there is significant interaction between networks in the modern society. Lots of wireless products, such as cellular mobile phone network, satellite TV services, wireless internet, etc, are making tremendous changes to our daily life. Wireless techniques and their applications in various kinds of networks, which can support higher data-rate, higher communication reliability, are the key hot topics in nowadays' research around the world.

This introduction chapter firstly covers the actualities of the wireless communication technology and networks. Some key techniques in recent research and future trends are introduced. Then, in Section 1.2, the development of the main research target of this thesis – wireless sensor networks, is discussed. Based on the design requirements of the wireless sensor network, the problems that need to be solved are stated in Section 1.3, which are also the aim of this thesis. Section 1.4 summarizes the contribution to knowledge. Finally, Section 1.5 gives a general outline of the remainder of the thesis.

1.1 Actualities of Wireless Communication Technology

In this digitized age, there is a wide variety of wireless networks, categorized by network architecture and transmission task requirements. Different wireless communication technologies and standards, such as Bluetooth, code division multiple access (CDMA), Global System for Mobile Communication (GSM), Infrared Data

Association (IrDA), Industrial, Scientific and Medical Radio (ISM), Ultra-Wide Band (UWB), Radio-Frequency Identification (RFID), Wi-Fi, Wi-Max, Zigbee, etc, are adopted in different type of networks according to the special requirements of transmission distance, data rate, bit-error-rate, and energy consumption, etc [1].

In the physical and MAC layers, TDMA, FDMA, and CDMA have already explored the time, frequency, and code multiplexing respectively. A breakthrough technology to explore the space multiplexing is MIMO (multiple-input multiple-output). By adopting multiple antennas at both the transmitter side (Tx) and the receiver side (Rx), a MIMO system can dramatically enhance the data rates and the communication reliability within a limited bandwidth and transmitting power. In addition, MIMO combined with OFDM can effectively resist frequency-selective fading and enhance the spectrum efficiency [2]. So, OFDM-MIMO has been considered as the key technique in 4G wireless communication networks.

1.2 Evolution of Wireless Sensor Networks

The research target of this thesis is wireless sensor network (WSN). It is a self-organized network composed of densely deployed sensor nodes. It was first proposed by the research group in Carnegie Mello University in 1978 for military use. Recently, its application has been broadened into civil use. There have been many research projects about wireless sensor networks since 1990s, such as SensIT (sensor information technology), WINS (wireless integrated network sensors), Smart Dust, μAMPS (micro-adaptive multi-domain power-aware sensors), Sea Web, etc [3].

Different from other wireless communication networks, the most important criterion in design of wireless sensor networks is energy-efficiency because sensor nodes are usually deployed in a large area and work using a non-rechargeable battery. Techniques used along the 7-layer OSI (open systems interconnection) model in this network all focus on the energy saving, especially in physical and MAC layers. IEEE has proposed two standards, IEEE 802.15.4 and IEEE 1451, in physical layer and MAC layer for wireless sensor networks [3]. However, there are only a few applications of WSN in use now and a lot of research work need to be done. So, this

thesis investigates the physical and MAC layers of WSN and hope to propose a more energy-efficient transmission framework.

1.3 Problem Statement

It is revealed that MIMO technology can increase the channel capacity because of the multiplexing gain, and the communication reliability because of the diversity gain. In another words, for the same bit-error-rate, a MIMO system uses less transmitting energy than traditional single-input single-output (SISO) mode. It is this idea that makes MIMO technology a possible option for data transmission in wireless sensor networks. Considering the strict limitation of sensors' physical size, it is impossible to install multiple antennas in one sensor node. So, the MIMO transmission in wireless sensor networks must be operated in a cooperative way, which means multiple sensor nodes with single-antenna in each of them, not multiple antennas, form this MIMO link [4]. This has brought out a question that although the transmitting energy can be dramatically reduced by the MIMO transmission mode, the extra circuit energy caused by information processing in multiple sensor nodes may make the total energy consumption of the cooperative MIMO system even higher than that of the simplest SISO mode. When it comes to two-hop or multi-hop communications, the comparison is more complicated and still not clear. The selection of the cooperative nodes and the relaying nodes are not clear too. In addition, the conditions under which a switch should be made between these two transmission modes need to be stated.

To solve these problems above, the operation feasibility of a cooperative MIMO framework in wireless sensor networks is investigated from a view of energy saving. The conditions that apply to cooperative MIMO and SISO modes are produced respectively.

1.4 Contributions to Knowledge

The main contributions of this thesis are now summarized as follows:

- The extended total energy consumption equations for different transmission modes in cluster-based wireless sensor networks are derived. The transmitting energy consumption and the circuit energy consumption are taken into account in both intra-cluster and inter-cluster phases respectively.

- A resource allocation framework is proposed for cluster-based cooperative MIMO on consideration of circuit energy. By introducing two adjusting parameters for the transmitting energy and the time slot allocation between intra-cluster and inter-cluster phases, this framework is designed to achieve the maximum data throughput of the whole system whilst maintaining the capacity and outage probability requirement in these two phases respectively.

- On comparison of various transmission modes in wireless sensor networks, a relatively energy-efficient mode switching framework is proposed for both single-hop and multi-hop transmissions. Based on the destination and the neighboring nodes' path-loss, the source node can decide which transmission mode, SISO or cooperative MISO, single-hop or multi-hop, should be chosen. Conditions for each mode switching are investigated. The possible existing area of the cooperative nodes and the relaying nodes can be obtained from this framework.

1.5 Organization of the Thesis

The remainder of this thesis is organized as follows.

Chapter 2 covers the background of the whole work in this thesis. General fundamentals of wireless fading channels and MIMO systems are introduced. Then the wireless sensor network and its key technologies for energy saving are discussed. Finally, the joint research actualities of MIMO and wireless sensor networks are stated. The gaps of others' work which will be solved in this thesis are also pointed out.

Chapter 3 first introduces several transmission modes in wireless sensor networks.

Then based on the function modules of a typical RF system, the extended total energy equations for different transmission modes are derived as the theoretical fundamentals of the research work.

Chapter 4 proposes a resource allocation framework for cluster-based cooperative MIMO transmission mode. Based on the underlying mathematics for wireless channels in both intra-cluster and inter-cluster phases, the time slot allocation and the power level allocation is discussed respectively. The comparison of the power allocation frameworks with or without consideration of the circuit energy is then made.

Chapter 5 first makes a comparison of all the single-hop transmission modes in wireless sensor networks. The energy components for each mode are analyzed. Then a path-loss based energy-efficient mode switching framework for single-hop transmission is proposed. By considering the geometry position of the cooperative node, its threshold area can be obtained.

Chapter 6 proposes a multi-hop path-loss based mode switching framework. Conditions for single-hop switching to multi-hop SISO and cooperative MISO modes are investigated respectively. The two-hop transmissions with ideal and non-ideal relaying position are both discussed. The treshold area for the relaying node (cluster) expressed by path-loss which makes sure the two-hop transmission is more energy-efficient than single-hop can be obtained from this framework.

Chapter 7 summarizes the most important conclusions drawn from the thesis and proposes several research paths for future work.

Chapter 2
Background and Literature Review

In this chapter, some basic concepts for wireless fading channels are introduced first. Then the background of MIMO communication and Wireless Sensor Networks are given, emphasizing the advantages of MIMO over the traditional technologies and the specialties of WSNs. Based on this, the necessity and feasibility of combining such two research fields can be clear, which also explains the source of this topic and the aim of this thesis. The literature review of recent cooperative MIMO technique in WSNs is also stated to clarify the contributions of the work.

2.1 Wireless fading channels

In wireless communications, fading is a common phenomenon. It refers to the attenuation and deviation of the power level when a carrier-modulated wireless signal is transmitted over certain propagation media. Due to the presence of reflectors and obstacles in the wireless environment, the signal arriving at the destination is a superposition of copies of transmitted signal, each experiencing a different physical propagation path and different attenuation, delay and phase shift [1]. A basic multipath propagation mechanism is shown in figure 2-1.

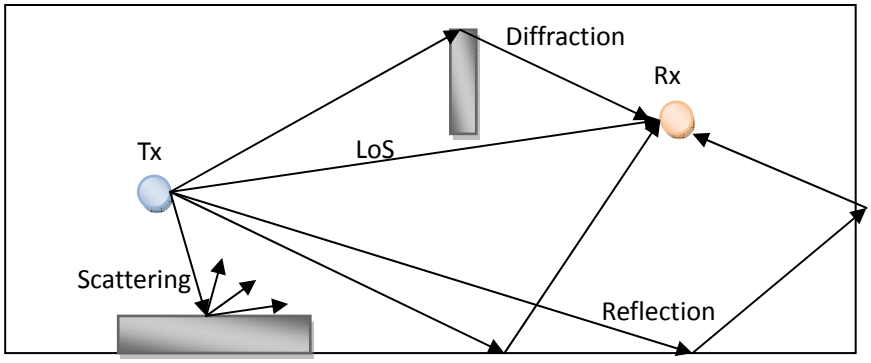

Figure 2-1 A basic multipath propagation mechanism

In figure 2-1, the transmitter and the receiver are named Tx and Rx. The signal directly transmitted to the receiver is the so called line-of-sight (LoS) signal. Other copies can also reach Rx through multipath propagation mainly caused by reflection, diffraction, and scattering. Then at the receiver side (Rx), amplification or attenuation of the signal power is seen because of superposition. The worst situation is so called deep fading which means a temporary failure of communication between Tx and Rx due to a severe drop of signal-to-noise ratio (SNR).

Fading is not always at a fixed value and is often modeled as a random process. It may vary with time, distance and radio frequency. So by different criterion, it can be categorized as slow and fast fading (or large scale and small scale fading), flat and frequency-selected fading.

2.1.1 Slow versus fast fading

The terms of slow and fast fading here refer to the rate at which the power and phase of the channel changes. A coherence time is defined to measure this, which means the minimum time required for the uncorrelated power change of the channel [5]. It is can be expressed as

$$T_c = \frac{k}{D_s} \tag{2.1}$$

where T_c is the coherence time, D_s is the Doppler spread, and k is a constant taking on values from 0.25 to 0.5.

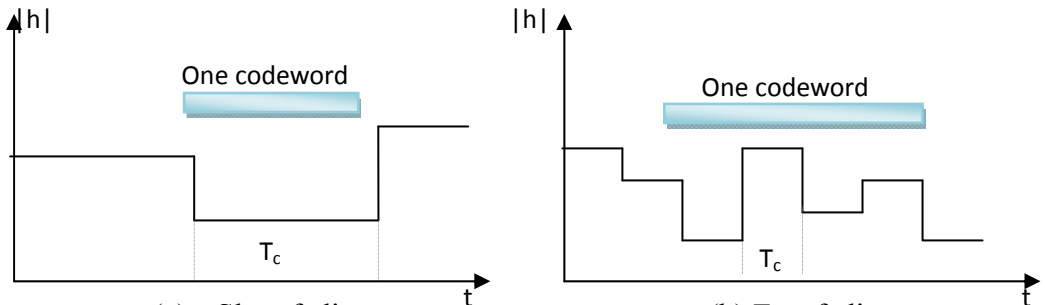

(a) Slow fading (b) Fast fading

Figure 2-2 Block fading models

When the coherence time of the channel is large enough compared with the delay constraint, we call this channel is in slow fading (figure 2-2(a)). In this situation, the power and phase change imposed by the channel can be considered as a constant [5]. Slow fading often occurs on a large scale due to the long distance transmission and some large obstacles like hills or buildings standing in the way, namely shadowing. It has been observed that the received signal power under a shadowing follows a log-normal distribution combined with a standard log-distance path loss [6]. The expression can be written as :

$$P_r = P_t \cdot d^{-\delta} \cdot 10^{\zeta/10} \tag{2.2}$$

P_r, P_t represent the signal power at the receiver and the transmitter respectively. $d^{-\delta}$ is the path loss, representing the mean energy loss along the transmission path. d denotes the propagation distance. δ is the path loss exponent. In an ideal free-space environment, $\delta = 2$, but in a practical environment, it is always in the range of 2 to 4 [7]. $\zeta \sim (0, \sigma_0^2)$ is a random variable drawn from a normal distribution with a mean of 0 and a standard deviation σ_0.

When the coherence time of the channel is small relative to the delay constraint of the channel, fast fading occurs (figure 2-2(b)). In this situation, the power and phase change imposed by the channel will vary considerably over the period of use. Fast fading often arises over small distances and is mainly caused by multipath propagation. For statistical analysis, there are three main distribution models to approach the fast fading, namely Rayleigh, Rician, and Nakagami.

- Rayleigh fading

Rayleigh fading is used to model the multipath propagation when there is no dominant LoS between the Tx and Rx. It assumes that there are a large number of independent scattering path from Tx to Rx. The amplitudes of the incoming signal at Rx are equal but with the random phases. Rayleigh fading is viewed as a reasonable model for tropospheric and ionospheric signal propagation as well as the effect of heavily built-up urban environments on radio signals [8][9].

In a discrete-time complex baseband model, the Rayleigh channel coefficient can be written as [10]:

$$h = a + bi \tag{2.3}$$

where a and b are independent identically distributed Gaussian random variables, $a \sim (0, \sigma_0{}^2/2)$, $b \sim (0, \sigma_0{}^2/2)$. The magnitude $|h|$ is described by a Rayleigh probability density function (PDF), given by:

$$p(x) = \frac{x}{\sigma_0^2} \exp\left\{\frac{-x^2}{2\sigma_0^2}\right\}, \quad x \geq 0 \tag{2.4}$$

Then the probability density function of power $|h|^2$ is

$$p(x) = \frac{1}{\sigma_0^2} \exp\left\{\frac{-x}{\sigma_0^2}\right\}, \quad x \geq 0 \tag{2.5}$$

- Rician fading

Rician fading occurs when there exists a dominant path, typically a LoS signal, which is much stronger than others. In a discrete-time complex baseband model, the Rician channel coefficient can be written as [11]:

$$h = (a + \tau) + bi \tag{2.6}$$

where $a \sim (0, \sigma_0{}^2/2)$, $b \sim (0, \sigma_0{}^2/2)$. τ is the peak amplitude of the dominant path and the power ratio of the dominant path and the scattered waves is defined as the Rician K-factor, given by:

$$K = \tau^2 / \sigma_0{}^2 \tag{2.7}$$

Two special values of $K = \infty$ and $K = 0$ represent two special channels respectively, a Gaussian channel with strong LoS and a Rayleigh channel without LoS [12]. The amplitude gain $|h|$ in the Rician channels is characterized by the Rician probability density function (PDF), given by:

$$p(x) = \frac{2x}{\sigma_0{}^2} \exp\left\{-(x^2 + \tau^2)/\sigma_0{}^2\right\} I_0\left[\frac{2x \cdot \tau}{\sigma_0{}^2}\right], \quad x \geq 0 \tag{2.8}$$

where $I_0(\cdot)$ is the modified Bessel function of first kind and zero order [13].

- Nakagami fading

Nakagami fading was initially proposed because it matched some empirical results with relatively large delay-time spreads and different clusters of reflected waves. Its corresponding PDF is [14]:

$$p(x) = \frac{2}{\Gamma(m_f)}\left(\frac{m_f}{\Omega}\right)^{m_f} x^{2m_f-1}\exp\left\{-m_f x^2/\Omega\right\}, x \geq 0 \qquad (2.9)$$

where $\Gamma(\cdot)$ is the Gamma function and $\Omega = E\left\{x^2\right\} \geq 0$ is the average power. m_f indicates the severity of fading and is determined by:

$$m_f = \frac{\Omega^2}{E\left\{(x^2-\Omega^2)\right\}} \geq 1/2 \qquad (2.10)$$

When $m_f = 1$, the Nakagami distribution reduces to Rayleigh fading. Both the Rician and the Nakagami models are two parameter distributions, so they are able to approximate more cases than Rayleigh model, which is a single parameter distribution.

2.1.2 Flat versus frequency-selective fading

Similarly to slow and fast fading, there is also a criterion named coherence channel bandwidth used to measure the flat or frequency-selective fading. The coherence bandwidth, which is the inversion of the time delay spread, indicates the minimum frequency separation at which the two frequency components become decorrelated [15].

Flat fading occurs when the coherence bandwidth is larger than the bandwidth of the signal. In that case, all frequency components of the signal will experience the same magnitude of fading. On the other hand, if the coherence bandwidth is small relative to the signal bandwidth, frequency-selective fading arises [15]. In this situation, different frequency components will experience different attenuation. In this thesis, the wireless channels are all flat fading ones.

2.2 Fundamentals of MIMO Communication

MIMO (Multiple-Input Multiple-Output) technology is a significant breakthrough in wireless communication and intelligent antenna research. The earliest ideas in this field can be traced back to the pioneering work during 1970s and 1980s by A.R. Kaye, D.A. George, W.van Etten, and Jack Winters, etc [16]. MIMO technology first originated from the antenna array used for military purposes. It aimed to provide improved diversity gain by exploiting more space dimensions and to suppress co-channel interference and noise in fading channels. Recently, some effort has also been made to incorporate MIMO technology into emerging communication standards, including the high speed downlink packet access (HSDPA) mode of third generation cellular networks, IEEE 802.11n for next-generation wireless local-area networks (WLAN), and IEEE 802.16 for outdoor fixed/nomadic wireless wide-area networks (WWAN) [17]. Its application has extended to our daily life, such as 3G mobile phones, and internet wireless accessing for our laptops, and promises to play an important role in the future.

2.2.1 General Structure of MIMO Systems

Different from the traditional single-transmitter single-receiver system, so-called SISO (single-input single-output), MIMO technology deploys multiple antennas at both the transmitter and the receiver side to improve communication performance. There are also some other systems derived from MIMO, which are known as SIMO, MISO. Diagrams illustrating SISO, SIMO, MISO and MIMO are shown in Figure 2-3.

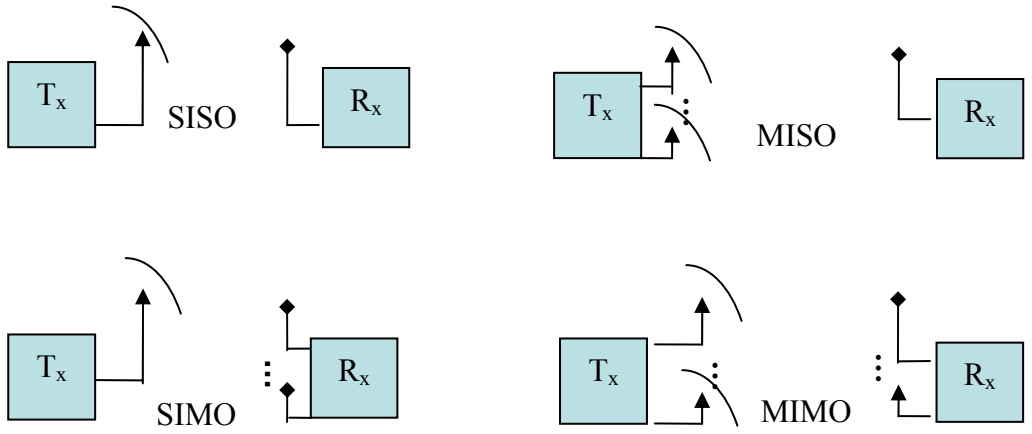

Figure 2-3 Sketch of SISO, SIMO, MISO, and MIMO systems

For MIMO systems, there are several sub-categories depending on the formation of antennas and number of users, such as single-user MIMO, multi-user MIMO (MU-MIMO), and cooperative MIMO (CO-MIMO).

- Single-user MIMO: a system with one transmitter equipped with multiple antennas communicating with only one receiver that has multiple antennas, shown as figure 2-4(a).

- Multi-user MIMO: a system with one multi-antenna transmitter communicating simultaneously with multiple receivers, each having one or multiple antennas (figure 2-4(b)).

- Cooperative MIMO: a system utilizing distributed antennas which belong to different users to form a virtual MIMO link at both transmission ends (figure 2-4(c)).

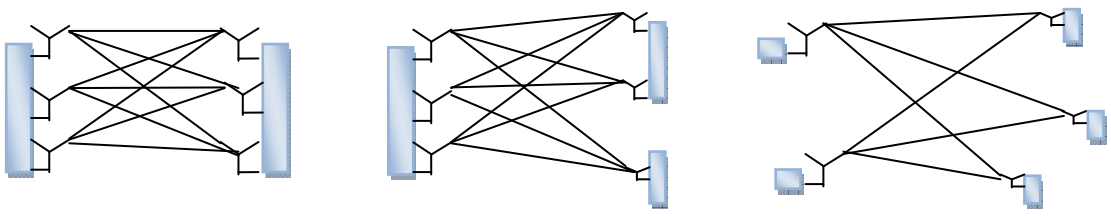

(a) (b) (c)

Figure 2-4 Single-user, multi-user, and cooperative MIMO systems

2.2.2 General methods for achieving MIMO

MIMO technology can be generally divided into three main fields, precoding, spatial multiplexing, and diversity coding.

- Precoding can be considered to be any spatial processing operations at the transmitter side. In a single-layer system (MISO), beamforming is used to send the same signal from each antenna with appropriate weighting such that the signal power is maximized at the receiver input. When there are more than one antennas at the receiver side, which is a MIMO system, precoding of multi-layer beamforming simultaneously maximize the signal level at all of the receive antennas [18]. Some examples of precoding strategies are singular value decomposition (SVD) [19] for single-user MIMO, linear precoding of minimum mean square error (MMSE), zero-forcing (ZF) and the nonlinear precoding of dirty paper coding (DPC) for multi-user MIMO systems [20]. All these strategies require knowledge of channel state information (CSI), full or limited, at the transmitter.

- Spatial multiplexing splits a high rate signal into multiple independent lower rate streams and each is emitted from a transmit antenna in the same frequency channel. It is a powerful technique for increasing channel capacity at higher signal-to-noise ratios (SNR) and can be adopted with or without channel state knowledge [21]. In an $N_t \times N_r$ system, where N_t and N_r represent the number of transmit and receive antennas respectively, the maximum spatial multiplexing order (capacity gain) is $N_s = \min(N_t, N_r)$.

- Diversity coding is used when there is no CSI at the transmitter side. In diversity methods, the data stream is coded by space-time block coding (STBC), which will be discussed in the following section, into several full or near orthogonal channels for transmission. Each transmit antenna emits one column of the codeword to combat fading. This technique reduces the probability that all the signal paths are in deep fade simultaneously and enhances the bit-error-rate performance [22][23].

2.2.3 MIMO channels

2.2.3.1 Mathematical definition

In an $N_t \times N_r$ MIMO system, the transmitted signal $\mathbf{x}(t) \in \mathbb{C}^{N_t \times 1}$ can be expressed as a vector:

$$\mathbf{x}(t) = [x_1(t), x_2(t) \cdots, x_{N_t}(t)]^T \tag{2.11}$$

where $x_i(t)\,(i = 1, 2, \cdots, N_t)$ is the data stream transmitted by the *i*-th transmitting antenna, and $[\cdot]^T$ represents matrix transposition. Then the received signal vector $\mathbf{y}(t) \in \mathbb{C}^{N_r \times 1}$ can be expressed as:

$$\mathbf{y}(t) = [y_1(t), y_2(t) \cdots, y_{N_r}(t)]^T \tag{2.12}$$

where $y_j(t)\,(j = 1, 2, \cdots, N_r)$ is the received data stream by the *j*-th receiving antenna. When the transmission delay is not considered, the input-output system function can be written as [15]:

$$\mathbf{y}(t) = \sqrt{\frac{\rho}{N_t}}\mathbf{H}(t)\mathbf{x}(t) + \mathbf{n}(t) \tag{2.13}$$

where ρ is the average SNR per antenna at the Rx and $\sqrt{\rho / N_t}$ represents the SNR per transmitting antenna at the source. $\mathbf{n}(t) \in \mathbb{C}^{N_r \times 1}$ is the complex circular additive white Gaussian noise (AWGN) vector which has zero mean and identity covariance matrix. $\mathbf{H}(t) \in \mathbb{C}^{N_r \times N_t}$ is the channel impulse response matrix containing all complex coefficients. It can be written as follows:

$$\mathbf{H}(t) = \begin{pmatrix} h_{11}(t) & h_{12}(t) & \cdots & h_{1N_t}(t) \\ h_{21}(t) & h_{22}(t) & \cdots & h_{2N_t}(t) \\ \vdots & \vdots & \ddots & \vdots \\ h_{N_r1}(t) & h_{N_r2} & \cdots & h_{N_rN_t}(t) \end{pmatrix} \tag{2.14}$$

h_{ji} $(j = 1, 2, \cdots, N_r,\ i = 1, 2, \cdots, N_t)$ in (2.14) describes the response between the *j*-th receiving antenna and the *i*-th transmitting element [24].

2.2.3.2 MIMO capacity

In information theory, channel capacity is the upper bound of information that a communication channel can transmit reliably. Given the input distribution, transmission power, noise level, and bandwidth, Shannon predicts the maximum achievable data rate for a communication system to obtain arbitrarily small error probability, which is widely known as the Shannon Formula [25]. This defines the channel capacity C as the maximum mutual information over all possible input distributions and gives the expression for an additive white Gaussian noise (AWGN) channel as [25]:

$$C = B\log\left(1+\frac{S}{N}\right) \tag{2.15}$$

B is the signal bandwidth and S/N is the signal-to-noise ratio (SNR) at the transmitter side. If channel gain is considered and C is measured in bits per second per Hertz, then the formula is rewritten as [25]:

$$C = \log_2\left(1+|h|^2\frac{S}{N}\right) \tag{2.16}$$

where $|h|^2$ is the channel gain.

In MIMO systems, as there exists a channel matrix, the capacity expression is more complicated than that of a SISO system (2.16). In addition, with different CSI at the transmitter, the capacity for MIMO systems can be quite different.

- Capacity with full CSI

In channels with perfect instantaneous channel state information at the transmitter, the ergodic $N_r \times N_r$ MIMO capacity is expressed as [26]:

$$C_{full-CSI} = \max_{\mathbf{Q};\mathbf{tr}(\mathbf{Q})\le P_t} \log_2\left(\det\left(\mathbf{I}_{N_r}+\frac{\rho}{N_t}\mathbf{HQH}^H\right)\right) \tag{2.17}$$

where $\mathbf{Q} = E\left\{\mathbf{xx}^H\right\}$ is the input covariance matrix and $\mathbf{tr(Q)}$ returns the trace of it

representing the total power transmitted at Tx. P_t is the transmitting power constraint. $[\cdot]^H$ denotes the Hermitian transpose. $I_{N_r} \in \mathbb{C}^{N_r \times N_r}$ is an $N_r \times N_r$ identity matrix and ρ is the average SNR per antenna at the Rx. This equation can be maximized by choosing $\mathbf{Q}$ optimally. Then the channel capacity with full CSI can be rewritten as [27]:

$$C_{full-CSI} = \sum_{i=1}^{\min(N_t, N_r)} \log_2\left(1 + \frac{\rho}{N_t} h_i \gamma_i\right) \tag{2.18}$$

where γ_i represents the subchannel weight. Equation (2.18) implies that by decomposing of the MIMO channel into several parallel channels, the optimal MIMO capacity with full CSI can be achieved by properly power allocation for each transmitting antenna.

- Capacity with statistical CSI

If the transmitter has only statistical channel state information, the ergodic channel capacity for a MIMO system can be expressed as [26][27]:

$$C_{statistical-CSI} = \max_{\mathbf{Q}} E_{\mathbf{H}}\left[\log_2\left(\det\left(\mathbf{I}_{N_r} + \frac{\rho}{N_t}\mathbf{H}\mathbf{Q}\mathbf{H}^H\right)\right)\right] \tag{2.19}$$

where the signal covariance $\mathbf{Q}$ can only be optimized in terms of the average mutual information. The capacity of this situation is smaller than that of the full CSI case and is strongly impacted by the spatial channel correlation.

- Capacity with no CSI

If there is no channel state information at the transmitter side, it has no preferred sub-channels. The input signal vector $\mathbf{x}(t)$ should be chosen using worst-case (non-preferential) statistics, which means $\mathbf{Q} = I_{Nr}$. So the capacity expression should be rewritten accordingly as [26][27]:

$$C_{no-CSI} = E_{\mathbf{H}}\left[\log_2\left(\det\left(\mathbf{I}_{N_r} + \frac{\rho}{N_t}\mathbf{H}\mathbf{H}^H\right)\right)\right] \tag{2.20}$$

2.2.3.3 Outage probability

The term of outage arises in slow fading channels or non-ergodic channels precisely speaking. In that case, the random channel realization $\mathbf{H}$ is fixed at the beginning of the transmission and stays constant over the duration of the codeword transmission. So there is a non-zero probability that a certain communication rate cannot be supported by the channel, which means the decoding error probability cannot be made arbitrarily small according to the Shannon theory [19][28]. Then this system is referred to as being in outage and the non-zero probability is named outage probability, denoted as P_{out}. The probability for reliable communication is then $1-P_{out}$.

For a SISO model, let an additive white Gaussian noise (AWGN) channel $CN(0,\sigma_0^2)$ with the received signal-to-noise ratio: $|\mathrm{h}|^2 P/\sigma_0^2$, where h is the channel vector and P is the transmitting power. Then the maximum rate of reliable communication will be $\log_2(1+|h|^2 P/\sigma_0^2)(\text{bits/s/Hz})$, which is so-called capacity. Suppose that the given data rate of a real system is R (bits/s/Hz), the outage situation will arise when R is above the maximum rate of reliable communication, i.e., $\log_2(1+|h|^2 P/\sigma_0^2) < R$. Therefore the outage probability can be defined as [26]:

$$P_{out}(R) = \Pr\{\log_2(1+|h|^2 P/\sigma_0^2) < R\} \tag{2.21}$$

where $\Pr\{\cdot\}$ is the cumulative density function (CDF).

Accordingly, for MIMO channels with a given input covariance matrix $\mathbf{Q} = E\{\mathbf{x}\mathbf{x}^H\}$, the outage probability can be defined as [27][28]:

$$P_{out}(R) = \inf_{tr(\mathbf{Q})\le P_t}\left\{\mathbf{Pr}\left\{\log_2 \det\left(\mathbf{I}_{N_r} + \frac{\rho}{N_t}\mathbf{H}\mathbf{Q}\mathbf{H}^H\right) < R\right\}\right\} \tag{2.22}$$

where $\inf\{\cdot\}$ denotes the infimum. It is the aim to minimize the outage probability by choosing a satisfactory form of codeword like space-time block code (STBC) for a given channel. For an energy average-split codeword, where $\mathbf{Q} = I_{Nr}$, (2.26) can be rewritten as [27][28]:

$$P_{out}(R) = \mathbf{Pr}\left\{\mathbf{log}_2 \mathbf{det}\left(\mathbf{I}_{N_r} + \frac{\rho}{N_t}\mathbf{H}\mathbf{H}^H\right) < R\right\}$$

$$= \mathbf{Pr}\left\{\sum_{i=1}^{\min(N_t,N_r)} \mathbf{log}_2\left(1+\frac{\rho\lambda_i}{N_t}\right) < R\right\} \quad (2.23)$$

where λ_i is the eigenvalue of $\mathbf{H}\mathbf{H}^H$.

2.2.4 Space-time Block Coding

Space-time block coding (STBC) is a coding technique for MIMO wireless communication. By space-time block coding on the transmitting antennas, the codewords are transmitted in multiple diversity data streams to improve the transmission reliability.

An STBC can be described as a matrix, with each row representing a time slot and each column representing one antenna's transmission over time [29]. A block codeword with *T* time slots is called *T* length coding. If an STBC block encodes k symbols of a signal, then the code rate can be expressed as [29]:

$$R = \frac{k}{T} \quad (2.24)$$

It is used to measure how many symbols this coding transmits per time slot on average. Then the system data rate is the product of symbol rate multiplying by the code rate.

STBC only provides diversity gain in space and time but no coding gain [30]. It is usually designed to be orthogonal, which means each column vector of the code block emitted from one antenna branch is uncorrelated with others from different branches. This can reduce the MIMO channel into parallel SISO channels. The advantages of orthogonality are less interference between channels and linear decoding at the receiver. However, due to the redundancy of coding, these advantages are always achieved at the sacrifice of proportional data rate [29][30].

2.2.4.1 Encoding

Orthogonal STBCs should be designed to achieve the maximum so-called diversity criterion [30]. Suppose a transmitting codeword

$$\mathbf{C}=\begin{bmatrix} s_{11} & s_{12} & \cdots & s_{1N_t} \\ s_{21} & s_{22} & \cdots & s_{2N_t} \\ \vdots & \vdots & \ddots & \vdots \\ s_{T1} & s_{T2} & \cdots & s_{TN_t} \end{bmatrix} \quad \downarrow \text{ T time-slots} \qquad (2.25)$$

N_t transmitting antennas →

and its decoded received codeword

$$\mathbf{C}'=\begin{bmatrix} s'_{11} & s'_{12} & \cdots & s'_{1N_t} \\ s'_{21} & s'_{22} & \cdots & s'_{2N_t} \\ \vdots & \vdots & \ddots & \vdots \\ s'_{T1} & s'_{T2} & \cdots & s'_{TN_t} \end{bmatrix} \qquad (2.26)$$

The error matrix

$$\mathbf{e}=\begin{bmatrix} s'_{11}-s_{11} & s'_{12}-s_{12} & \cdots & s'_{1N_t}-s_{1N_t} \\ s'_{21}-s_{21} & s'_{22}-s_{22} & \cdots & s'_{2N_t}-s_{2N_t} \\ \vdots & \vdots & \ddots & \vdots \\ s'_{T1}-s_{T1} & s'_{T2}-s_{T2} & \cdots & s'_{TN_t}-s_{TN_t} \end{bmatrix} \qquad (2.27)$$

has to be full-rank to satisfy the maximum possible diversity order.

The most famous and widely used STBC is the Alamouti scheme, invented in 1998 [31]. It was designed for a simple two-transmitting-antenna system. Its coding matrix is:

$$\mathbf{C}_{Alamouti}=\begin{pmatrix} s_1 & s_2 \\ -s_2^* & s_1^* \end{pmatrix} \qquad (2.28)$$

where "$*$" denotes complex conjugate. It is apparent that Alamouti is a 1-rate code (two symbols transmitted in two time slots).

In the research field of coding, a set of higher order STBCs have been invented [32]. Some straightforward examples for 3 and 4 antennas are listed below.

$$\mathbf{C}_{3,1/2}=\begin{bmatrix} s_1 & s_2 & s_3 \\ -s_2 & s_1 & -s_4 \\ -s_3 & s_4 & s_1 \\ -s_4 & -s_3 & s_2 \\ s_1^* & s_2^* & s_3^* \\ -s_2^* & s_1^* & -s_4^* \\ -s_3^* & s_4^* & s_1^* \\ -s_4^* & -s_3^* & s_2^* \end{bmatrix} \qquad \mathbf{C}_{3,3/4}=\begin{bmatrix} s_1 & s_2 & \frac{s_3}{\sqrt{2}} \\ -s_2^* & s_1^* & \frac{s_3}{\sqrt{2}} \\ \frac{s_3^*}{\sqrt{2}} & \frac{s_3^*}{\sqrt{2}} & \frac{-s_1-s_1^*+s_2-s_2^*}{2} \\ \frac{s_3^*}{\sqrt{2}} & -\frac{s_3^*}{\sqrt{2}} & \frac{s_2+s_2^*+s_1-s_1^*}{2} \end{bmatrix}$$

$$\mathbf{C}_{4,1/2}=\begin{bmatrix} s_1 & s_2 & s_3 & s_4 \\ -s_2 & s_1 & -s_4 & s_3 \\ -s_3 & s_4 & s_1 & -s_2 \\ -s_4 & -s_3 & s_2 & s_1 \\ s_1^* & s_2^* & s_3^* & s_4^* \\ -s_2^* & s_1^* & -s_4^* & s_3^* \\ -s_3^* & s_4^* & s_1^* & -s_2^* \\ -s_4^* & -s_3^* & s_2^* & s_1^* \end{bmatrix} \qquad \mathbf{C}_{4,3/4}=\begin{bmatrix} s_1 & s_2 & s_3 & 0 \\ -s_2^* & s_1^* & 0 & s_3 \\ -s_3 & 0 & s_1^* & -s_2 \\ 0 & -s_3^* & s_2^* & s_1 \end{bmatrix} \tag{2.29}$$

The above codewords reach the code rate of 1/2, 3/4, 1/2, 3/4 respectively. It has been proved that the highest code rate for N_t antennas should be [32]:

$$r_{\max}=\frac{n_0+1}{2n_0}, \quad n_0=\begin{cases} N_t/2 & (N_t \text{ is even}) \\ (N_t+1)/2 & (N_t \text{ is odd}) \end{cases} \tag{2.30}$$

From (2.30) we can see that the maximum code rate for all possible numbers of antennas is 1, and only the 2-antenna Alamouti scheme can achieve such a rate. In another word, only the Alamouti code can achieve its full diversity gain without sacrificing its data rate. So, to obtain diversity advantages in a system with higher data rate restriction, the Alamouti scheme is a better choice than other STBCs. More importantly, since all the communication instruments can easily modulate the signal into complex symbols and all the constellation diagrams rely on these complex modulations, the Alamouti code is much more widely used than other STBCs, especially in research, even though the higher order STBCs can sometimes achieve a better bit-error-rate performance.

2.2.4.2 Decoding

As mentioned above, one of the big advantages for orthogonal STBCs is linear processing at the decoding end, which is called maximum likelihood decoding. The received signal at antenna *j* is expressed as:

$$y_j(t) = \sum_{i=1}^{N_t} h_{ji} x_i(t) + n_j(t), \quad j = 1, 2, \cdots, N_r, \quad i = 1, 2, \cdots, N_t \tag{2.31}$$

where $x_i(t)$ is the signal transmitted by antenna *i*, and h_{ji} is the path gain from transmitting antenna *i* to receiving antenna *j*. $n_j(t)$ is the AWGN at antenna *j*. The maximum-likelihood detection rule is to form the decision variables [33]

$$X_i = \sum_{k=1}^{T} \sum_{j=1}^{N_r} y_j h_{\varepsilon_k(i) j} \delta_k(i) \tag{2.32}$$

where $\delta_k(i)$ is the sign of s_i in the *k*-th row of the coding matrix, $\varepsilon_k(i) = q$ denotes that s_i is the (*k*,*q*) element of the coding matrix, and then decide on constellation symbol s_i that satisfies

$$s_i = \arg\min_{s \in \Lambda} \left(\left| R_i - s \right|^2 + \left(-1 + \sum_{k,j} \left| h_{kj} \right|^2 \right) \left| s \right|^2 \right) \tag{2.33}$$

with Λ the constellation alphabet [32][33].

2.2.5 Advantages of MIMO over SISO

After a short investigation of MIMO channels and some basic techniques for MIMO communication in the former part of this section, we can now come to conclude the comparison results regarding MIMO and SISO transmission modes.

The benefits of a MIMO system over a SISO system arise from two aspects . The first one is spatial multiplexing gain [5][15], which is apparent from its multiple-antenna system structure. Multiple antennas in both transmitting and receiving ends extend the degree of space freedom and makes it possible to transmit a number of individual (orthogonal in most cases) data streams simultaneously. In a general $N_t \times N_r$ MIMO system, the maximum multiplexing gain is upper limited by $\min(N_t, N_r)$. This also means that in a high SNR environment, the capacity supported by a MIMO system is

$\min(N_t, N_r)$ times of that of a SISO system. However, this conclusion only refers to the maximum possible channel capacity, and it doesn't promise that the data rate for a real MIMO system is better than that of SISO, because some coding strategies at the source, such as STBCs, introduces redundancy and sacrifices part of data rate to achieve other benefits.

The second big advantage of MIMO mode over SISO is spatial diversity gain [5][15]. It is obtained by transmitting the same message for each transmitter through different sub-channels and then combining them at the receiver side. Diversity reduces the probability that all the branches are in deep fade thus can significantly enhance the reliability of the system, shown by bit-error-rate performance. Theoretically speaking, the more antennas deployed at the transmitting and receiving sides, the more diversity gain can be obtained. In a $N_r \times N_r$ MIMO system, the maximum diversity gain is upper limited by $N_t N_r$.

However, there is an inherent trade-off between spatial multiplex and spatial diversity, which means the maximum multiplexing gain and maximum diversity gain cannot be achieved simultaneously [5]. The increase of diversity gain requires more repeated data stream to enhance the BER performance, which will cut down the system data rate and expenses the multiplexing gain, and vice versa. So the diversity-multiplexing trade-off of a MIMO system is a more reasonable measure for its performance and can be used to compare with SISO systems.

The disadvantage of MIMO system is the complexity of its structure. More antennas introduce more complicated modulation and synchronization schemes at both Tx and Rx which arouses more circuit energy consumption. This explains why more N_t and N_r are not necessarily better.

2.3 Fundamentals of Intelligent Wireless Sensor Networks

In recent years, along with the development of computer science, telecommunication, automation, artificial intelligence, and micro-electro-mechanism system (MEMS), a new kind of monitoring network, wireless sensor network (WSN), has been paid more

and more attention and becomes one of the hot topics in IT research field [34]. Different from other computer and wireless communication networks, WSN has some particular features and its own criterion for design. In the section, we will give a fundamental introduction of its structure and some important techniques for its operation.

2.3.1 Basic structure for wireless sensor networks

A wireless sensor network is composed of a large number of sensor nodes that are densely and randomly deployed in specific terrains, like battlefields or inaccessible environments, for monitoring [34]. The position of sensor nodes need not be engineered or predetermined and even during its lifetime, the topology of the network still keeps on changing. Information gathered from the collector node can be delivered node by node to the target one. This case is called node-based communication. In addition, by using selection strategies, these nodes can also form several clusters to do the same job, termed cluster-based communication. The sketch of a sensor network and its basic operating mode are shown in Figure 2.5

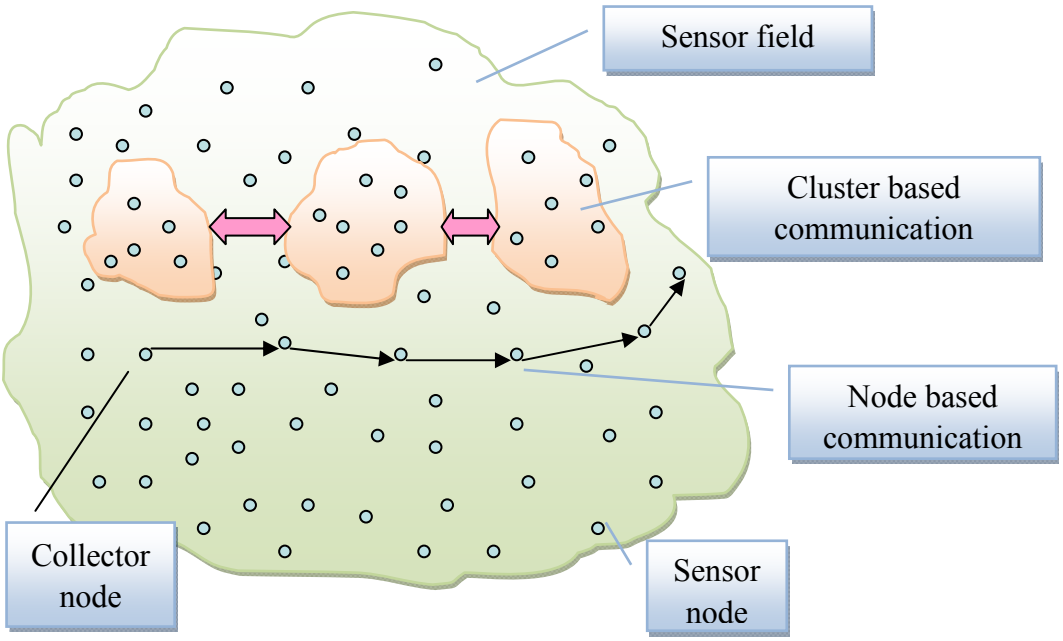

Figure 2-5 A wireless sensor network

Many protocols and algorithms proposed for traditional wireless ad hoc networks can

be directly applied to WSNs. However, WSNs do have some unique features which are different from Ad Hoc networks [35]:

- The number of sensor nodes in a sensor network can be several orders of magnitude higher than the nodes in an ad hoc network.
- The topology of a sensor network changes frequently.
- Sensor nodes are limited in power, computational capacity, memory storage, and prone to failure.
- Sensor nodes may not have global identification (ID) because of the large associated overhead and large number of sensors.

According to the physical structure of sensor nodes, there are two kinds of sensor networks: homogeneous WSNs, in which the sensor nodes are all the same; inhomogeneous WSNs, in which sensor nodes are designed with different energy and capabilities [34]. However, in both kinds of WSNs, a basic sensor node is made up of four fundamental components: a sensing unit, a processing unit, a transceiver unit, and a power unit [35]. As shown in Figure 2-6, there may also be some additional application-dependent components such as a power generator and a location finding system. Because all the functions performed by the sensor node are powered by a small onboard battery that is quite difficult to be recharged or replaced, the lifetime of a sensor network is mainly determined by duration of these batteries. Hence, energy conservation and power management become the most important factor in design of WSNs.

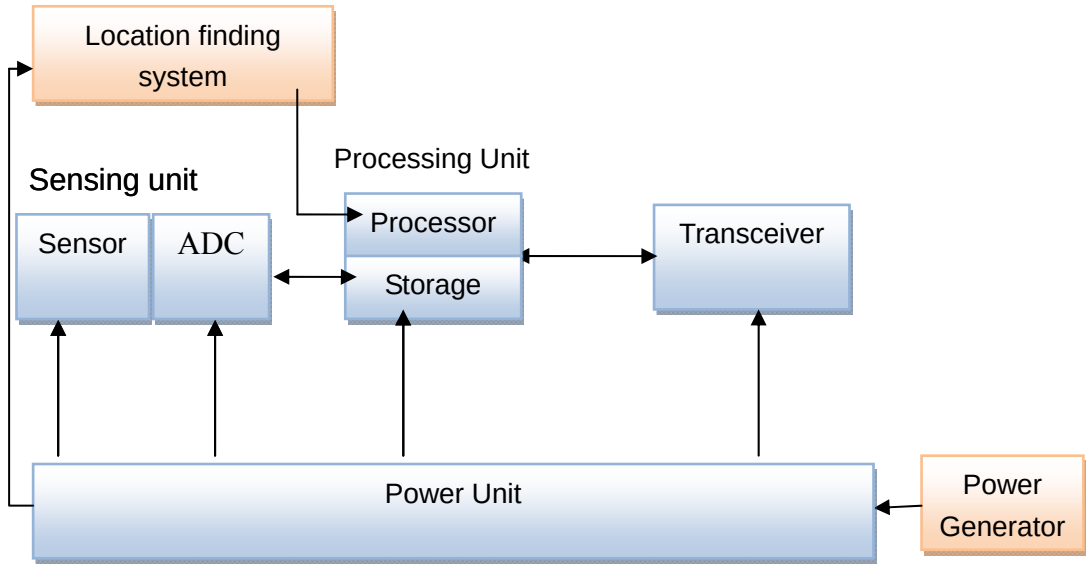

Figure 2-6 The components of a sensor node

2.3.2 Techniques for wireless sensor networks

As a communication system, wireless sensor networks also obey the 7-layer Open Systems Interconnection (OSI) model. The main techniques for WSNs can be divided into three categories from bottom to the top of the model: communication and network forming, service management, and application system [34][35], as shown in figure 2.7.

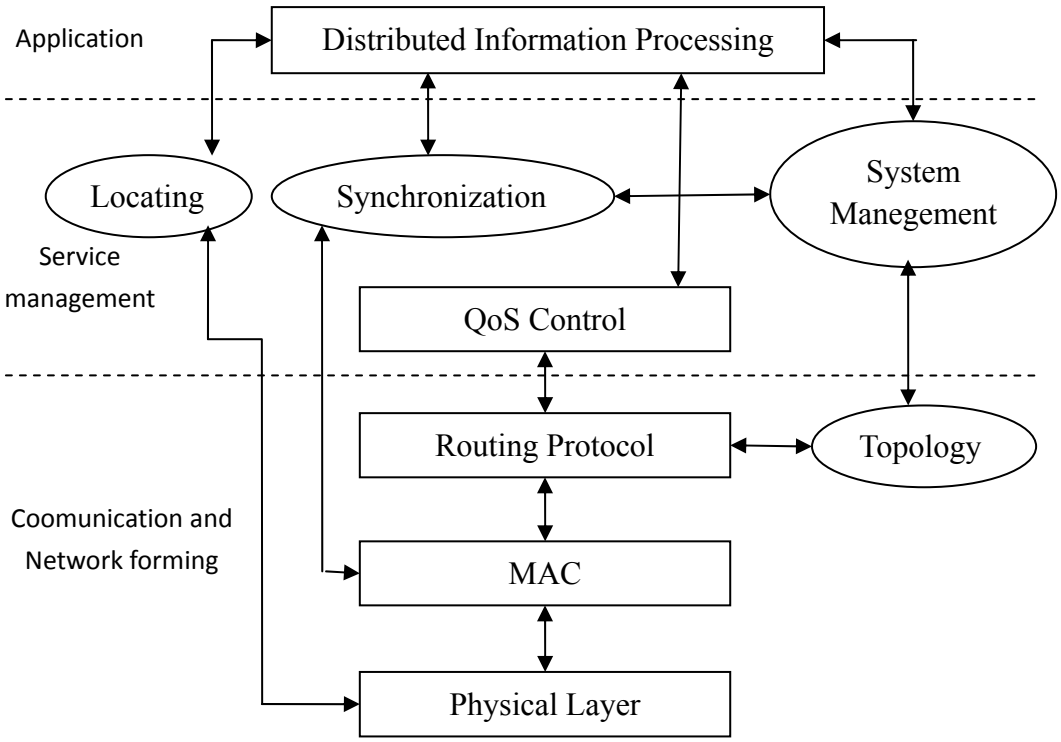

Figure 2-7 Main techniques for wireless sensor networks

Among the techniques in figure 2-7, we will focus on channel access technology, routing, and energy management, which have a close relationship to the problem we want to solve in this thesis.

2.3.2.1 Channel access technology

Channel access technology is a method used to set up reliable 1-to-1, 1-to-multipoint, and multipoint sharing communication links [36]. When there exists a large number of

transmitting nodes and each of them always bursts to emit data, it is the responsibility of data-link layer to allocate proper channel resources for each node using a media access control (MAC) protocol [37]. The channel access protocols for a common wireless network can be divided into three groups: competition-based techniques, fixed-allocation techniques, and requirement-based techniques[38].

- Competition-based channel access

  Competition-based channel access is a typical dynamic, random access strategy. The nodes with a communication requirement occupy the channels by competition. Examples for this strategy are ALOHA [39], Carrier Sense Multiple Access/Collision Detect (CSMA) [40], busy-tone multiple access (BTMA) [41], split channel reservation multiple access (SRMA) [42], and mini-slotted alternating priorities (MSAP) [43]. The main problems faced by all these protocols are frame collision, hidden and exposed stations. The former one can be solved by binary exponential backoff (BEB) and multiplicative increase linear decrease (MILD) algorithms [44], while the latter one can be solved by a Request To Send/Clear To Send (RTS-CTS) strategy [45].
- Fixed-allocation channel access

  If a sharing channel is split into several isolated sub-channels and each is used by named one or more nodes, then we call this strategy fixed-allocation channel access [46]. Typical protocols for this are frequency-division multiple access (FDMA) [47], time-division multiple access (TDMA) [48], code-division multiple access (CDMA) [49], and space-division multiple access (SDMA) [50]. Among these, TDMA, FDMA, and CDMA are already widely used by other wireless networks. SDMA can be obtained by adaptive antenna array with each antenna identified.
- Requirement-based channel access

  Requirement-based channel access means that an enquiry is sent sequentially to each node in the network to ask if they have data packet to transmit [38]. If a certain node receives the enquiry and has such a transmission task, it then sends the packets immediately. Otherwise, it will pass the enquiry to the next one. Based on different kinds of enquiry control, there are two models for this channel access protocol. One is the central coordination algorithm, which means a central node, or cluster-head, is set to operate the sequential enquiry. A typical example

for this is point coordination function (PCF) in IEEE 802.11 [51]. The other algorithm is distributed coordination, where each node has the responsibility to manage the channel resources in the network cooperatively. An example for this is wireless token ring protocol (WTRP) in IEEE 802.5 [52].

As sensor networks are used for environment monitoring, we can assume that the nodes remain inactive for long periods of time, but then become active when something is detected. This is different from traditional wireless MACs such as IEEE 802.11 because energy conservation and self-configuration are primary goals for WSNs, while per-node fairness and latency are less important. Therefore, not all of the MAC protocols mentioned above can be adopted directly in WSNs. Here we introduce some protocols designed specially for WSNs.

- Sensor-MAC (S-MAC) [53]

  There are three novel techniques used in S-MAC. To reduce energy consumption in listening to an idle channel, a sensor node periodically falls asleep. Its neighbours form a *virtual cluster* and auto-synchronize on this sleep schedule. S-MAC also sets the radio transmitter to sleep during communications of other nodes, where only in-channel signaling is in use. Finally, S-MAC uses message passing to reduce contention latency for sensor-network applications that require store-and-forward processing as data moves through the network [54].
- Distributed energy-aware MAC (DE-MAC) [55]

  DE-MAC is based on TDMA. The core idea of DE-MAC is to elect a local winner with the lowest remaining energy and allocate more sleep slots for it. The local election phase is based on TDMA so there is no loss of data throughput for the whole system. All the time slots have been pre-allocated for each node, so there is no frame competition and expense for controlling.
- Mediation device (MD) [56]

  MD protocol focuses on supporting a reliable communication to sensor nodes without precise synchronization. By recording the time deviation in an enquiry frame, the pair of nodes can be synchronized dynamically only when communication arises.

2.3.2.2 Routing technology

Another important element of wireless sensor networks is routing. In this thesis, routing technology is not the main focus of the research work, however, all the cluster-heads used for the cluster-based transmissions in this thesis are selected from from a kind of pre-set routing protocol. So, in this section, the usual routing protocols are introduced in brief.

Given the energy and memory limitation of the sensor nodes and dynamic topology of WSNs, it is difficult to directly adopt routing protocols of other Ad Hoc networks to WSNs. The design of routing protocols for WSNs should satisfy the following requirements: a) energy efficiency to cut unnecessary cost and maximally extend the network lifetime, b) data fusion capability to cut redundant information, c) distributed processing, d) robustness for dynamic network topology, e) security [35].

Since 1999, scientists have designed a set of protocols for WSNs specially, such as sensor protocol for information via negotiation (SPIN) [57], directed diffusion (DD) [58], highly-resilient energy-efficient multipath routing (HREEMR) [59], sequential assignment routing (SAR) [60], low-energy adaptive clustering hierarchy (LEACH) [61], power-efficient gathering in sensor information system (PEGASIS) [62], threshold sensitive energy efficient sensor network protocol (TEEN) [63], small minimum energy communication network (SMECN) [64], and geographic and energy aware routing (GEAR) [65], etc. All these protocols above can be divided into different categories based on criteria such as flat or hierarchical routing, with or without geography location assistant, supporting QoS or not. Here we will introduce some most popular routing protocols which are closely related to this dissertation.

- DD

  Directed diffusion (DD) is based on the idea of converging data from different sources. It is composed of three steps. The first is route building, during which the sink node broadcasts its interest within the network and all the other nodes can set up a grads to the sink node depending on the interest [58]. The second step is data transmission, during which the information is transmitted from the source to the sink node following the grads. The relay nodes as well as the sink

node may receive data streams from multiple neighbours and then do the data fusion by a local algorithm. The final step is to set up a strengthened route. The sink node send a route-strengthen requirement to the neighbour with highest SNR, and this requirement is then passed by the neighbour sequentially to the source node with the same decision criterion. Thus a strengthened multi-hop single route is set up and following communication is mainly on this route [58]. Because DD is based on the interest of the sink node, it is not fit for environment monitoring applications based on an emergency drive model.

- LEACH

  LEACH is a low power hierarchical routing protocol, proposed by Chandrakasan and his colleagues in MIT in 2000 [66]. Its basic idea is to repeatedly choose cluster-heads randomly; the total energy of the network can be spread over every sensor node. Simulation results shows that LEACH can extend the network life time by 15% compared to other flat routing protocols [61]. The communication within the network is a cluster-based model. The chosen of cluster-heads is based on the total number of clusters and the times of each node been chosen as the cluster-head before. Once a cluster-head is selected, it will use a TDMA mode to communicate with other members in the cluster. To reduce the energy cost, the duration for a stable communication should be much longer than that for cluster forming. However, because the cluster-heads selection mechanism of LEACH assumes all the sensor nodes have the same energy at the first selection and the selection only depends on the times that a sensor node has been chosen, not on its remaining energy, it is not fit for the energy non-even distributed networks.

- GEAR

  GEAR is a geography assisted algorithm, which considers both energy and location information to route to the destination area. GEAR requests each node sustain an estimated cost, representing the remaining energy and the distance to the destination, and a learning cost, which is a modification to the estimated cost when no neighbours are nearer to the sink node than itself [67]. When a certain packet reaches the destination successfully, the learning cost for the last hop will be passed to the former hop for adjusting.

2.3.2.3 Energy management

Based on the former discussion, we can see that all the techniques applied in lower layers of the WSNs have a common aim, to cut the energy cost and to make the network last as long as possible. In higher layers, this is still the case. So energy management techniques are involved in each layer of design for WSNs.

A common energy management strategy is sleep scheduling [35]. Its main idea is that when there is no data to transmit, the sensor node will switch off all its modules and turn to a quite low-power state, namely sleep. When the need for communication arises, the node need to be woken to the work state. So how to switch between these two states is the key point of this energy management, for bad switching schemes may cause time delay and even more energy consumption.

Nowadays, there are several ways to support this sleep scheduling strategy. The first relies on the hardware. Some microprocessors, like Strong ARM and Crusoe, support adjusting the voltage and frequency of operation. In addition, recent RF instruments can also switch to one of four states: transmitting, receiving, idle, and sleep. The second lies on the software, like dynamic voltage scaling (DVS) proposed by Pering in 1998 [68]. Sinha also proposed a five-state sleep model based on the prediction of system load [69]. The third way is by the MAC protocols discussed above, such as DE-MAC, MD, and S-MAC [53~56].

Another useful energy management strategy is multi-hop communication. The energy consumed in transmission will increase dramatically with the increase of communication distance. So, to reduce the energy consumption, we should try to make the single-hop shorter and adopt a multi-hop mode for data transmission. This strategy is one of the key topics in this thesis and will be discussed in the following chapters.

2.4 Review of Cooperative Technologies for WSNs

As MIMO technology has the potential to dramatically increase the channel capacity

and at the same time reduce transmission energy consumption [70], the idea of connecting these two research fields, MIMO and WSNs, has become popular in recent research. However, due to the physical limitation of a sensor node which can typically support only one antenna, it is impractical to apply multi-antenna devices into sensor networks directly [71]. So cooperation between individual single antenna nodes is needed to form a cooperative MIMO, or virtual MIMO, for information transmission and reception.

The idea of cooperative MIMO in WSNs first came out in [72~74], based on the original work of Cover and El Gamal [75]. In cooperative networks, nodes combine the received signal at the physical layer and relay each other's messages to provide spatial diversity [76]. There are three approaches to achieve cooperative diversity in WSNs. The first is based on the physical layer multi-hop structure introduced in [77]. Multi-hop is considered as a multiple relay channel with source-relay, relay-relay and relay-destination communications. The second approach is based on the data flooding scheme proposed in [78][79]. The source node starts to transmit data to the destination node directly, while other network nodes transmit a cooperative signal after they have decoded the broadcast data. The third is cluster-based approach presented in [71]. The sensor nodes are grouped into so-called cooperative clusters. All clusters transmit and receive information from other cooperative clusters. Limiting cooperation inside the cluster reduces synchronization and resource management complexity [76]. [80] shows the network capacity of restricting relaying to a finite cluster. Cluster design and a corresponding energy saving strategy can be found in [81][82], where the relationship between the long haul distance and the optimum number of clusters is derived.

Outage probability discussed in [72] and Shannon capacity in [83] show that increasing the number of nodes can improve the performance of cooperative diversity in single-hop communication. Likewise, in a multi-hop situation, benefits from node cooperation are also shown in [84]. Results in [85] show the benefits of cooperation in terms of a low transmission power budget. Nevertheless, although in many situations cooperative transmission can potentially improve system performance, a number of issues such as synchronization among nodes, distributed control and resource management may complicate its practical application. Even in the energy technology

field, there is a lot of work to do. Traditional energy-efficient communication techniques mainly focus on the transmission power only. That is the case in long-range applications where the transmission power is the dominant element of the total energy consumption [71]. However, in short-range applications, the circuit energy consumption is comparable to or even dominates the transmission power. Hence, although cooperative MIMO technology can effectively reduce the power consumption during the transmission, it doesn't necessarily cut down the total power consumption within the network [71][86~88] . So a total energy-efficient model from a global view of the whole network is the starting point of the work in this thesis. Based on this, a clear comparison of cooperative MIMO and SISO in both single-hop and multi-hop transmissions needs to be discussed in details, which is the main task of the thesis.

Chapter 3
Transmission and Energy Consumption Models for Wireless Sensor Networks

The most common application for wireless sensor networks is environmental monitoring. In this thesis, it is assumed that a large number of sensor nodes with a single-antenna are deployed within an area and work on a Sleep Scheduling strategy, as discussed in Chapter 2, for information gathering. For a common long time period, all the sensor nodes are inactive or in state of sleep to keep the energy expense as low as possible. However, when something arises within the area, reflected in the information the network is interested in, and is detected by one node, namely the source node, part of the network is woken. The information gathered from the source node will be transmitted wirelessly within the network by some routing protocol to the so-called sink node or base station (BS) for further processing.

In this chapter, several transmission modes in WSNs will be introduced first. If a wireless sensor network is organized by clusters, then the transmission mode is cluster-based, otherwise it is node-based. In addition, depending on the physical distance from the source node to the sink node, these transmissions can also be categorized as single-hop and multi-hop. The structure, transmission process, and channel characteristics for each mode will be discussed in detail in Section 3.1. Then in Section 3.2, a total energy consumption model for the RF transmission system is stated. Based on this model, the extended energy equations for different transmission modes in wireless sensor networks can be derived. Both these two sections are the foundation of research work in this thesis.

3.1 Transmission Model

3.1.1 Node-based transmission mode

The simplest and most traditional transmission mode in WSNs is point-to-point SISO. Data gathered from the source node is transmitted to the sink node or BS directly without any relay. Only the pair of communication ends are activated while any other nodes in the network keeps on sleeping to save energy. The basic structure of a single-hop SISO system in a WSN is shown in figure 3-1.

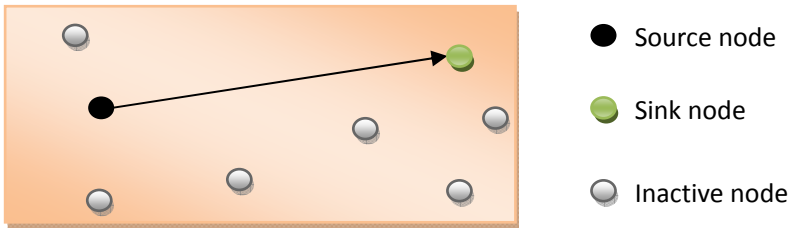

Figure 3-1 Single-hop SISO in a WSN

The communication channel in figure 3-1 is a basic SISO channel, with the capacity expression of (2.16) for ergodic channels and the outage probability expression of (2.23) for non-ergodic channels. The single-hop SISO system is usually used in a relatively small network where the distance between the source node and the sink node is short. However, when the source node is far away from the destination, there will be a higher energy consumption for this single-hop mode. This is because the signal power transmitted experiences a drop in power along the path (path loss) related to the path length, so to maintain the same signal-to-noise ratio as well as the bit-error-rate at the receiver side, more power is needed at the transmitter. For the long distance situation, a multi-hop mode is preferred instead of the single-hop one. The structure of a multi-hop SISO transmission mode is shown in figure 3-2.

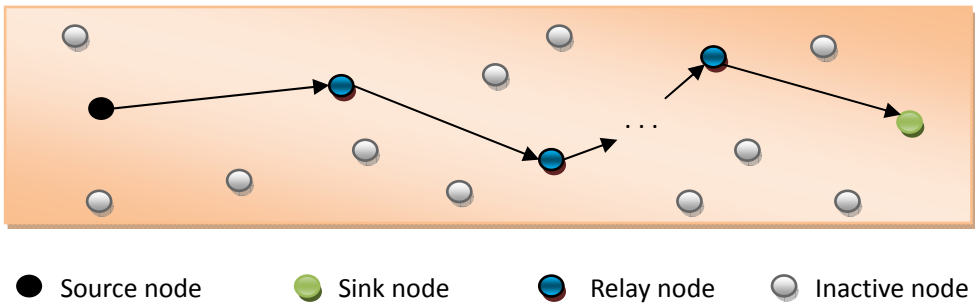

Figure 3-2 Multi-hop SISO in a WSN

In figure 3-2, the information is passed node by node to the destination. The routing protocol can be chosen from any of the schemes discussed in chapter 2. (It is not the routing protocols but the energy consumptions for each transmission mode that are the main concerns in this thesis.) The transmission distances for each hop in figure 3-2 can be equal or unequal, but are not fixed. Because the system throughput is determined by the weakest hop, the end-to-end channel capacity for this multi-hop mode can be written as:

$$C_{multi-hop} = \mathbf{min}(C_1, C_2, \cdots C_K) \tag{3.1}$$

where $C_1, C_{2,} \cdots C_K$ represent the channel capacity for each hop respectively and $K = 1, 2, \cdots$ is the number of hops. If there is no error correction scheme at the relay nodes, errors will accumulate at the destination and the bit error-rate can be written as:

$$P_{e,multi-hop} = 1 - (1 - P_{e1})(1 - P_{e2}) \cdots (1 - P_{eK}) \tag{3.2}$$

where P_{e1}, P_{e2}, … , P_{eK} represent the bit-error-rate for each hop. The choice of optimal relay nodes and the number of hops K will be discussed in later chapters.

3.1.2 Cluster-based cooperative transmission modes

When a wireless sensor network is composed of clusters, the transmission mode is cluster-based [89]. All the sensor nodes in the network are grouped into clusters and there may or may not be a cluster-head for each of them, depending on the cluster forming algorithm or routing protocol. The node-based sleep scheduling strategy then turns to cluster-based one. Clusters not involved in the communication remain in sleep mode [90]. A typical one-hop cluster-based cooperative transmission mode is

displayed in the following figure.

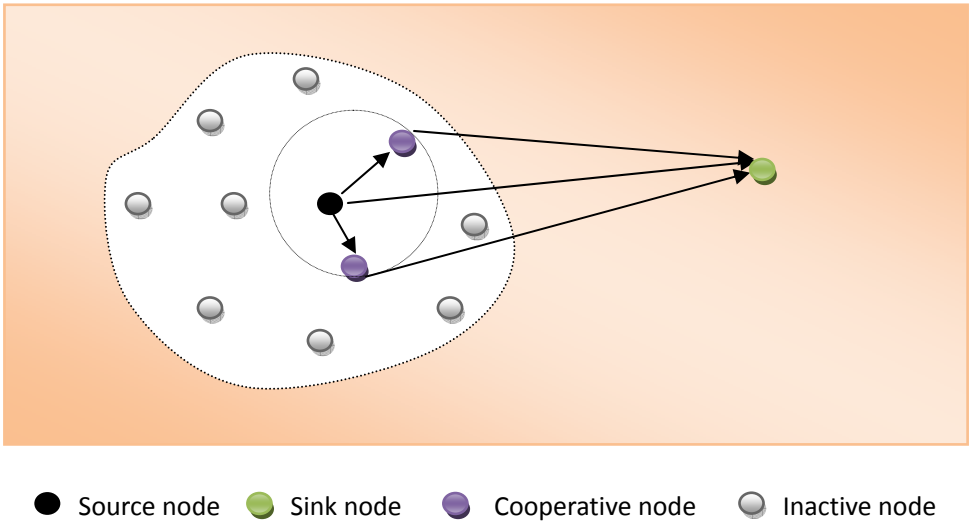

Figure 3-3 One-hop cluster-based cooperative transmission mode

In figure 3-3, if a source node has gathered information to transmit, it first broadcasts the data within the cluster it belongs to, which is called intra-cluster (ITA) transmission. Some of its neighbours within the same cluster are wakened and selected as the cooperative nodes. Then the cooperative nodes, together with the source node, form a virtual MIMO transmission to the destination, which is named inter-cluster (ITE) transmission. As there is only one hop to the sink node shown in figure 3-3, this virtual MIMO channel is actually a MISO channel. Sensors not selected as the cooperative nodes within the source cluster remain sleeping or inactive.

An obvious question that rises in this mode is how to select the cooperative nodes. The selection criterion can be geographical distance or more practically path-loss between the source and the sink nodes, which will be discussed in the following chapters. Another question here is how many cooperative nodes should be selected. Although more cooperative nodes can form a more reliable MISO link, it is no good selecting as many cooperative nodes as possible, for more nodes wakened means more energy consumed and the lifetime of the whole network will be shortened. There should be a tradeoff between the energy-efficiency and the communication reliability. Comparisons for different numbers of cooperative nodes will also be discussed in following chapters of this thesis.

Similar to the SISO transmission mode, when the transmission distance is far enough, multi-hop transmissions can be also adopted for cluster-based cooperative mode [91]. Depending on an information exchange phase occurring in each of the relaying clusters, the multi-hop cluster-based cooperative transmission has two kinds of structures.

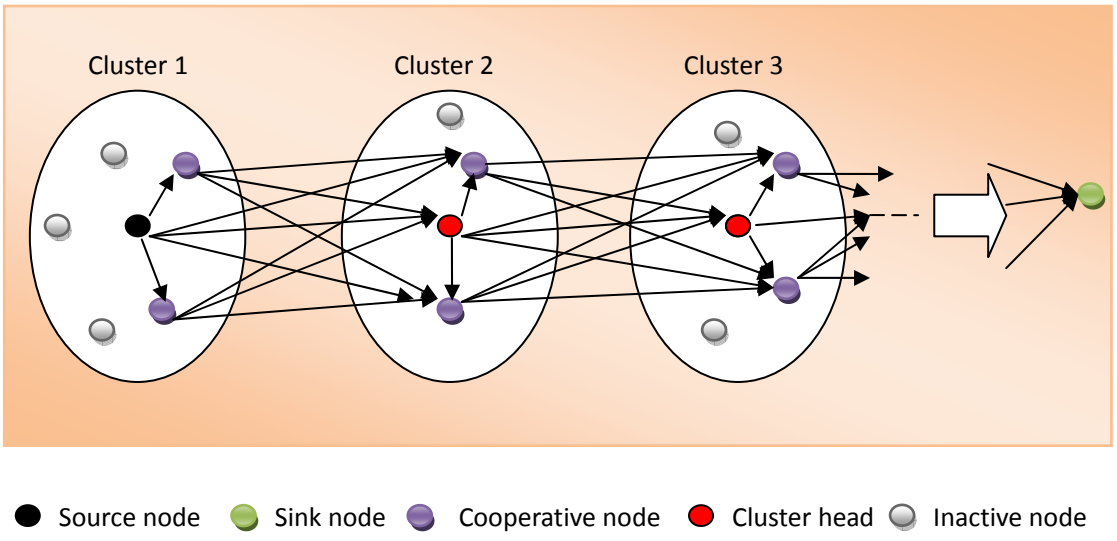

Figure 3-4 Multi-hop cluster-based cooperative transmission with data exchange

Figure 3-4 shows the structure of multi-hop cluster-based cooperative transmission with data exchange in each relaying cluster. The transmission process is described in more detail as follows.

Based on a time-division scheme, the source node first encodes the information and broadcasts it with power p_1 within the cluster in an intra-cluster time slot (ITA). When the selected cooperative nodes receive the information, they re-encoded it together with the source node and transmit it to the relaying cluster (cluster 2) on a cooperative MIMO channel with power P_1 in an inter-cluster time slot (ITE). Space-time coding can be used here. The local distance within the cluster and the distance between these two clusters can be represented as d_{ITA} and d_{ITE} respectively. In the first relaying cluster (cluster 2), a number of cooperative nodes receive the information and decode it. The one with the highest SNR among these cooperative nodes is then selected as the cluster-head of cluster 2 and repeats the actions of the source node in cluster 1. Firstly, in an intra-cluster time slot, it broadcasts the information with power p_2 to the other cooperative nodes. Then these nodes combine this broadcasted information with that received in last hop to make a

decision or perform error correction. This phase is called data exchange. After that, all the cooperative nodes and the cluster-head re-encode the data and form a cooperative MIMO transmission to the next cluster (cluster 3) with power P_2 in an inter-cluster time slot. This process in cluster 2 is repeated cluster by cluster until the last relaying cluster forms a cooperative MISO link to the sink node.

The advantage of this structure is that by data exchange, each relaying cluster can do error correction for the former hop and utilize STBCs to form a more reliable cooperative MIMO transmission for the next hop. However, one point needs to be stated here is that for each relaying cluster, it is assumed that the cooperative receiving nodes are already known before the transmission, which is a little bit unreasonable in practice since there is no existing algorithm to select and preset these cooperative nodes. In addition, the selection scheme for the cluster-head in each relaying cluster is complicated, for there exists an enquiry phase among the cooperative nodes to decide which one has the highest SNR. To avoid this cluster-head selection phase, one possible transform of the structure discussed above is to operate the scheme without data exchange in each relaying cluster, as shown in figure 3-5 [92].

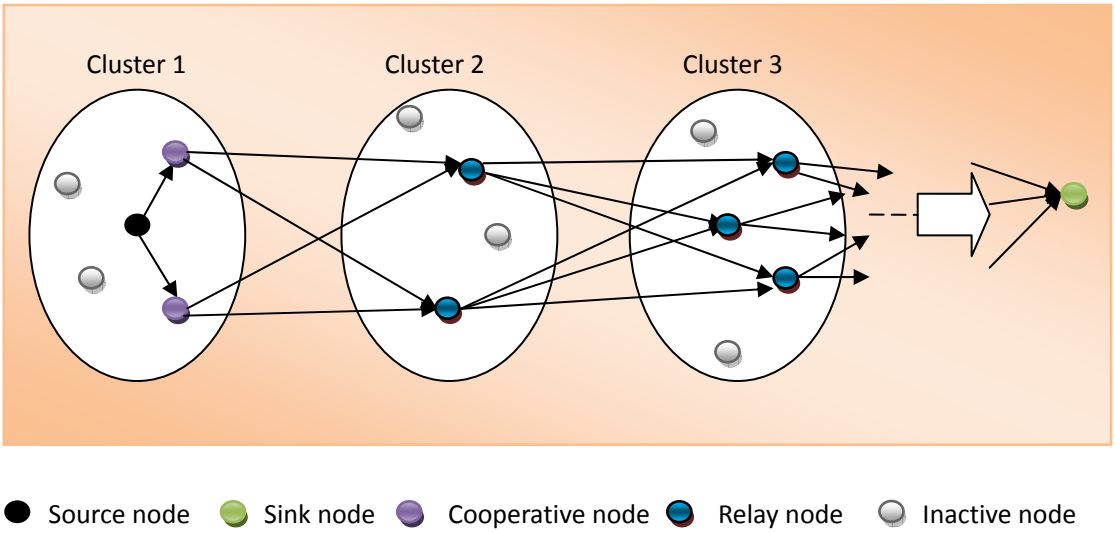

Figure 3-5 Multi-hop cluster-based cooperative transmission without data exchange

In the structure of figure 3-5, each relay node receives copies of the information stream from last hop and makes a decision independently. There is no cluster-head selection scheme needed in each relaying cluster and no data exchange happens. As a

result, STBCs are not applicable for each relaying cluster. Each relay node performs a cooperative SIMO transmission for the next hop. Since the inter-cluster transmission distances are relatively long, SIMO channel links between relaying clusters are vulnerable and frequently experience deep fades. Then errors that occur during the decision phase of one relay node can accumulate in the following hops and decrease the communication reliability. Although this structure exploits more special multiplexing gain than a multi-hop SISO system, it is fundamentally a decision-and-broadcast system and doesn't fully utilize the advantages of cooperative MIMO.

In addition, similar to the former structure discussed (figure 3-4), it doesn't solve the presetting problem of the relaying cooperative nodes as well. Therefore, to avoid the selection of receiving cooperative nodes for each relaying cluster and utilize the advantages of cooperative techniques, another multi-hop structure is proposed for wireless sensor networks that have clusters with cluster-head, namely cooperative MISO, as shown in figure 3-6 [93].

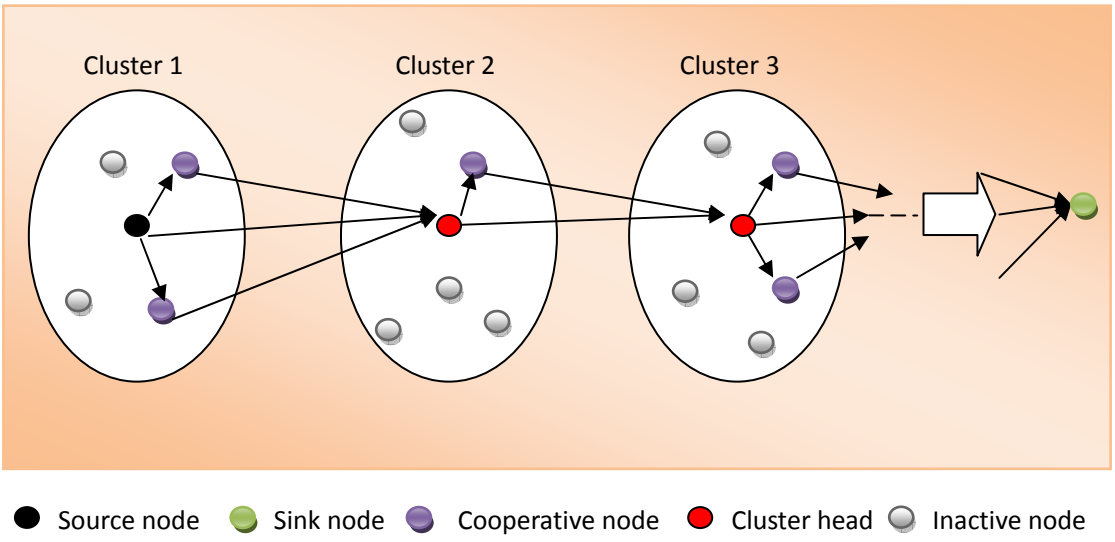

Figure 3-6 Multi-hop cluster-based cooperative MISO transmission

Figure 3-6 shows the structure of a multi-hop cluster-based cooperative MISO transmission system. This system assumes that all the relaying clusters have their own cluster-head, selected either by the remaining energy or the specially designed physics (in an inhomogeneous network, cluster-heads are designed with more energy and more complicated structure). The broadcasting phase in cluster 1, during the

intra-cluster time slot, is the same as that for the other cluster-based transmission structures, but during the inter-cluster time slot, the cooperative nodes together with the source node form a cooperative MISO, not MIMO, channel to communicate with the cluster-head of cluster 2. Then the cluster-head of cluster 2 repeats the same time-divided phases as the source node in cluster 1 and the information is transmitted in a multi-hop way with each hop operating in MISO mode until reaching the sink node.

This cooperative MISO mode also has the data exchange phase in each relaying cluster and STBCs can be adopted to increase the communication reliability. This structure avoids the presetting of receiving cooperative nodes in each relaying cluster and only the cluster-head is selected to receive the signal from last cluster. In a homogeneous WSN, where the sensor nodes are all the same in physical structure, these cluster-heads can be selected by any of the cluster forming and routing algorithms discussed in chapter 2. In an inhomogeneous WSN, sensors designed with more energy and capabilities can be chosen as the cluster-heads.

The algorithm for selection of cooperative transmitting nodes for each relaying cluster is based on the location of the cluster-head, which will be proposed in following chapters. Compared to cooperative MIMO, this cooperative MISO structure may sacrifice some diversity gain because there is only one node at the receiving side, but in return, it may save more energy due to the simplicity. In the following section, an energy consumption model for the sensor node is introduced. Detailed energy consumption analysis and energy equations for each transmission mode will be given later as well.

3.2 Energy Consumption Model

The energy consumption of a wireless sensor transmission system is composed of two parts: the transmitting energy used for signal emitting and the circuit energy used for signal processing within the sensor node. References [70~74] have already revealed that for long distance communication, the transmitting energy is the dominant part of the total system energy consumption, however, for relatively short distance

communication, the circuit energy consumption cannot be omitted and may even be of the same order as the transmitting one. Therefore, an investigation into the system energy consumption from a global view is needed and is the main task in this section.

A typical RF system with functional blocks in both the transmitter and the receiver is shown in figure 3-7. [71]

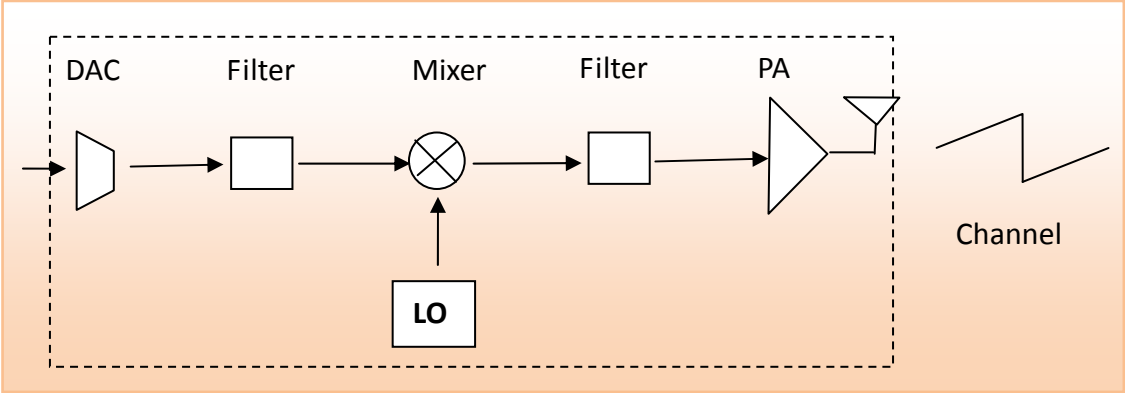

Figure 3-7 (i) Functional blocks in the transmitter

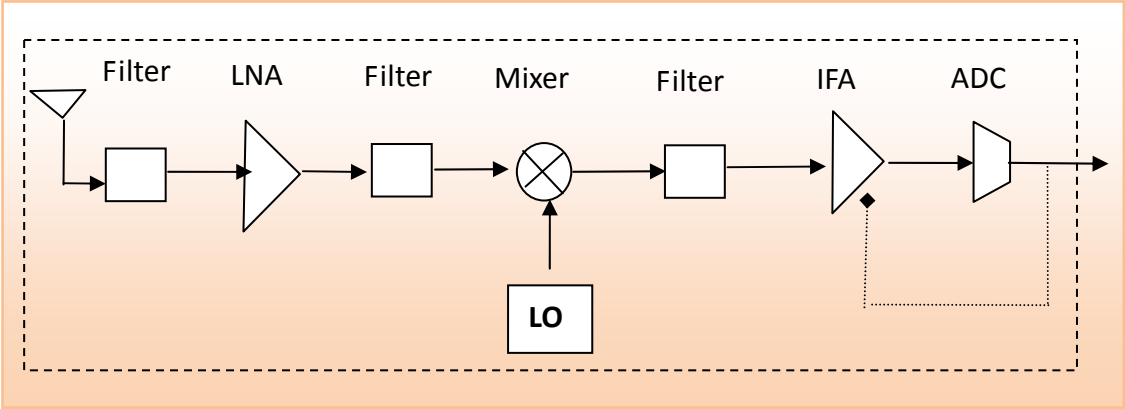

Figure 3-7 (ii). Functional blocks in the receiver

In figure 3-7, DAC, PA, LO, LNA, IFA, and ADC represent the blocks of digital-analog converter, power amplifier, local oscillator, low noise amplifier, intermediate frequency amplifier, and analog-digital converter. To keep the model from becoming over-complicated, no baseband signal processing and error correction blocks are considered.

3.2.1 Transmitting Energy

The total power consumption of this RF system along the signal path consists of two components: the power consumed in the amplifiers P_{PA} and the power consumed in all the other circuit blocks P_c. The first term P_{PA} is decided by the transmitting power P_{tran} [94]:

$$P_{PA} = (1+\varepsilon)P_{tran} \tag{3.3}$$

where $\varepsilon = \xi / \eta - 1$ with η the drain efficiency of the RF power amplifier [95] and ξ the Peak-to-Average Ratio which depends on the modulation scheme and the associated constellation size [87].

When squared power path loss is considered, P_{out} can be calculated by the link budget relationship as [94]:

$$P_{tran} = \bar{E}_b \times \frac{R_b (4\pi d)^2}{G_t G_R \lambda^2} M_l N_f \tag{3.4}$$

where $\bar{E}_b$ is the mean required energy per bit at the receiver for a given BER requirement. R_b is the bit rate of the RF system. d is the transmitting distance. G_t and G_R are the antenna gain of the transmitter and the receiver respectively. λ is the wavelength of the signal. M_l is the link margin compensating the hardware process variations and other additive background noise or interference. N_f is the receiver noise figure defined as $N_f = (N_s / N_0)$ with N_s as the power spectral density of the total effective noise at input of the receiver and N_0 as the power spectral density of the single-sided thermal noise [71][94].

3.2.2 Circuit Energy

According to the structure of a RF system in figure 3-7, the circuit power consumption at a transmitter can be calculated as [71][94]:

$$P_{ct} = P_{DAC} + P_{mix} + P_{fil} + P_{syn} \tag{3.5}$$

Similarly, the circuit power consumption at a receiver can be calculated as [71][94]:

$$P_{cr} = P_{LNA} + P_{mix} + P_{IFA} + P_{fil} + P_{ADC} + P_{syn} \tag{3.6}$$

To estimate the power level for each block, expressions have been adopted from a number of references. The parameter of P_{DAC} can be obtained from the binary-weighted current-steering DAC model proposed in [96]. P_{ADC} can be evaluated by the Nyquist-rate ADC model proposed in [97]. Other parameters such as P_{mix}, P_{fil}, P_{syn}, P_{LNA}, and P_{IFA} can be approximated as constants and are quoted from some publications [98~105].

For a general MIMO link with n_t transmitters and n_r receivers, the circuit power consumption along the signal path can be written as:

$$P_c = n_t \cdot P_{ct} + n_r \cdot P_{cr} \tag{3.7}$$

So based on (3.3) to (3.7), the total energy consumption per bit for a MIMO communication with fixed data can be expressed as:

$$E_{bt\_MIMO} = \frac{P_{PA} + P_c}{R_b}$$

$$= (1+\varepsilon) \cdot \bar{E}_b \times \frac{(4\pi d)^2}{G_t G_R \lambda^2} M_l N_f + \frac{n_t \cdot (P_{DAC} + P_{mix} + P_{fil} + P_{syn})}{R_b}$$

$$+ \frac{n_r \cdot (P_{LNA} + P_{mix} + P_{IFA} + P_{fil} + P_{ADC} + P_{syn})}{R_b} \tag{3.8}$$

3.2.3 Energy Equations for Different Transmission Modes

Based on the energy model discussed above, the energy equations for different transmission modes in wireless sensor network, such as SISO, cluster-based cooperative MIMO, and cluster-based cooperative MISO can be derived. For a fair comparison, the transmission distance in a SISO mode equals to the distance between two relaying clusters in the cluster-based modes, denoted as d_{ITE}. The transmission distance within the cluster is denoted as d_{ITA}.

In one-hop SISO mode, shown in figure 3-1, there is only one transmitter and one receiver corresponding to one P_{ct} and one P_{cr} in the duration of T for a data packet transmission. Here we set T=1s. The total energy consumption per bit in this mode can be written as:

$$E_{bt\_SISO} = \frac{P_{PA} + P_{ct} + P_{cr}}{R_b}$$

$$= (1+\varepsilon)\cdot \bar{E}_b \times \frac{(4\pi d_{ITE})^2}{G_t G_R \lambda^2} M_l N_f + \frac{P_{DAC} + P_{mix} + P_{fil} + P_{syn}}{R_b}$$

$$+ \frac{P_{LNA} + P_{mix} + P_{IFA} + P_{fil} + P_{ADC} + P_{syn}}{R_b} \tag{3.9}$$

In one-hop cluster-based cooperative MIMO mode described in figure 3-4, there are two parts of transmitting energy consumption corresponding to the distances of d_{ITA} in the intra-cluster phase and d_{ITE} in the inter-cluster phase respectively. The circuit energy consumptions in these two phases are also different. Considering an $n_t \times n_r$ cooperative MIMO link, there should be one transmitter and r $(r = n_t - 1)$ receivers in the intra-cluster broadcasting phase, while n_t transmitters and n_r receivers in the inter-cluster transmission phase. The total energy consumption per bit in this mode can be written as:

$$E_{bt\_Co\_MIMO} = \frac{P_{PA\_ITA} + P_{PA\_ITE} + t_1 \cdot [P_{ct} + (n_t - 1)P_{cr}] + t_2 \cdot (n_t \cdot P_{ct} + n_r \cdot P_{cr})}{R_b}$$

$$= (1+\varepsilon)\cdot \bar{E}_{b\_ITA} \times \frac{(4\pi d_{ITA})^2}{G_t G_R \lambda^2} M_l N_f + (1+\varepsilon)\cdot \bar{E}_{b\_ITE} \times \frac{(4\pi d_{ITE})^2}{G_t G_R \lambda^2} M_l N_f$$

$$+ (t_1 + t_2 \cdot n_t)\cdot \frac{P_{DAC} + P_{mix} + P_{fil} + P_{syn}}{R_b}$$

$$+ [t_1 \cdot (n_t - 1) + t_2 \cdot n_r]\cdot \frac{P_{LNA} + P_{mix} + P_{IFA} + P_{fil} + P_{ADC} + P_{syn}}{R_b} \tag{3.10}$$

where t_1 and t_2 $(t_1 + t_2 \le T)$ are the time slots allocated to the intra-cluster and inter-cluster phases. $\bar{E}_{b\_ITA}$ and $\bar{E}_{b\_ITE}$ represent the received energy per bit for a

given BER requirement in the ITA and ITE slot respectively.

The one-hop cluster-based cooperative MISO mode described in figure 3-6 can be viewed as a special example of cooperative MIMO with $n_r = 1$. Its expression of total energy consumption per bit can be written as:

$$E_{bt\_Co-MISO} = \frac{P_{PA\_ITA} + P_{PA\_ITE} + t_1 \cdot [P_{ct} + (n_t - 1)P_{cr}] + t_2 \cdot (n_t \cdot P_{ct} + P_{cr})}{R_b}$$

$$= (1+\varepsilon) \cdot \bar{E}_{b\_ITA} \times \frac{(4\pi d_{ITA})^2}{G_t G_R \lambda^2} M_l N_f + (1+\varepsilon) \cdot \bar{E}_{b\_ITE} \times \frac{(4\pi d_{ITE})^2}{G_t G_R \lambda^2} M_l N_f$$

$$+ (t_1 + t_2 \cdot n_t) \cdot \frac{P_{DAC} + P_{mix} + P_{fil} + P_{syn}}{R_b}$$

$$+ [t_1 \cdot (n_t - 1) + t_2] \cdot \frac{P_{LNA} + P_{mix} + P_{IFA} + P_{fil} + P_{ADC} + P_{syn}}{R_b} \qquad (3.11)$$

In multi-hop situations with *m* as the number of hops, the total energy per bit is *m* times of the equations discussed above for each mode.

For fixed d_{ITA} and d_{ITE} in (3.10) and (3.11), different power levels at the transmitter side in ITA and ITE phases can generate different $\bar{E}_{b-ITA}$ and $\bar{E}_{b-ITE}$, which then affect the transmitting energy consumption of the whole system. To compare with the SISO mode, there should be a power level allocation between the ITA and ITE phases to minimize the value of transmitting energy under a fixed bit-error-rate requirement. In respect of the circuit energy, it can be seen from the equations that the circuit energy is decided by parameters of n_t, n_r, as well as t_1 and t_2. In addition, the data throughput in a time-division system is largely dependent on the allocation of t_1 and t_2. So, before comparing these transmission modes, a time slot allocation framework for the ITA and ITE phases is also needed. These allocations of power level and time slot for ITA and ITE phases will be discussed in Chapter 4. Based on the allocation framework, a detailed comparison of these modes in single-hop transmission will be made in Chapter 5. Then in Chapter 6, the situation of multi-hop will be discussed.

Chapter 4
Resource Allocation for Cluster-based Cooperative Communication

In Chapter 3, several transmission modes for wireless sensor networks have been introduced, of which the cluster-based cooperative transmission is the focus of this thesis. All the transformations of the cluster-based modes include an intra-cluster broadcasting phase and an inter-cluster transmitting phase either in the first hop or the intermediate relaying hops. As the local cluster size is different, usually much shorter, from the distance between two clusters, the power needed to maintain a level of communication reliability in these two phases should not be the same. The power level allocation for the intra-cluster and the inter-cluster communications needs to be determined. In addition, based on the time division scheme adopted and the energy equations derived in the last chapter, the end-to-end data throughput and the circuit energy consumption of the whole scheme has a strong relationship with the duration of these two time slots. Thus time slot allocation also needs to be considered in this mode. The allocations for power and time slots constitute the resource allocation.

Several schemes to solve similar resource allocation problems have already been proposed by others. In [106~108], capacity regions for different kinds of fading channels and their corresponding optimal power allocation strategies are analyzed. However, these strategies only achieve the capacity bound of downlink broadcasting channels by optimally allocating power to each sub-link. They do not consider MIMO channels and multi-hop situations. [109] proposed an explicit numerical optimisation for power allocation in distributed MIMO channels, but still didn't solve the relationship of power levels between intra-cluster and inter-cluster phases in this cluster-based transmission model. Reference [28] proposed a mathematical expression for joint power and time slot allocation, however it is a multi-dimensional function and there is no closed form expression for both the power and time slot allocation. In addition, the formula in [28] takes the minimum outage probability in inter-cluster

phase as the only criterion for system optimization, the broadcasting channels in intra-cluster phase and the data throughput of the whole system are not considered.

Another thing to note is that none of these references above consider both the transmitting energy and the circuit energy when managing power allocation. The common method in these publications is to only consider the transmitting energy. However, as circuit energy cannot be omitted, it is unfair to compare SISO with cluster-based cooperative MIMO on this basis.

Therefore, it is the aim in this chapter to propose a new resource allocation framework for cluster-based cooperative MIMO transmission with, and without, accounting for the circuit energy. This framework can maximize the data throughput and at the same time maintain a level of communication reliability by optimally assigning time fractions and power levels for intra-cluster and inter-cluster phases,

This chapter is organised as follows. In Section 4.1, the underlying mathematics for wireless channels in both intra-cluster and inter-cluster phases are introduced. For broadcasting channels in the intra-cluster phase, the channel capacity is the main focus, while for cooperative MIMO channels in inter-cluster phase, it is the outage probability that is of concern. Based on this, a resource allocation framework for cluster-based cooperative communication is proposed in Section 4.2, which can support a reliable, maximum data throughput communication for the whole system. For different situations like single data packet communication, full duplex continuous communication, and half duplex continuous communication, different time division models are shown in this section corresponding to different resource allocation frameworks. The power allocation framework proposed here considers the situations when circuit energy consumption is ignored, and when it is taken into account. The simulations and results discussion for all these situations are shown in Section 4.3. Then Section 4.4 sums up this chapter.

4.1 Underlying Mathematics

Consider a single relaying hop of the cluster-based cooperative MIMO mode with data exchange, shown in figure 3-4. Let a transmitting cluster (TxC) composed of N_t nodes communicate with a N_r-node-receiver cluster (RxC). n_t and n_r are the active cooperative sensors in TxC and RxC respectively, where $2 \le n_t \le N_t$, $n_r \le N_r$. The time-division scheme for this communication is shown in the following figure.

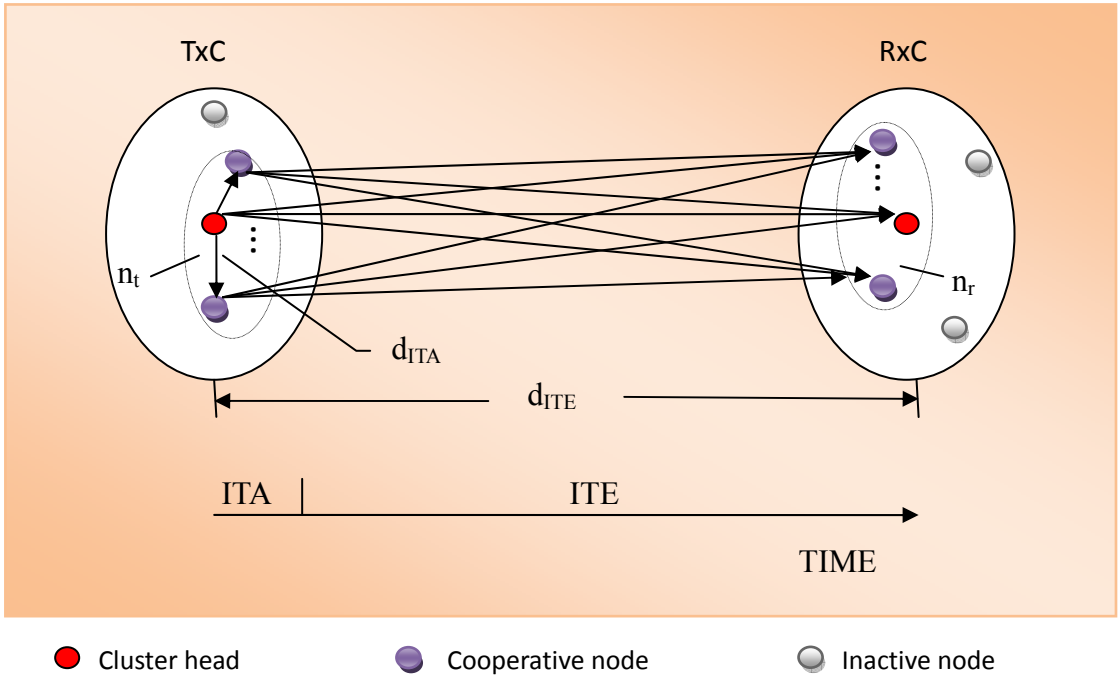

Figure 4-1. Time-division scheme for single-hop cooperative MIMO Communication

In figure 4-1, ITA and ITE represent the intra-cluster broadcasting and inter-cluster transmission time slots respectively. Correspondingly, d_{ITA} and d_{ITE} represent the distances for the intra-cluster transmission and inter-cluster transmission. As $d_{ITA} \ll d_{ITE}$ and because of the spatial separation of the sensor nodes within the cluster, the broadcasting channel during the ITA slot can be assumed to be an ergodic SIMO channel with Rician fading. A light-of-sight (LoS) path exists for each sub-channel. The cluster-head is assumed to know the full channel-state-information (CSI) within the cluster. However, for the inter-cluster transmission, because of the longer transmission distance and the possibility of multipath propagation with no dominant LoS signal, the channel for the ITE time slot can be modelled as an ergodic MIMO channel with Rayleigh fading. There is no assumption of the CSI being known between these two clusters. Factors of path loss and outage probability need to be

considered in this communication.

For the SIMO broadcast in the ITA slot, the channel capacity can be written as follows based on (2.17) [109]:

$$C_{SIMO\_fullCSI} = E_H \left\{ \mathbf{log}_2 \, \mathbf{det}\left(I_r + \rho \mathbf{H}\mathbf{H}^H \right) \right\} \tag{4.1}$$

where $r = n_t - 1$ is the number of cooperative nodes receiving signal during the broadcasting slot. ρ is the average SNR per antenna at each cooperative node and $\mathbf{H}$ is the impulse response matrix for the SIMO channel. $[\cdot]^H$ denotes the Hermitian transpose. For only one transmitter, the cluster-head broadcasts in this time slot, and there is only one eigenvalue of $\mathbf{H}\mathbf{H}^H$. Inserting the joint probability density function (PDF) of this eigenvalue derived from reference [16], the SIMO channel capacity with full CSI can be written as [109]:

$$C_{1\times r} = \hat{C}_{r-1}(\rho) / \Gamma(r) \tag{4.2}$$

where $\Gamma(n)$ is the Gamma Function: $\Gamma(n) = (n-1)!$ for $n \in N$. $\hat{C}_\zeta(a)$ is referred to as the Capacity Integral with the expression [109]:

$$\hat{C}_\zeta(a) \triangleq \int_0^\infty \mathbf{log}_2(1+ax) x^\zeta e^{-x} dx \tag{4.3}$$

$\hat{C}_\zeta(a)$ has a closed form deduced in [109][110]:

$$\hat{C}_\zeta(a) = \sum_{\mu=0}^{\zeta} \frac{\zeta!}{(\zeta-\mu)!} [(-1)^{\zeta-\mu-1} (\frac{1}{a})^{\zeta-\mu} e^{1/a} Ei(\frac{-1}{a})$$

$$+ \sum_{k=1}^{\zeta-\mu} (k-1)! (\frac{-1}{a})^{\zeta-\mu-k}] \tag{4.4}$$

As for the cooperative MIMO transmission in the ITE slot, due to the long distance transmission, a given transmission rate Φ may not always be supported by the channel $\mathbf{H}$. Thus outage probability is the main concern in this situation. When Rayleigh fading is considered, and assuming all sub-channel gains for the cooperative MIMO transmission are equal, $\gamma_1 = \cdots = \gamma_{n_t}$, the outage probability for one sensor node at the receiver side can be derived as follows [19].

$$P_{out}(\Phi) = \frac{1}{\Gamma(n_t)} \Upsilon\left(n_t, (2^{\Phi} - 1) \cdot \frac{n_t / \gamma}{\rho} \right) \tag{4.5}$$

where $\Upsilon(\cdot)$ is the lower incomplete Gamma function [109][111].

$$\Upsilon(s, x) = \int_0^x t^{s-1} e^{-t} dt \tag{4.6}$$

When a Space-Time Block Code (STBC) with code rate R ($0 < R \leq 1$, R=1 only when the Alamouti scheme is used) is applied, the normalised capacity for a MIMO channel with equal sub-channel gain γ can be expressed as [112]

$$C_{MIMO\_STBC} = R \log_2 (1 + \frac{1}{R} \cdot \frac{\gamma}{n_t} \cdot \rho) \tag{4.7}$$

If outage arises, the outage probability for a given desired communication rate (bits/s/Hz) can be written as:

$$P_{out}(\Phi) = \Pr(R \cdot \log_2 (1 + \frac{1}{R} \cdot \frac{\gamma}{n_t} \cdot \rho) < \Phi) \tag{4.8}$$

Similar to (4.5), by some changes in variables, the outage probability for cooperative MIMO channels using STBCs can be rewritten as [113]:

$$P_{out}(\Phi) = \frac{1}{\Gamma(n_t)} \Upsilon\left(n_t, \left(2^{\Phi/R} - 1\right) \cdot \frac{n_t / \gamma}{\rho} \cdot R \right) \tag{4.9}$$

Based on the formulas (4.4) and (4.9) discussed above, a power and time slot allocation framework can be derived in the following section.

4.2 Resource Allocation Framework

4.2.1 Time Slot Allocation

Before we derive the resource allocation framework, the time-division models for single packet transmission, half duplex continuous communication, and full duplex

continuous communication should be discussed first, which require different time slot allocation frameworks.

For single packet transmission, each cluster goes into a sleep state after they transfer the information packet to the next cluster. So the time slot allocation mainly focuses on the intra-cluster and inter-cluster phases for each hop. Let a uniform parameter α ($0 \le \alpha < 1$) representing the fraction of time for ITA slots, then the fraction of time for ITE slots can be expressed as $1-\alpha$. If $\alpha = 0$, the cluster-based transmission degrades to multi-hop SISO transmission. The time-division scheduling is shown in figure 4-2.

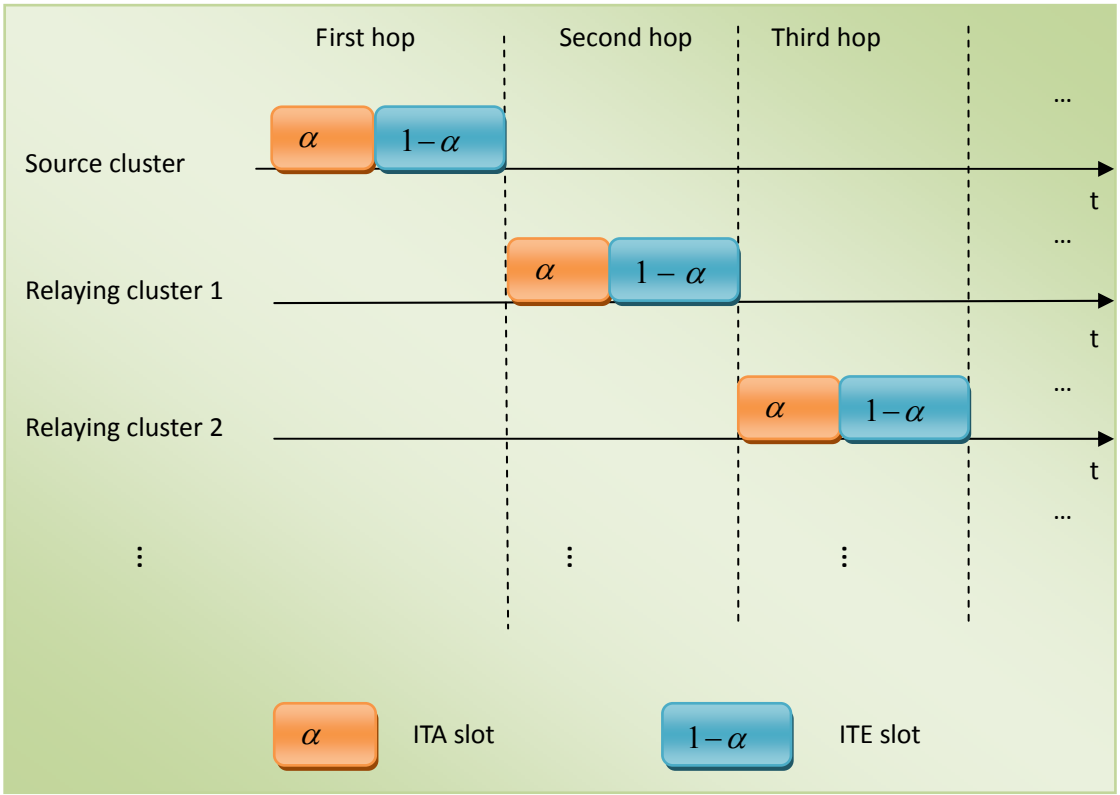

Figure 4-2 Time-division model for single packet transmission

If the sensor antenna operates in a half duplex mode, it cannot receive and transmit data at the same time. Thus the receiving phase for each relaying cluster shouldn't be omitted and the duration of this phase is equal to the ITE slot of the last cluster. Assuming α as the ITA slot and all the clusters operate the same time allocation framework, the ITE slot needs to be divided into two parts, both of length $(1-\alpha)/2$.

The time-division scheduling for the half duplex continuous communication is shown in the following figure.

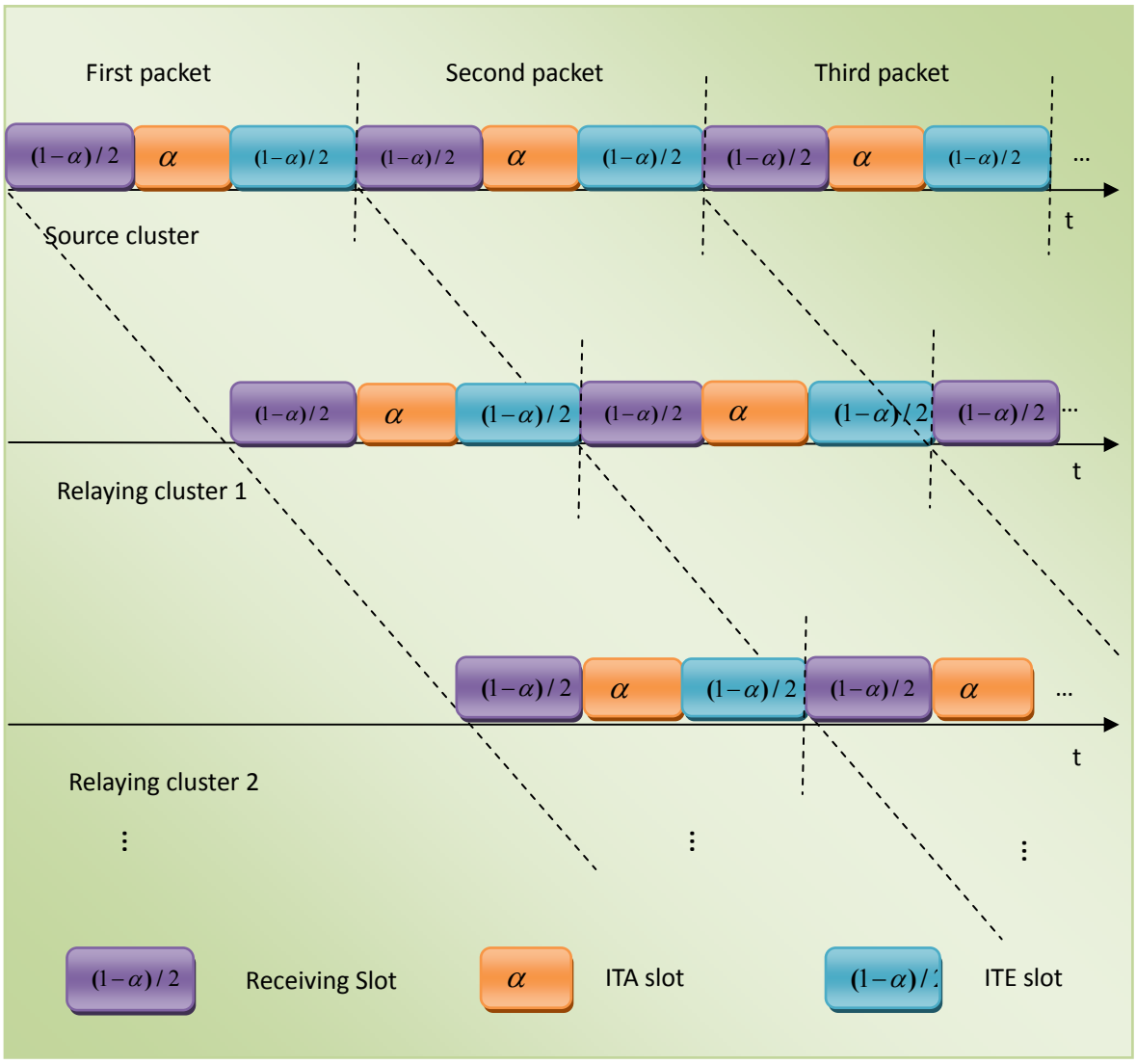

Figure 4-3 Time-division model for half duplex continuous communication

It can be seen in figure 4-3 that in continuous half duplex communication, each relaying cluster has three time slots, which are the ITE receiving slot, the ITA slot, and ITE transmission slot in order. The cycle of packet processing for each cluster starts at the ITE slot of the former one, so the intra-cluster and inter-cluster phases are not synchronized among clusters.

If the sensor antennas work in a full duplex way, each of them can simultaneously receive and transmit data. In this situation, there is no need for relaying clusters to

assign a time slot for information receiving specially. The time slot allocation of this method is similar to that of the single packet transmission but in a continuous way where receiving phase is considered. This is shown in figure 4-4.

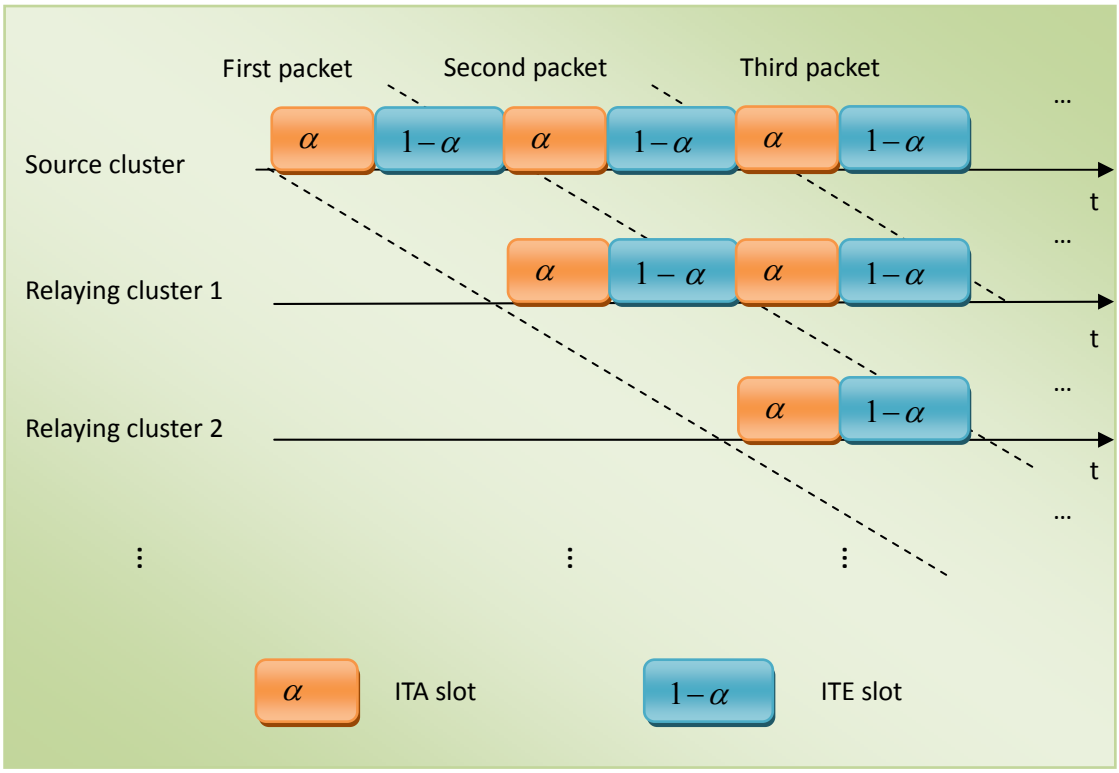

Figure 4-4 Time-division model for full duplex continuous communication

In figure 4-4, it is shown that in full duplex continuous communication, only ITA and ITE slots need to be considered for time allocation. The ITA and ITE slots for all the clusters in the network are synchronized. The ITE slot in each relaying cluster is used for the receiving phase of the last hop as well as the inter-cluster transmitting phase of the next hop.

The aim for time slot allocation is to maximize the end-to-end data throughput. Let the maximum symbol rate of a sensor antenna be Φ (symbol/s) and assume all the antennas within the network work at the highest symbol rate Φ. In the situation of single packet transmission or full duplex communications, the maximum data throughput of the ITA slot for one hop equals $\Phi \cdot R_{\text{intra}} \cdot \alpha \cdot T$ (bit/s), where T is the processing duration of one data packet in the relaying cluster, $R_{\text{intra}} > 0$ is the modulated code rate in intra-cluster phase. Given the STBC with code rate R_{inter}

used in cooperative MIMO communication, the data throughput of the ITE slot is $R_{\text{inter}} \cdot \Phi \cdot (1-\alpha) \cdot T$. To waste no useful information, the data throughput of the two phases should be the same and equal to the overall data throughput of the single-hop system. Then the following equation is derived,

$$\Phi'_{full-duplex} = R_{\text{inter}} \cdot \Phi \cdot (1-\alpha) \cdot T = \Phi \cdot R_{\text{intra}} \cdot \alpha \cdot T \tag{4.10}$$

Φ' represents data throughput. From (4.10), it can be obtained that

$$\alpha = \frac{R_{\text{inter}}}{R_{\text{inter}} + R_{\text{intra}}} \tag{4.11}$$

and

$$\Phi'_{full-duplex} = \frac{R_{\text{inter}} \cdot R_{\text{intra}}}{R_{\text{inter}} + R_{\text{intra}}} \cdot \Phi \cdot T \tag{4.12}$$

As the STBCs code rate R_{inter} satisfy $R_{\text{inter}} \le 1$ [34], $\alpha \le 1/(1+R_{\text{intra}})$. (4.12) is maximised only when $R_{\text{inter}} = 1$ (the Alamouti scheme).

$$\Phi'_{\max-full-duplex} = \frac{R_{\text{intra}}}{1+R_{\text{intra}}} \Phi \cdot T, \text{ (when } R_{\text{inter}} = 1) \tag{4.13}$$

In half duplex continuous communication, the data throughput of the ITE slot is $R_{\text{inter}} \cdot \Phi \cdot (1-\alpha)/2$. The overall data throughput for the single-hop system can be written as

$$\Phi'_{half-duplex} = R_{\text{inter}} \cdot \Phi \cdot \frac{(1-\alpha)}{2} \cdot T = \Phi \cdot R_{\text{intra}} \cdot \alpha \cdot T \tag{4.14}$$

from which α can be obtained as:

$$\alpha = \frac{R_{\text{inter}}}{R_{\text{inter}} + 2R_{\text{intra}}} \tag{4.15}$$

So (4.14) can be rewritten as:

$$\Phi'_{semiduplex} = \frac{R_{\text{inter}} \cdot R_{\text{intra}}}{R_{\text{inter}} + 2R_{\text{intra}}} \cdot \Phi \cdot T \le \frac{R_{\text{intra}}}{1+2R_{\text{intra}}} \Phi \cdot T, \text{ (when } R_{\text{inter}} = 1) \tag{4.16}$$

It can be seen from (4.13) to (4.16) that the time allocation for ITA and ITE slots is dependent on the code rate R_{intra} used for intra-cluster broadcasting modulation and R_{inter} of STBCs used in inter-cluster cooperative MIMO communication. R_{intra} is a

preset parameter decided by the modulation code used for the broadcasting within the cluster. The maximum data throughput of the system can be achieved only when the Alamouti scheme is adopted for a fixed R_{intra}, which means two cooperative transmitters for the inter-cluster transmission has the advantage in data throughput than more transmitting antennas. When the symbol rates in intra-cluster and inter-cluster phases are different and lower than Φ, the time allocation parameter α will vary according to the symbol rates and the system data throughput will be lower.

4.2.2 Power Level Allocation

As the local cluster size is usually shorter than the distance between clusters, the transmitting power levels for intra-cluster and inter-cluster transmission shouldn't be the same and can be defined to save energy under certain requirement of communication reliability. This power allocation framework is proposed based on the comparison with the single-hop SISO transmission. Depending on whether or not the circuit energy consumption is taken into account, this framework has two expressions.

- Without consideration of circuit energy

In this situation, it is assumed that all the available energy is used for transmitting only, which is a common assumption in recent research publications. To make a fair comparison, the total transmitting energy consumption of the whole cluster-based single-hop cooperative transmitting system should be set the same as that of the single-hop SISO mode. Assuming the average transmitting power of an antenna in SISO mode for full duplex communication is *P* and for half duplex communication it is P', $P \cdot T$ and $P' \cdot T/2$ are the transmitting energy consumption in one packet processing duration for full and half duplex communication respectively. Then the problem of power allocation for the cluster-based cooperative system transforms to the one of transmitting energy allocation for the ITA and ITE phases with the same total value of the corresponding SISO mode.

By introducing a fraction energy allocation parameter $\beta (0 \le \beta \le 1)$, the energy used for full duplex transmitting in the intra-cluster phase is $P \cdot T \cdot \beta$ ($P' \cdot \beta \cdot T/2$ for the half duplex communication) and that in the inter-cluster phase is $P \cdot T \cdot (1-\beta)$ ($P' \cdot (1-\beta) \cdot T/2$ for the half duplex communication). The resource allocation

expressions and data throughput for each time slots and the whole system compared with a SISO mode are listed in table 4-1 and 4-2 for completeness.

Table 4-1 Parameter expressions for single packet or full duplex continuous communication without consideration of circuit energy

	Intra-cluster Phase	Inter-cluster Phase	Whole System	SISO Mode
Transmitting Energy Consumption	$P \cdot T \cdot \beta$	$P \cdot T \cdot (1-\beta)$	$P \cdot T$	$P \cdot T$
Time Slot	$\alpha \cdot T$	$(1-\alpha) \cdot T$	T	T
Transmitting Power	$\frac{P \cdot \beta}{\alpha}$	$\frac{P \cdot (1-\beta)}{1-\alpha}$	P	P
Date Rate	$\Phi \cdot R_{\text{intra}}$	$\Phi \cdot R_{\text{inter}}$	$\frac{R_{\text{intra}} \cdot R_{\text{inter}}}{R_{\text{inter}} + R_{\text{intra}}} \cdot \Phi$	$\Phi \cdot R_{\text{intra}}$
Date Throughput	$\Phi \cdot R_{\text{intra}} \cdot \alpha \cdot T$	$\Phi \cdot R_{\text{inter}} \cdot (1-\alpha) \cdot T$	$\frac{R_{\text{intra}} \cdot R_{\text{inter}}}{R_{\text{inter}} + R_{\text{intra}}} \cdot \Phi \cdot T$	$\Phi \cdot R_{\text{intra}} \cdot T$
SNR (Receiver Side)	$\frac{P \cdot \beta \cdot d_{ITA}^{-\delta}}{\alpha \cdot N}$	$\frac{P \cdot (1-\beta) \cdot d_{ITE}^{-\delta}}{N \cdot (1-\alpha)}$	$\frac{P \cdot (1-\beta) \cdot d_{ITE}^{-\delta}}{N \cdot (1-\alpha)}$	$\frac{P \cdot d_{ITE}^{-\delta}}{N}$

In Table 4-1, The code rate of SISO mode is the same as that in intra-cluster broadcasting. d_{ITA} and d_{ITE} represent the local distance within the cluster and the distance between two relaying clusters respectively. Because the power allocation happens at the transmitting side of each phase, path loss needs to be considered when calculating SNR at the receiving side of each phase. δ is the path loss exponent. N is denoted as the power of noise and all the noise levels in the system are set to the same value.

Table 4-2 Parameter expressions for half duplex continuous communication without consideration of circuit energy

	Intra-cluster Phase	Inter-cluster Phase	Receiving Phase	Whole System	SISO Mode
Transmitting Energy Consumption	$\frac{P'\cdot T\cdot\beta}{2}$	$\frac{P'\cdot T\cdot(1-\beta)}{2}$	0	$\frac{P'\cdot T}{2}$	$\frac{P'\cdot T}{2}$
Time Slot	$\alpha\cdot T$	$\frac{(1-\alpha)}{2}\cdot T$	$\frac{(1-\alpha)}{2}\cdot T$	T	$\frac{T}{2}$
Transmitting Power	$\frac{P'\cdot\beta}{2\alpha}$	$\frac{P'\cdot(1-\beta)}{1-\alpha}$	0	$\frac{P'}{2}$	P'
Date Rate	$\Phi\cdot R_{\text{intra}}$	$\Phi\cdot R_{\text{inter}}$	$\Phi\cdot R_{\text{inter}}$	$\frac{R_{\text{inter}}\cdot R_{\text{intra}}}{R_{\text{inter}}+2R_{\text{intra}}}\cdot\Phi$	$\Phi\cdot R_{\text{intra}}$
Date Throughput	$\Phi\cdot R_{\text{intra}}\cdot\alpha\cdot T$	$\frac{\Phi\cdot R_{\text{inter}}\cdot(1-\alpha)\cdot T}{2}$	$\frac{\Phi\cdot R_{\text{inter}}\cdot(1-\alpha)\cdot T}{2}$	$\frac{R_{\text{inter}}\cdot R_{\text{intra}}}{R_{\text{inter}}+2R_{\text{intra}}}\cdot\Phi\cdot T$	$\Phi\cdot R_{\text{intra}}\cdot\frac{T}{2}$
SNR (Receiver Side)	$\frac{P'\cdot\beta\cdot d_{ITA}^{-\delta}}{2\alpha\cdot N}$	$\frac{P'\cdot(1-\beta)\cdot d_{ITE}^{-\delta}}{N\cdot(1-\alpha)}$	$\frac{P'\cdot(1-\beta)\cdot d_{ITE}^{-\delta}}{N\cdot(1-\alpha)}$	$\frac{P'\cdot(1-\beta)\cdot d_{ITE}^{-\delta}}{N\cdot(1-\alpha)}$	$\frac{P'\cdot d_{ITE}^{-\delta}}{N}$

In table 4-2, there is an additional receiving phase in the packet processing duration T because of the half duplex communication method. In a cluster-based cooperative MIMO system, this receiving time slot is $(1-\alpha)\cdot T/2$, while in the SISO system, the receiving time slot is $T/2$ and the remaining $T/2$ slot is used for signal transmission. So the total transmitting energy for each of these two systems is set as $P'\cdot T/2$. For the received SNR in the receiving phase is generated from the transmitting power of the last hop, no transmitting energy of the current hop is needed to be allocated to this phase. Only the intra-cluster and inter-cluster phases need the transmitting energy allocation with a different time slots allocation from the full duplex communication situation in table 1.

From table 1 and 2, it can be seen that the system data throughput of the cluster-based

cooperative MIMO communication is always less than the SISO mode. This is generated from the time-division scheme adopted and cannot be eliminated. What we can do is try to achieve this maximum data throughput of the cooperative system and enhance the communication reliability compared to SISO mode with the same transmitting energy budget.

By using the mathematical theory discussed in Section 4.1 and parameters given in table 1, one can get the capacity limit in intra-cluster broadcasting phase for single packet transmission or full duplex communication:

$$C_{1\times r-full} = \hat{C}_{r-1}\left(\frac{P\cdot\beta\cdot d_{ITA}^{-\delta}}{\alpha\cdot N}\right)/\Gamma(r) \geq \Phi\cdot R_{\text{intra}} \tag{4.17}$$

From (4.9), the outage probability for the inter-cluster transmission in this situation can be rewritten as:

$$P_{out-MIMO-full}(\Phi R_{\text{inter}}) = \frac{1}{\Gamma(n_t)}\Upsilon\left(n_t, \left(2^{\Phi}-1\right)\cdot\frac{n_t}{\gamma}\cdot\frac{N\cdot(1-\alpha)}{P\cdot(1-\beta)\cdot d_{ITE}^{-\delta}}\cdot R_{\text{inter}}\right) \tag{4.18}$$

The aim of power allocation is to keep the $P_{out}(\Phi R)$ as low as possible. As the Capacity Integral in (4.17) and the outage probability in (4.18) are both increasing functions of β, when equality of (4.17) is established, (4.18) will reach the possible minimum value. If a β establishing the equality of (4.17) produces an outage probability within the outage tolerance of the inter-cluster transmission, such a β can be chosen as the fraction of transmitting energy allocation. Then the power level ratio of intra-cluster and inter-cluster phases in this framework is $\beta(1-\alpha)/\alpha(1-\beta)$. Otherwise, there is no power allocation for reliable communication with this symbol rate Φ and the code rate R_{intra}. A lower data rate is needed to meet the requirement of outage probability with sacrifice of data throughput.

Similarly, in half duplex continuous communication, by power allocation, the communication reliability for the system can be enhanced. The expression of capacity limit for the intra-cluster broadcasting and outage probability for the inter-cluster transmission in this situation can be written as:

$$C_{1\times r-half} = \hat{C}_{r-1}\left(\frac{P'\cdot\beta\cdot d_{ITA}^{-\delta}}{2\alpha\cdot N}\right)/\Gamma(r) \geq \Phi\cdot R_{\text{intra}} \tag{4.19}$$

$$P_{out-MIMO-half}(\Phi R_{\text{inter}}) = \frac{1}{\Gamma(n_t)} \Upsilon\left(n_t, \left(2^{\Phi \cdot R_{\text{inter}}} - 1\right) \cdot \frac{n_t}{\gamma} \cdot \frac{N \cdot (1-\alpha)}{P' \cdot (1-\beta) \cdot d_{ITE}^{-\delta}} \cdot R_{\text{inter}} \right) \quad (4.20)$$

On choosing the time slot of α, equality of (4.19) can be established by adjusting β and then (4.20) meets the outage requirment. The power level ratio of the two phases in half duplex communication is $\beta(1-\alpha)/2\alpha(1-\beta)$.

SISO modes used for comparison in the full-duplex and half-duplex situations have the outage probability expressions as

$$P_{out-SISO-full}(\Phi \cdot R_{\text{intra}}) = \frac{1}{\Gamma(1)} \Upsilon\left(1, \left(2^{\Phi \cdot R_{\text{intra}}} - 1\right) \cdot \frac{1}{\gamma} \cdot \frac{N}{P \cdot d_{ITE}^{-\delta}} \right) \quad (4.20)$$

and $$P_{out-SISO-half}(\Phi R_{\text{inter}}) = \frac{1}{\Gamma(1)} \Upsilon\left(1, \left(2^{\Phi \cdot R_{\text{inter}}} - 1\right) \cdot \frac{1}{\gamma} \cdot \frac{N}{P' \cdot d_{ITE}^{-\delta}} \right) \quad (4.21)$$

- With consideration of circuit energy

In this situation, the total available energy needs to be split into two parts, one for the transmitting consumption and the other for the circuit consumption. For fair comparison, we cannot set the equal transmitting energy for both SISO and cooperative MIMO but the total available energy. Assuming the same average transmitting power in SISO mode (P for full duplex communication and P' for half duplex communication), the energy used for data transmitting in cluster-based cooperative transmission satisfies the equations as follows.

For full duplex communication:

$$E_{tran\_full} + \alpha \cdot T \cdot [P_{ct} + (n_t - 1) \cdot P_{cr}] + (1-\alpha) \cdot T \cdot (n_t \cdot P_{ct} + n_r \cdot P_{cr}) = P \cdot T + P_{ct} \cdot T + P_{cr} \cdot T \quad (4.22)$$

For half duplex communication:

$$E_{tran\_half} + \alpha \cdot T \cdot [P_{ct} + (n_t - 1) \cdot P_{cr}] + \frac{(1-\alpha)}{2} \cdot T \cdot (n_t \cdot P_{ct} + n_r \cdot P_{cr}) = P' \cdot \frac{T}{2} + P_{ct} \cdot \frac{T}{2} + P_{cr} \cdot \frac{T}{2} \quad (4.23)$$

P_{ct} and P_{cr} in the equations above represent the circuit power for one transmitter and one receiver respectively, as is introduced in Chapter 3. Then the power allocation for the cluster-based cooperative system with consideration of circuit energy transforms to the transmitting energy allocation between the ITA and ITE phases with the sum of $E_{tran-full}$ and $E_{tran-half}$. The resource allocation expressions and data throughput for each time slots and the whole system compared with a SISO mode in this situation can also be listed in table 4-3 and 4-4 for explicitness.

Table 4-3 Parameter expressions for single packet or full duplex continuous communication with consideration of circuit energy

	Intra-cluster Phase	Inter-cluster Phase	Whole System	SISO Mode
Transmitting Energy Consumption	$E_{tran\_full} \cdot \beta$	$E_{tran\_full} \cdot (1-\beta)$	E_{tran_full}	$P \cdot T$
Time Slot	$\alpha \cdot T$	$(1-\alpha) \cdot T$	T	T
Transmitting Power	$\frac{E_{tran\_full} \cdot \beta}{\alpha \cdot T}$	$\frac{E_{tran\_full} \cdot (1-\beta)}{(1-\alpha) \cdot T}$	$\frac{E_{tran\_full}}{T}$	P
Date Rate	$\Phi \cdot R_{\text{intra}}$	$\Phi \cdot R_{\text{inter}}$	$\frac{R_{\text{inter}} \cdot R_{\text{intra}}}{R_{\text{inter}} + R_{\text{intra}}} \cdot \Phi$	$\Phi \cdot R_{\text{intra}}$
Date Throughput	$\Phi \cdot R_{\text{intra}} \cdot \alpha \cdot T$	$\Phi \cdot R_{\text{inter}} \cdot (1-\alpha) \cdot T$	$\frac{R_{\text{inter}} \cdot R_{\text{intra}}}{R_{\text{inter}} + R_{\text{intra}}} \cdot \Phi \cdot T$	$\Phi \cdot R_{\text{intra}} \cdot T$
SNR (Receiver Side)	$\frac{E_{tran\_full} \cdot \beta \cdot d_{ITA}^{-\delta}}{\alpha \cdot T \cdot N}$	$\frac{E_{tran\_full} \cdot (1-\beta) \cdot d_{ITE}^{-\delta}}{N \cdot (1-\alpha) \cdot T}$	$\frac{E_{tran\_full} \cdot (1-\beta) \cdot d_{ITE}^{-\delta}}{N \cdot (1-\alpha) \cdot T}$	$\frac{P \cdot d_{ITE}^{-\delta}}{N}$

Table 4-4 Parameter expressions for half duplex continuous communication with consideration of circuit energy

	Intra-cluster Phase	Inter-cluster Phase	Whole System	SISO Mode
Transmitting Energy Consumption	$E_{tran\_half}\cdot\beta$	$E_{tran\_half}\cdot(1-\beta)$	E_{tran_half}	$\frac{P'\cdot T}{2}$
Time Slot	$\alpha\cdot T$	$\frac{(1-\alpha)}{2}\cdot T$	T	$\frac{T}{2}$
Transmitting Power	$\frac{E_{tran\_half}\cdot\beta}{\alpha\cdot T}$	$\frac{E_{tran\_half}\cdot(1-\beta)}{(1-\alpha)\cdot T/2}$	$\frac{E_{tran\_half}}{T}$	P'
Date Rate	$\Phi\cdot R_{\text{intra}}$	$\Phi\cdot R_{\text{inter}}$	$\frac{R_{\text{inter}}\cdot R_{\text{intra}}}{R_{\text{inter}}+R_{\text{intra}}}\cdot\Phi$	$\Phi\cdot R_{\text{intra}}$
Date Throughput	$\Phi\cdot R_{\text{intra}}\cdot\alpha\cdot T$	$\frac{\Phi\cdot R_{\text{inter}}\cdot(1-\alpha)\cdot T}{2}$	$\frac{R_{\text{inter}}\cdot R_{\text{intra}}}{R_{\text{inter}}+2R_{\text{intra}}}\cdot\Phi\cdot T$	$\Phi\cdot R_{\text{intra}}\cdot\frac{T}{2}$
SNR (Receiver Side)	$\frac{E_{tran\_half}\cdot\beta}{\alpha\cdot T\cdot N\cdot d_{ITA}^{\delta}}$	$\frac{E_{tran\_half}\cdot(1-\beta)}{N\cdot(1-\alpha)\cdot T\cdot d_{ITE}^{\delta}}$	$\frac{E_{tran\_half}\cdot(1-\beta)}{N\cdot(1-\alpha)\cdot T\cdot d_{ITE}^{\delta}}$	$\frac{P'\cdot d_{ITE}^{-\delta}}{N}$

The ITA capacity limit and the ITE outage probability for full duplex and half duplex communication taking circuit energy into account can be then expressed as:

$$C_{1\times r-full}=\hat{C}_{r-1}\left(\frac{E_{tran\_full}\cdot\beta\cdot d_{ITA}^{-\delta}}{\alpha\cdot T\cdot N}\right)/\Gamma(r)\geq\Phi\cdot R_{\text{intra}} \tag{4.24}$$

$$P_{out-MIMO-full}(\Phi R_{\text{inter}})=\frac{1}{\Gamma(n_t)}\Upsilon\left(n_t,\left(2^{\Phi\cdot R_{\text{inter}}}-1\right)\cdot\frac{n_t}{\gamma}\cdot\frac{N\cdot(1-\alpha)\cdot T}{E_{tran\_full}\cdot(1-\beta)\cdot d_{ITE}^{-\delta}}\cdot R_{\text{inter}}\right) \tag{4.25}$$

$$C_{1\times r-half} = \hat{C}_{r-1}\left(\frac{E_{tran\_half}\cdot\beta\cdot d_{ITA}^{-\delta}}{\alpha\cdot T\cdot N}\right)/\Gamma(r) \geq \Phi\cdot R_{\text{intra}} \tag{4.26}$$

$$P_{out-MIMO-half}(\Phi R_{\text{inter}}) = \frac{1}{\Gamma(n_t)}\Upsilon\left(n_t, \left(2^{\Phi\cdot R_{\text{inter}}}-1\right)\cdot\frac{n_t}{\gamma}\cdot\frac{N\cdot(1-\alpha)\cdot T}{E_{tran\_half}\cdot(1-\beta)\cdot d_{ITE}^{-\delta}}\cdot R_{\text{inter}}\right) \tag{4.27}$$

Based on (4.22) to (4.27), the power allocation in consideration of circuit energy can be obtained. Simulations for this proposed time slots and power level allocation framework compared with SISO mode will be made in the following section.

4.3 Simulations

In this section, we first consider no circuit energy in the simulations. The preset parameters for simulating are listed in table 4-5.

Table 4-5 Preset parameters for simulating

Φ	T	d_{ITA}	d_{ITE}	δ	P/N
5 symbol/s	1 s	3 m	10 m	2.7	20 dB

Based on the time slot allocation discussed in Section 4.2, the maximum data throughput of the cluster-based cooperative MIMO transmission system can only be achieved when the STBCs adopted has the code rate $R_{\text{inter}}=1$. So firstly, the Alamouti scheme is investigated with $n_t=2$, $R_{\text{inter}}=1$, $r=n_t-1$. The sub-channel gains for the MIMO communication are set equal as $\gamma=1$. The time allocation parameter α is then decided by R_{intra}. For simplicity, we assume no code modulation is added in the intra-cluster broadcasting in all the simulations of this chapter, which means R_{intra} is fixed at 1.

In single packet transmission or full duplex continuous communication, the time slot $\alpha = 0.5$ for the Alamouti scheme based on (4.11). Then the channel capacity for the ITA slot, the outage probability for the ITE slot, and the SISO mode versus the transmitting energy allocation parameter β can be plotted, as shown in figure.4-5.

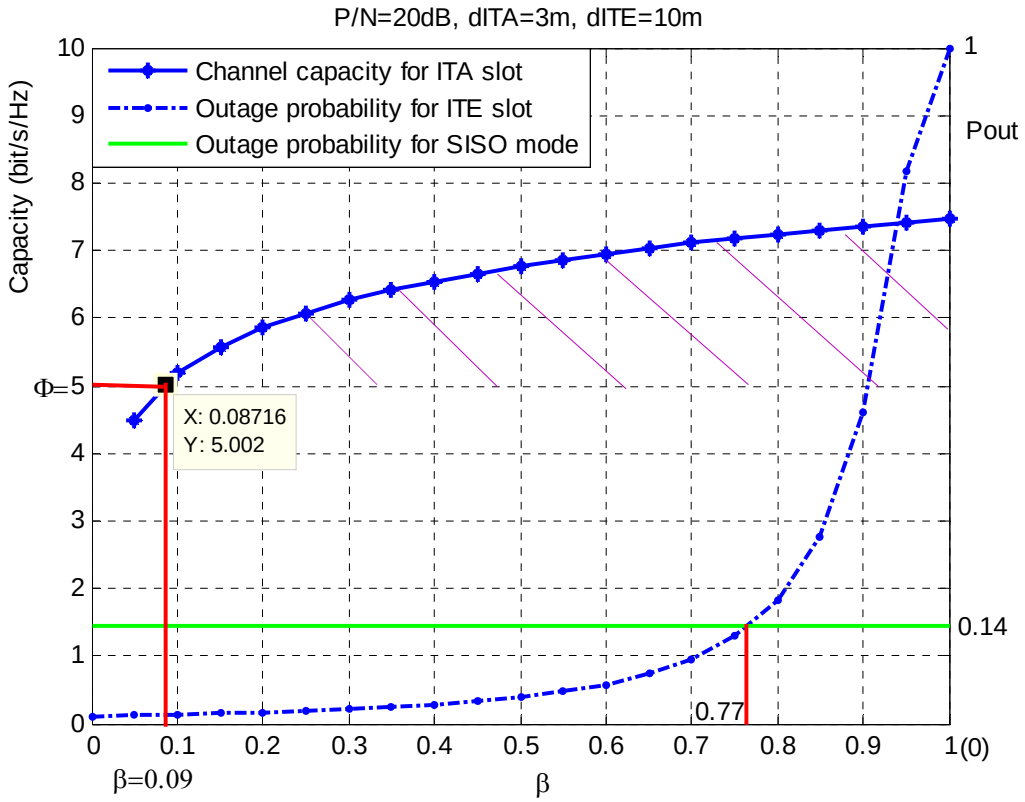

Figure 4-5 Transmitting energy allocation for full duplex communication

Figure 4-5 shows the transmitting energy allocation framework for the full duplex communication using the Alamouti scheme. The left y-axis represents the channel capacity and the right y-axis represents the outage probability. The hatched area represents the possible reliable data rate for the intra-cluster broadcasting under the transmitting energy allocated in this phase. The leftmost point of this area, which is the cross point of $C_{1\times r-full}$ and $\Phi = 5$, represents the adjustment of β considering both the communication reliability and minimum energy cost in the intra-cluster phase. As the total transmission energy is fixed, less energy allocated to the intra-cluster phase means more energy can be assigned to the inter-cluster phase, which decreases the outage probability of the inter-cluster transmission and enhances the reliability of the whole system. The allocation parameter β in figure 4-5 is 0.09 with 2% as the minimum outage probability of the inter-cluster phase as well as the

whole system. Then the power ratio of these two phases is obtained as $\beta(1-\alpha)/\alpha(1-\beta)=1/10$ with the chosen α and β. Thus the power level allocation is achieved. If the requirement of system outage probability is set to be lower than a certain value, the possible available β would be a closed zone with the one in figure as the leftmost point and the rightmost point corresponding to the required maximum outage probability value.

The outage probability curve of the full duplex SISO mode intersects that of the cluster-based cooperative MIMO system at the abscissa of $\beta=0.77$ in figure 4-5, corresponding to the power level ratio of these two phases $\beta(1-\alpha)/\alpha(1-\beta)=1/0.3$. This can also be derived theoretically from (4.18) and (4.20) using the Alamouti scheme ($R_{\text{inter}}=1$, $\alpha=0.5$). The β obtained in figure 4-5 is smaller than this threshold of 0.77, which means that under this selection values of α and β, the communication reliability of the cluster-based cooperative MIMO system is better than that of SISO system with the same total transmitting energy budget. In another words, with the same communication reliability requirement, the cooperative MIMO system uses less transmitting energy than the SISO system under these parameter conditions.

However, based on (4.17), (4.18) and (4.20), the parameter β and the crossing point of the two outage probability curves are affected by d_{ITA} and d_{ITE} for a fixed total transmitting energy and noise level. For different d_{ITA} and d_{ITE}, the parameter β may not always lie to the left side of the cross point. It can even fall into the right side of the threshold, which is shown in figure 4-6.

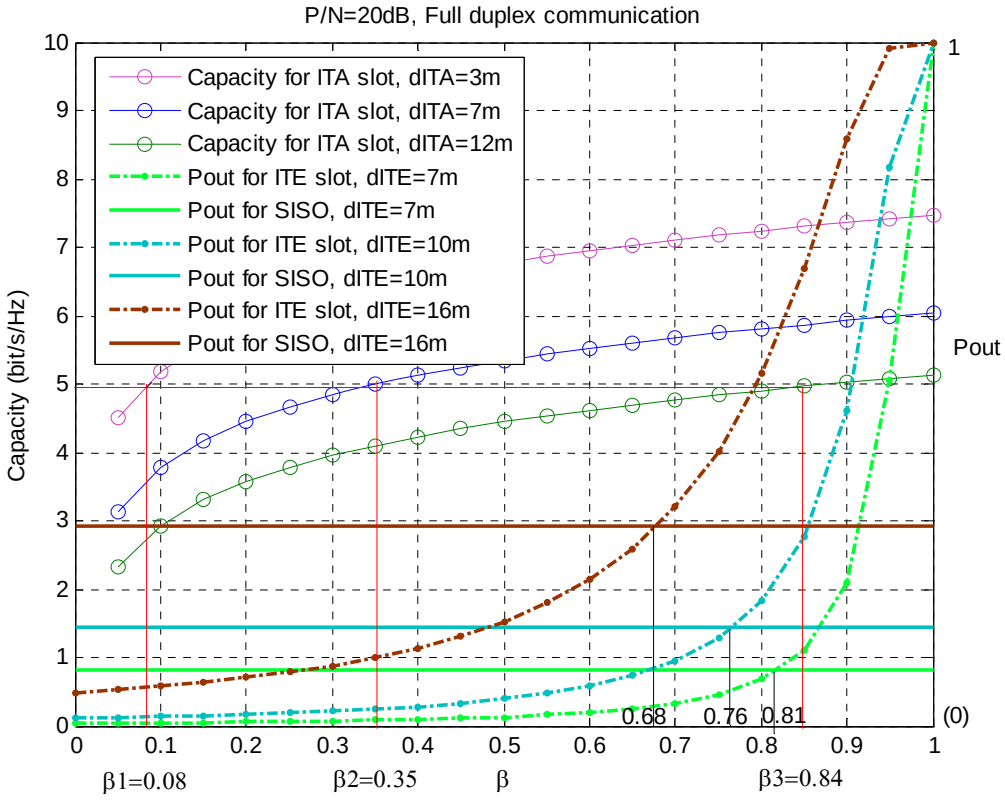

Figure 4-6 Transmitting energy allocation for different d_{ITA} and d_{ITE}

It can be seen from figure 4-6 that the capacity curve for the ITA slot goes down as d_{ITA} increases which makes the possible power allocation parameter β move rightwards, while the crossing point of outage probability curves of SISO and cooperative MIMO moves leftwards as d_{ITE} increases. Only when the possible β produces a reasonable (meets the requirement of outage probability) outage probability, it can be used as a proper power allocation parameter. In this figure, when we set $d_{ITA}=12\,\mathrm{m}$ and $d_{ITE}=16\,\mathrm{m}$, the possible parameter $\beta=0.84$ falls into the right side of the threshold $\beta=0.68$, which means the cooperative MIMO system is no better than the SISO system in these conditions. In this situation, the possible parameter β is actually not correct for power allocation. The transmission distances for the ITA and ITE slots, especially d_{ITA}, are too far to support a reliable communication under a total transmitting energy budget. The solution to this may be subdividing the cluster and adding a number of hops, or adopting a SISO mode directly instead of the cluster based cooperative MIMO. How many hops (single-hop or multi-hop) should be used and which mode should be adopted for each hop will be discussed in the following chapter.

Another factor which can affect the transmitting energy allocation is P/N. The selection of the β with different R/N is investigated in figure 4-7 below.

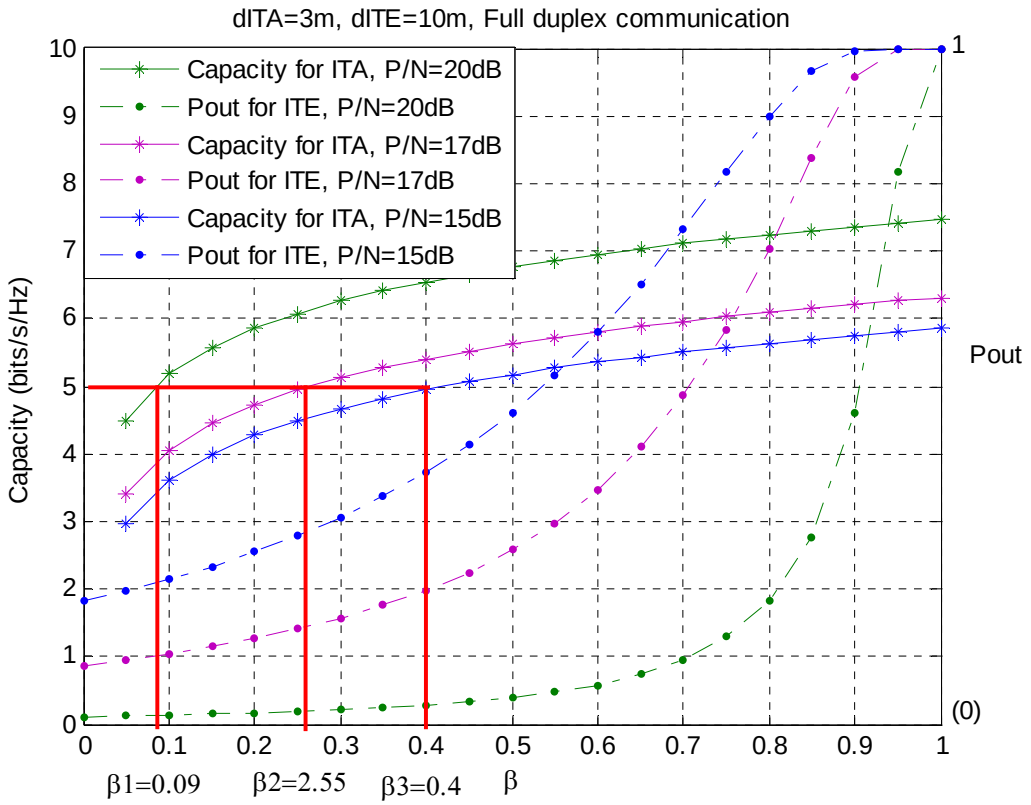

Figure 4-7 Transmitting energy allocation with different P/N

In figure 4-7, the allocation parameter β reduces as the ratio of P/N grows. For a fixed d_{ITA} and noise level, the transmitting energy used to get the lower bound of capacity for reliable communication within the cluster is a constant. When P/N grows with a fixed N, it is the total available transmitting energy of the system that grows, so the constant energy used for broadcasting during the intra-cluster phase constitutes a smaller fraction of the total energy budget. Clearly, the performance of outage probability in cooperative transmission will improve with increasing the energy allocation in the ITE slot.

If the number of transmitting nodes increases during the inter-cluster cooperative MIMO communication, various STBCs with different code rate R_{inter} can be adopted. The energy allocation parameter β for different numbers of cooperative transmitters versus P/N is shown in figure 4-8.

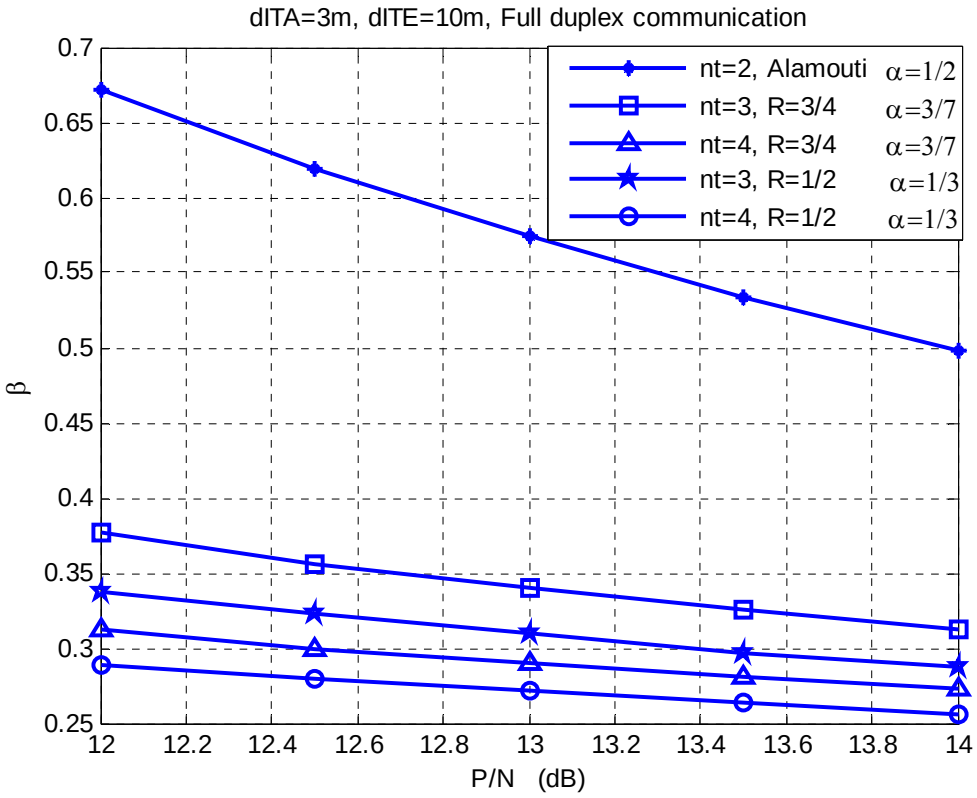

Figure 4-8 β versus P/N for different STBCs

In figure 4-8, STBCs with higher code rates, R_{inter}, correspond to a longer time slot allocation for ITA. This is because a relatively short slot allocation for ITE can also satisfy the data throughput requirement with a higher R_{inter}. For a fixed P/N and d_{ITA}, it is understandable that a bigger time slot, α, requires an increased energy allocation, β, with the same ratio to maintain the transmitting power and the capacity limit of (4.17). So the curve in figure 4-8 with $\alpha = 1/2$ is above those with $\alpha = 3/7$, which are also above those with $\alpha = 1/3$.

For the same R_{inter}, because the $1 \times r$ SIMO broadcasting capacity in (4.17) is the increasing function of r and r satisfies $r = n_t - 1$, more receiving antennas in the ITA broadcasting phase (or transmitting antennas in ITE cooperative MIMO communication) can support a bigger SIMO channel capacity under the same transmitting energy budget. In another words, to achieve the lower bound of capacity

in the ITA slot, less energy needs to be allocated to the intra-cluster phase with a bigger n_t. This explains why the curves with $n_t = 3$ in figure 4-8 are above those with $n_t = 4$ with the same R_{inter}. Under lower noise conditions, the energy spent on cooperative MIMO transmission becomes the dominant consumption, as the communication reliability of the whole system depends on this phase. The outage performance of the SISO mode and the cooperative MIMO system after resource allocating by the proposed framework is shown in figure 4-9.

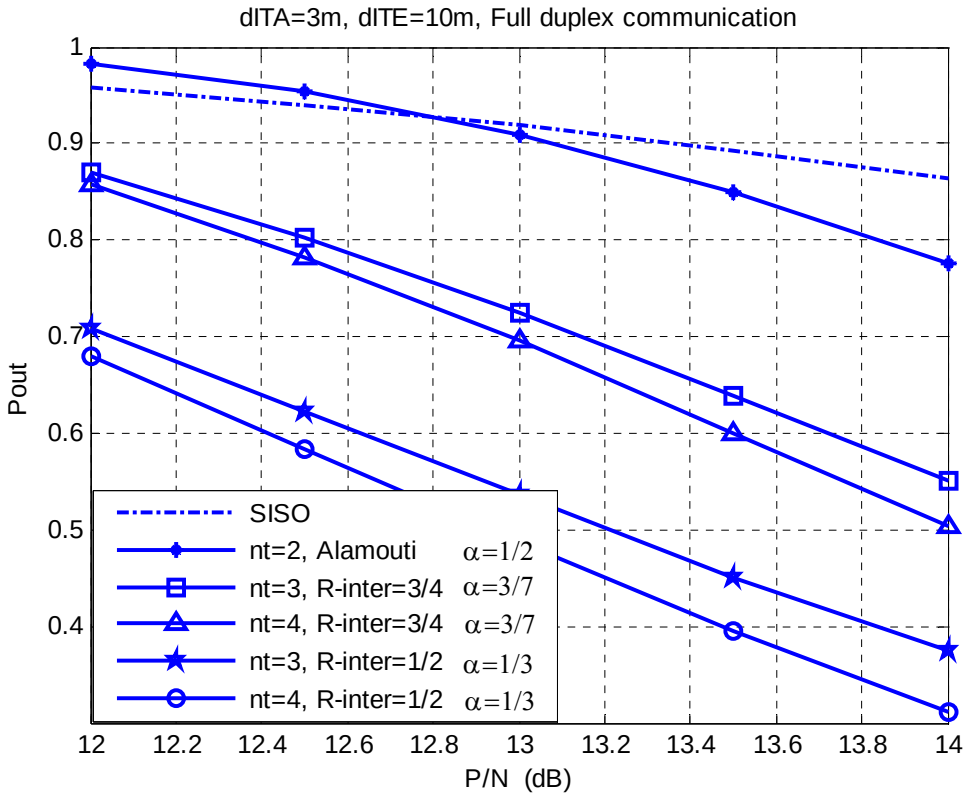

Figure 4-9 Outage performance after using the resource allocation framework

It is clear in figure 4-9 that all the outage performances of different transmission methods improve when the noise level goes down. The intersection of curves of SISO and Cooperative Alamouti modes represents the abscissas of the energy allocation point and the threshold point in figure 4-5 overlap as P/N changes for the fixed d_{ITA} and d_{ITE}. For the general low noise level field, the outage performance of the cluster-based cooperative MIMO system is better than that of the SISO system under the same total transmitting energy. For the same n_t, to achieve the same capacity limit of (4.17), the ITA slot allocation of α is directly-proportional to the energy allocation of β. So for different STBCs with the same n_t, a higher R_{inter}

corresponds to a bigger α and results in a bigger outage probability for the ITE communication based on (4.18). This is why the curves with $R_{\text{inter}} = 3/4$ are above those with $R_{\text{inter}} = 1/2$ in the figure above. Similarly, for different n_t with the same R_{inter}, bigger n_t requires less energy allocated in ITA slot to achieve the lower bound of SIMO channel capacity, which derives a lower outage probability from (4.18). So, for each R, the outage performance of $n_t = 4$ is better than that of $n_t = 3$.

Although more transmitting nodes in the ITE slot tends to get a better outage perfromance based on figure (4-9), considering the time division system and the data rate R_{inter} of STBCs used is less than 1 (except for Alamouti), there is a loss of data throughput for the cooperative MIMO system compared to the SISO mode. The outage performance improvement can be seen as a sacrifice of system data rate. In addition, the energy allocation discussed in this chapter is only the energy used for signal transmitting. When the energy used for signal processing in each sensor node is considered, it may not be the case that the cooperative MIMO system is always better than the SISO mode. A trade off between the energy saving, data throughput, and communication reliability is needed for the transmission method selection.

The full duplex mode needs to isolate the transmitted signal from the receiver antenna. The separation can either be physical – the transmitter transmits in one direction, away from the receiving antenna – but that is very hard to organize in an ad-hoc network, or it could be in terms of frequency, but then this would require planning.

If the antennas of the sensor nodes all work in a half duplex way, the resource allocation framework is then based on (4.19) and (4.20). To make a fair comparison, the energy used for data transmitting in full duplex and half duplex communication should be the same. So, the transmitting power of the half duplex SISO mode should be $P' = 2P$. The transmitting energy allocation for the Alamouti scheme in this situation can be shown in figure (4-10).

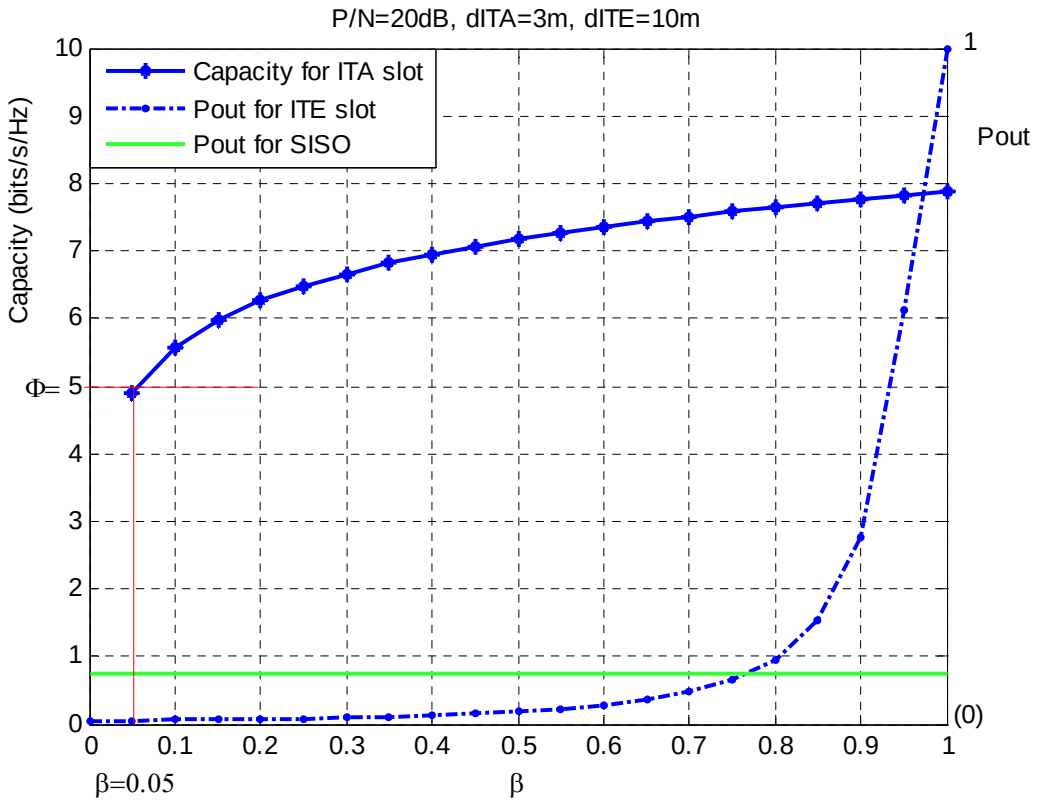

Figure 4-10 Transmitting energy allocation for half duplex communication

Figure 4-10 is plotted under the same noise conditions of figure 4-5, where $P'/N = 2P/N \approx 23\,\text{dB}$. As is shown in (4.17) and (4.19), the SIMO channel capacity for full duplex and half duplex communications have the same expression when $P' = 2P$. So, to achieve the same lower bound of SIMO channel capacity, the parameters α and β in these two figures should satisfy the equation below:

$$\frac{\beta_{full\_duplex}}{\alpha_{full\_duplex}} = \frac{\beta_{half\_duplex}}{\alpha_{half\_duplex}} \tag{4.28}$$

Based on (4.11) and (4.15), the time allocation parameter α for the full duplex and half duplex communications are 1/2 and 1/3 respectively. By inserting them to (4.35), one can obtain $\beta_{half\_duplex} = 2\beta_{full\_duplex}/3$. This explains why the transmitting energy allocated in ITA slot for half duplex continuous communication is smaller than that for full duplex communication. In figure 4-10, the allocation parameter β is 0.05. Then the power ratio of the ITA and ITE phases in this situation is obtained as $\beta(1-\alpha)/2\alpha(1-\beta) = 1/19$, which is smaller than that in figure 4-5. Higher power level in ITE slot results a better outage performance in figure 4-10 than that in figure 4-5.

Similar to the full duplex communication, the β versus P/N ($P'=2P$) for different STBCs in half duplex communication is shown in figure 4-11.

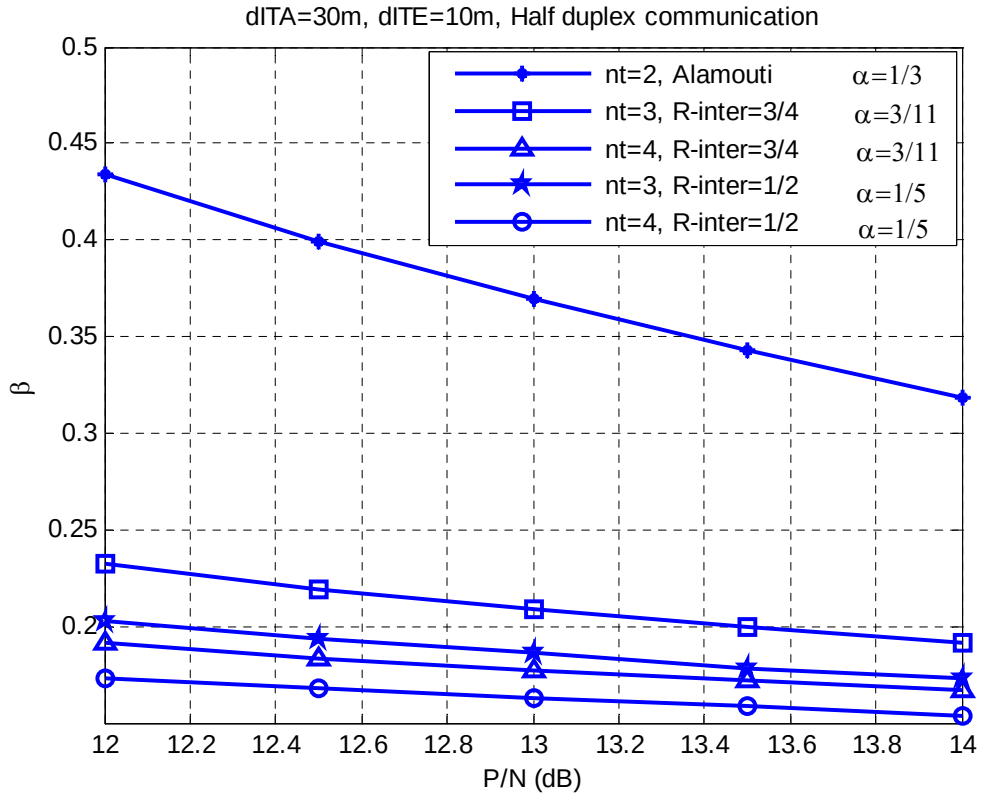

Figure 4-11 β versus P/N for different STBCs

Based on (4.15), the time slots allocation of α for different R_{inter} R in figure 4-11 are different from those in figure 4-8. By inserting (4.11) and (4.15) to (4.22), one can obtain:

$$\beta_{half\_duplex} = \frac{R_{\text{inter}} + R_{\text{intra}}}{R_{\text{inter}} + 2R_{\text{intra}}} \cdot \beta_{full\_duplex} \tag{4.29}$$

Equation (4.29) mathematically explains the relationship of figure 4-11 and 4-8.

Similar to figure 4-9, the outage performances for different STBCs after choosing the resource allocation parameters α and β are shown in figure 4-12.

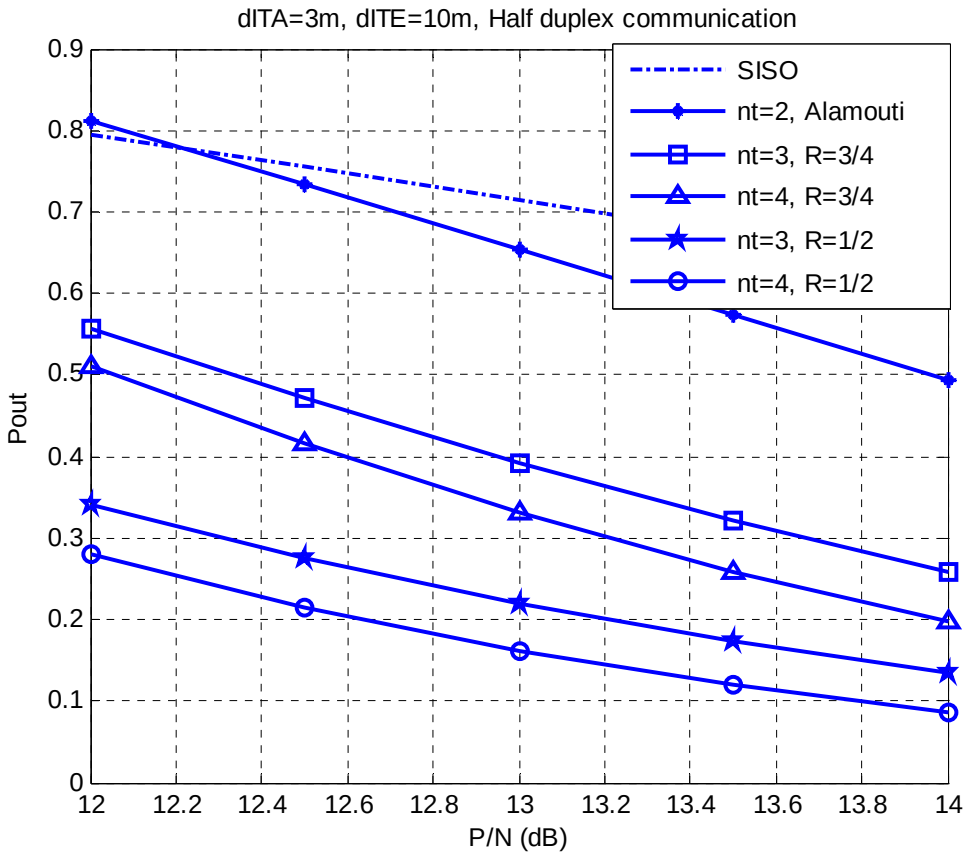

Figure 4-12 Outage performance after using the resource allocation framework

For a certain P/N, because more transmitting energy is allocated to a smaller inter-cluster time slot, which results in an even higher transmitting power level, the outage performance for different STBCs in figure 4-12 are better than that in figure 4-9. Considering the better outage performance and the maximum data throughput of $1/3\cdot\Phi\cdot T$ (when $R_{intra}=1$) versus $1/2\cdot\Phi\cdot T$ of SISO for half duplex communication ($1/2\cdot\Phi\cdot T$ versus $\Phi\cdot T$ for full duplex communication), there is a large posibility that the cluster-based cooperative MIMO system surpasses the SISO mode in the half duplex method.

When circuit energy is considered, the power allocation framework is based on (4.24) to (4.27). To calculate the circuit energy consumption P_{ct} and P_{cr} in this situation, parameters for each circuit block need to be preset [98~105].

Table 4-6 Parameters of circuit energy

$P_{mix} = 30\,\text{mW}$	$P_{LNA} = 20\,\text{mW}$
$P_{fil} = 2.5\,\text{mW}$	$P_{DAC} = 15.5\,\text{mW}$
$P_{IFA} = 3\,\text{mW}$	$P_{ADC} = 6.7\,\text{mW}$
$P_{syn} = 50\,\text{mW}$	$N = -23\,\text{dB/Hz}$

The simulations of the resource allocation framework with consideration of circuit energy in full-duplex mode are shown in figure 4-13 ($n_t = 2$, $n_r = 2$). To make a comparison, the curves without consideration of circuit energy are also plotted into the same figure.

In figure 4-13, since the transmitting energy of SISO mode is set the same in both with and without circuit energy consideration, there is no difference for the outage performace of SISO mode between these two situations. In aspect of cluster-based cooperative transmission, it can be seen that when circuit energy consumption is considered, the transmitting energy allocation parameter β moves rightward compared to that without consideration of circuit energy. This is because, with the same total energy in these two situations, the energy available to be allocated for data transmitting in cluster-based transmission with consideration of circuit energy is actually less than that without circuit energy taken into account. Even with different total energy but the same transmitting energy of SISO mode in these two situations, as is the assumptions in this simulation, this is still the case, since more nodes are activated in cooperative transmission where more circuit energy consumption occurs. As a result, to achieve the same capacity lower bound decided by a certain transmitting power in ITA slot, the fraction of energy allocated in this phase should be bigger. Less transmitting power in ITE phase also causes a worse outage

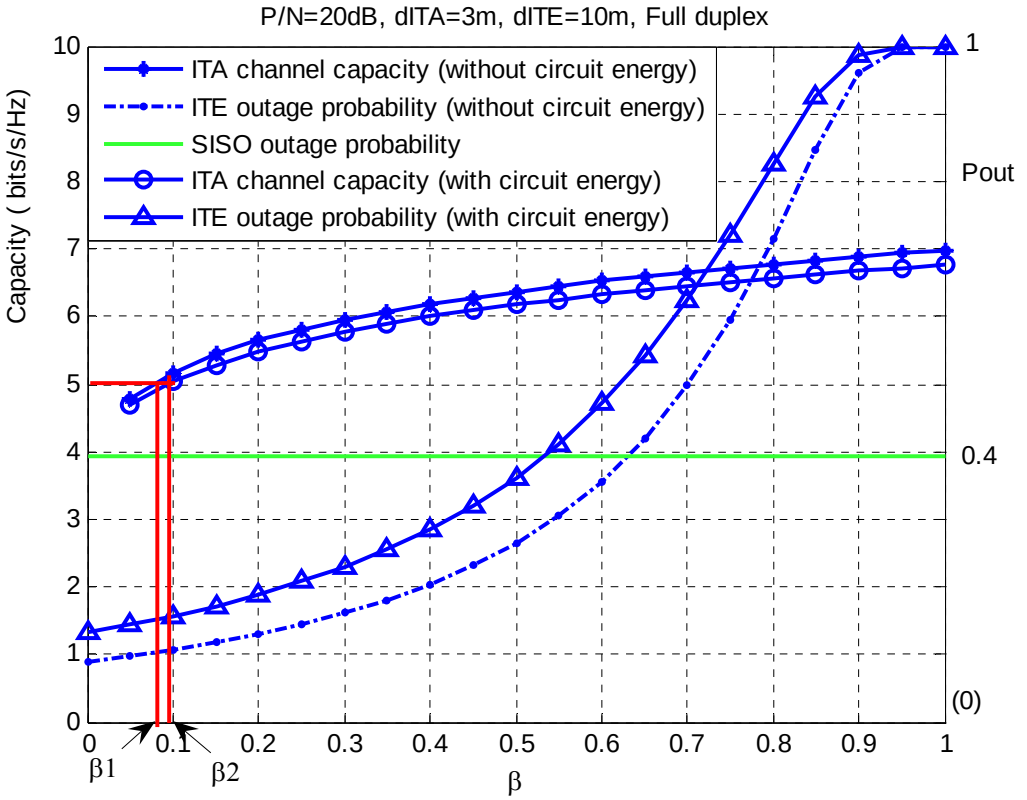

Figure 4-13 Power allocation with and without circuit energy (full-deplex)

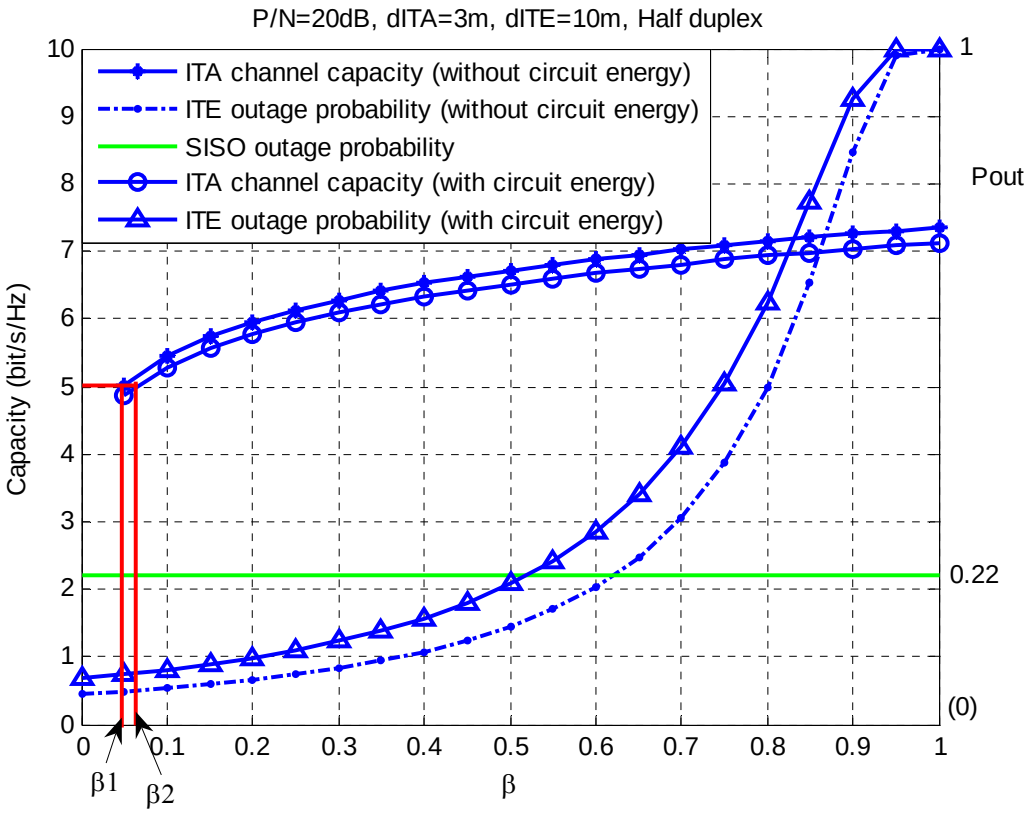

Figure 4-14 Power allocation with and without ciruit energy (half-duplex)

perormance. This difference in cluster-based cooperative transmission generated by the circuit energy depends on the preset circuit parameters and the number of transmitters and receivers in each transmission phase. More circuit energy consumption in each node and more activated nodes involved in each phase make the difference between these two situations even bigger. If the circuit energy isn't considered, the comparison results can be overly optimistic about the benefits of cooperative MIMO.When the circuit energy consumption grows to the same order or even larger than the transmitting energy consumption, usually in quite a short distance communication, the power allocation parameter β for cluster-based transmission may move to the right of the outage performance intersection, which means no power allocation can make the cluster-based cooperative tranmission better than SISO in communication reliability with the same energy budget. A similar analysis also holds for half-duplex communication, shown in figure 4-14.

4.4 Conclusions

In cluster-based cooperative MIMO transmission, the research of resouce allocation mainly focuses on time slot allocation and power level allocation. The topic of time slot allocation arises because of the time-division scheme adopted in this system. Information received by the relaying cluster is firstly broadcasted by the cluster-head within the cluster which is called intra-cluster phase (ITA). Then the cooperative nodes including the cluster head will form a cooperative MIMO transmission with next cluster, where STBCs may be adopted in this inter-cluster phase (ITE). Compared to the SISO transmission mode, this time-division scheme will result in a data rate loss with the same symbol rate with SISO. However, by properly allocating each time slot, the loss of throughput for the whole system can be minimized.

The problem of power level allocation for ITA and ITE phases has been brought out on the consideration of energy efficiency. As the local distance in the ITA slot is always much shorter than that in the ITE slot, the antennas in these two phases shouldn’t work at the same power level. Under a certain requirment of communication reliability, antennas used for the shorter distance transmission can properly lower its transmitting power to save more energy. So, the power level

allocation for the ITA and ITE phases can significantly affect both the communication reliability and the lifetime of the sensor network.

In this chapter, a resource allocation framework for the cluster-based cooperative MIMO system is proposed. Two adjusting parameters, α and β, are introduced for the time slot and transmitting energy allocation respectively. The time allocation parameter α is obtained based on no redundant information in this system and is decided by the code rate used in both intra-cluster broadcasting and inter-cluster transmission phases. The power allocation parameter β is got by reducing the outage probability of the cooperative MIMO transmission as low as possible or under a threshold requirment, and at the same time maintaining the reliability of the broadcasting transmission in ITA slot. Then the power level ratio for these two phases can be obtained based on this pair of selected α and β.

Simulations of this proposed framework in full duplex and half duplex communication methods are made and compared with the SISO system. The situations with and without circuit energy consumption are both analysed. The simulation results show that when the circuit energy is small enough compared with the transmitting energy, usually in a long distance transmission, the cluster-based cooperative MIMO system with the proposed resource allocation overcomes the SISO system in outage performance and transmitting energy saving. When circuit energy becomes considerable and cannot be omitted, consideration of the circuit energy is important when comparing different modes. Without doing this, comparison results of the benefits about cooperative MIMO mode can be overly optimistic. For different STBCs adopted in the inter-cluster phase, more transmitters can get an even better communication reliability of the whole system with the same total transmitting energy. However, when the energy consumed for the data processing within the sensor nodes is considered, more cooperative nodes may increase the energy consumption of the whole network. Based on the resource allocation framework proposed in this chapter and the energy equations derived in Chapter 3, a detailed comparison of varies transmission modes in wireless sensor network can be made in the following parts of this thesis.

Chapter 5
Single-hop Mode Switching Framework

From the discussions in the former chapter, it is known that the performance of a wireless communication system is measured in three ways: the system data rate, communication reliability, and energy consumption. Specifically, because the data streams in wireless sensor networks are usually transmitted at a low data rate, energy-efficiency and communication reliability become the two priority requirements which need to be considered in sensor network design. By comparing the energy consumption for each transmission mode under a fixed bit-error-rate requirement, researchers have found that there is not a single unique energy-efficient transmission mode for all wireless sensor networks [82~86][98~100]. Based on different conditions, such as the transmission distance, the energy-efficient transmission mode changes from SISO to cooperative MIMO/MISO, and from single-hop to multi-hop. The transmission method which dynamically changes the transmission mode is called a mode switching framework.

However, to the best of my knowledge, there is no published work that explains how this mode switching framework can be used in practice. Firstly, although some papers [98~100] consider circuit energy, they do not take into account the energy consumption in the intra-cluster phase for cluster-based cooperative MIMO/MISO. Secondly, all the mode switching frameworks proposed by other researchers perform the mode switching only based on the destination transmission distance, but do not explain how the distance information in a densely deployed wireless sensor network can be determined [98~100]. A more practical parameter fit for mode switching should be path-loss, which is easy to measure in distributed nodes. Thirdly, no angle position relationship of the sensor nodes is taken into account on choosing of transmission mode. The affect caused by the location of the cooperative nodes within the cluster is not stated. Fourthly, when it comes to the multi-hop situation, all the published frameworks made an assumption that the relaying nodes (clusters) are all at

equally spaced points along the signal path. However, how this framework works when the relaying nodes (clusters) are not ideally situated like this is still not clear.

So, to solve the problems above, an improved path-loss based mode switching framework for wireless sensor networks is proposed in this thesis. In this chapter, this framework for single-hop transmission is introduced and the multi-hop situation will be dealt with in Chapter 6.

The structure of this chapter is as follows. In Section 5.1, a comparison of all the single-hop transmission modes in wireless sensor networks (SISO, cluster-based cooperative MIMO, and cluster-based cooperative MISO) will be made from the view of total energy consumption under a fixed bit-error-rate requirement. Both the transmitting energy consumption and the circuit energy consumption for the intra-cluster phase and inter-cluster phase are taken into account. Based on this, the single-hop path-loss based mode switching framework is introduced in Section 5.2. How this framework operates in practice is stated. Resource allocation frameworks proposed in Chapter 4 that incorporate circuit energy are used in the simulations of this chapter.

5.1 Energy Comparison for Different Transmission Mode

In Chapter 3, a typical energy consumption model of RF systems with functional blocks is introduced. Expressions of the total energy consumption per bit for different transmission modes in wireless sensor networks are derived based on this model. For convenience of comparison, these energy equations are re-stated here with resource allocation being considered.

- Single-hop SISO

$$E_{bt\_SISO} = \frac{P_{PA} + P_{ct} + P_{cr}}{R_b}$$

$$= (1+\varepsilon)\cdot \bar{E}_b \times \frac{(4\pi d_{ITE})^2}{G_t G_R \lambda^2} M_l N_f + \frac{P_{DAC} + P_{mix} + P_{fil} + P_{syn}}{R_b}$$

$$+\frac{P_{LNA}+P_{mix}+P_{IFA}+P_{fil}+P_{ADC}+P_{syn}}{R_b} \tag{5.1}$$

- Single-hop cooperative MIMO

$$E_{bt\_Co-MIMO}=\frac{P_{PA\_ITA}+P_{PA\_ITE}+\alpha\cdot[P_{ct}+(n_t-1)P_{cr}]+(1-\alpha)\cdot(n_t\cdot P_{ct}+n_r\cdot P_{cr})}{R_b}$$

$$=(1+\varepsilon)\cdot\bar{E}_{b\_ITA}\times\frac{(4\pi d_{ITA})^2}{G_tG_R\lambda^2}M_lN_f+(1+\varepsilon)\cdot\bar{E}_{b\_ITE}\times\frac{(4\pi d_{ITE})^2}{G_tG_R\lambda^2}M_lN_f$$

$$+[\alpha+(1-\alpha)\cdot n_t]\cdot\frac{P_{DAC}+P_{mix}+P_{fil}+P_{syn}}{R_b}$$

$$+[\alpha\cdot(n_t-1)+(1-\alpha)\cdot n_r]\cdot\frac{P_{LNA}+P_{mix}+P_{IFA}+P_{fil}+P_{ADC}+P_{syn}}{R_b} \tag{5.2}$$

- Single-hop cooperative MISO

$$E_{bt\_Co-MISO}=\frac{P_{PA\_ITA}+P_{PA\_ITE}+\alpha\cdot[P_{ct}+(n_t-1)P_{cr}]+(1-\alpha)\cdot(n_t\cdot P_{ct}+P_{cr})}{R_b}$$

$$=(1+\varepsilon)\cdot\bar{E}_{b\_ITA}\times\frac{(4\pi d_{ITA})^2}{G_tG_R\lambda^2}M_lN_f+(1+\varepsilon)\cdot\bar{E}_{b\_ITE}\times\frac{(4\pi d_{ITE})^2}{G_tG_R\lambda^2}M_lN_f$$

$$+[\alpha+(1-\alpha)\cdot n_t]\cdot\frac{P_{DAC}+P_{mix}+P_{fil}+P_{syn}}{R_b}$$

$$+[\alpha\cdot(n_t-1)+(1-\alpha)]\cdot\frac{P_{LNA}+P_{mix}+P_{IFA}+P_{fil}+P_{ADC}+P_{syn}}{R_b} \tag{5.3}$$

In the equations above, the exact $\bar{E}_b$ ($\bar{E}_{b-ITA}$ and $\bar{E}_{b-ITE}$) can be obtained from the bit-error-rate performance using Monte Carlo simulation. In MIMO transmission with equal sub channel gains, an upper bound for $\bar{E}_b$ can be derived using the Chernoff bound in the high SNR region [112]:

$$\bar{E}_b\le\frac{n_tN_0}{P_e^{1/n_t}} \tag{5.4}$$

where n_t is the number of transmitters and P_b is the bit-error-rate. The expression of (5.4) can be used to estimate the transmitting power in independent channels. The detailed energy model for each circuit block is not the main focus of this thesis, so the parameters for each block are drawn from several references [71] for simulation. The preset simulation parameters in this section are listed below [98~105].

Table 5-1 System Parameters

$P_e = 10^{-5}$	$P_{IFA} = 3\,\text{mW}$
$N_0 / 2 = -174\,\text{dBm/Hz}$	$P_{syn} = 50\,\text{mW}$
$\xi = 1$	$P_{LNA} = 20\,\text{mW}$
$\eta = 0.35$	$P_{DAC} = 15.5\,\text{mW}$
$R_b = 10\,\text{Kbit/s}$	$P_{ADC} = 6.7\,\text{mW}$
$P_{mix} = 30\,\text{mW}$	
$P_{fil} = 2.5\,\text{mW}$	

From the energy equations derived in (5.2) and (5.3), it can be seen that after setting the circuit parameters in table 5-1, the total energy consumption per bit for cooperative transmission depends on the received energy per bit ($\bar{E}_{b-ITA}$ and $\bar{E}_{b-ITE}$) in each phase, the transmitting distance (d_{ITA} and d_{ITE}), and the number of transmitters and receivers (n_t and n_r). For simplicity, $\bar{E}_b$, $\bar{E}_{b-ITA}$ and $\bar{E}_{b-ITE}$ are all assumed equal to the approximation of (5.4) in this section; this is a common assumption in published research. No power level allocation in ITA and ITE phases is considered for the time being.

The total energy consumption per bit versus d_{ITE} for SISO and cluster-based cooperative MISO modes with different n_t is shown in figure 5-1. As only the repeated data streams are considered in the inter-cluster cooperative transmission and no STBCs are adopted, in full duplex communications, the time allocation parameter α is set to 0.5 (assume $R_{\text{intra}} = 1$) in the simulation.

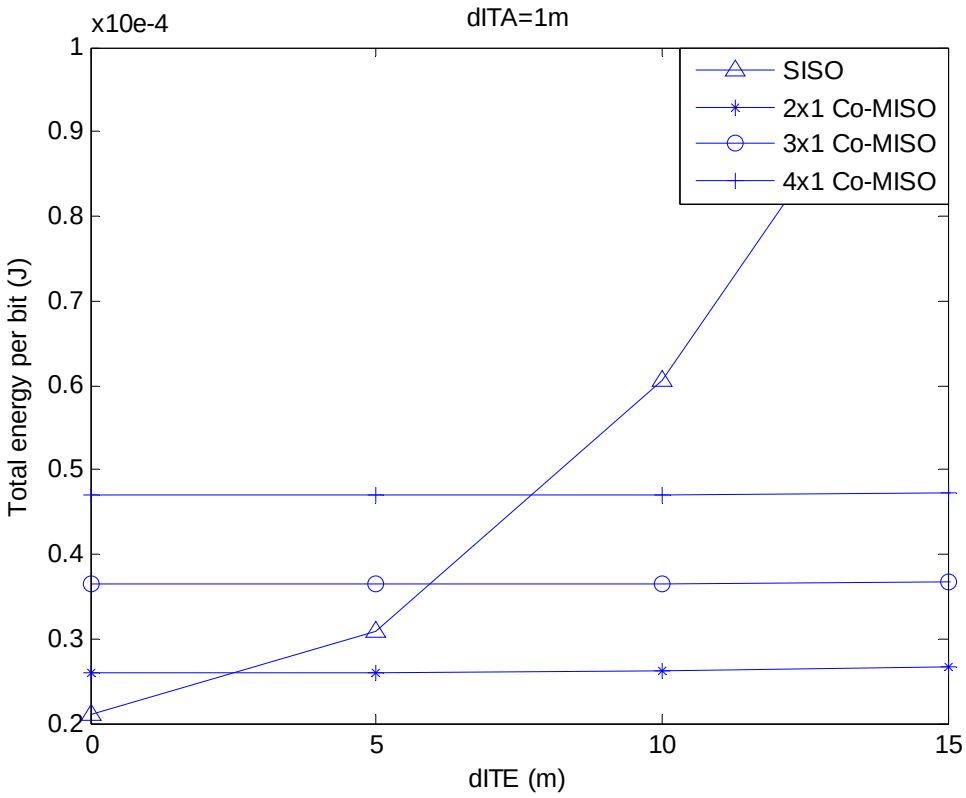

Figure 5-1 One-hop energy consumption of Co-MISO vs SISO

In figure 5-1, the transmission distance of SISO is set to the value of d_{ITE} in the Co-MISO mode. It can be seen that for a small range of d_{ITE}, operating in a SISO mode uses less energy than a Co-MISO mode because the extra circuit energy consumption generated by introducing more nodes in the Co-MISO modes overcomes the power saved by the cooperative gain for this short d_{ITE}. However, when d_{ITE} grows, the total energy consumption of the SISO mode increases dramatically and is less energy efficient than the Co-MISO modes, which means the transmitting energy becomes the dominant part of the total consumption in this situation and the benefit of cooperative transmission in transmitting energy saving outweighs the circuit energy consumed.

The curves of the Co-MISO modes with different n_t increase slightly in figure 5-1. This is because the transmitting energy for the inter-cluster phase is cut to a rather small value and the circuit energy is the dominant part within this range of d_{ITE}. Larger n_t means more P_{cr} is required in the intra-cluster phase and more P_{ct} used in the inter-cluster phase and this added extra circuit energy overcomes the differences

in transmitting energy consumption caused by adding n_t in this range of d_{ITE}. This is why the curves with larger n_t are above those with small ones in the figure above. However, when d_{ITE} continues to increase, the saving of transmitting energy caused by adding n_t may be bigger than the cost of extra circuit energy and these curves of Co-MISO modes may intersect then.

The comparison of Co-MISO and Co-MIMO over a large range of d_{ITE} is shown in figure 5-2.

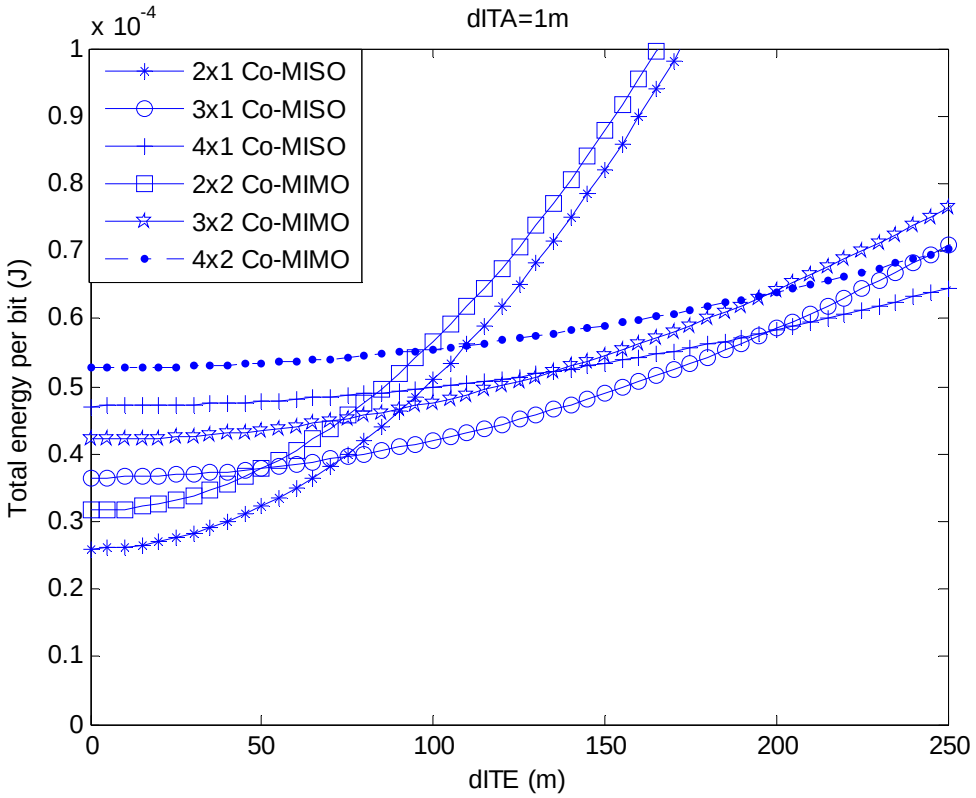

Figure 5-2 One-hop energy consumption of Co-MISO vs Co-MIMO

In figure 5-2, it can be easily seen that all the energy consumption curves go up as d_{ITE} increases. This is apparent because the transmitting energy consumed in the inter-cluster transmission is directly proportional to the path loss. For this scale of d_{ITE}, the curves with the same n_r but different n_t intersect at the point that the benefit in transmitting energy saving caused by adding cooperative nodes offsets the addition of circuit energy consumption. But the curves with a bigger n_r are all above those with the same n_t. These differences between the pairs of 2x1 and 2x2, 3x1 and

3x2, 4x1 and 4x2 are the same and kept as a constant because they are all generated by an additional P_{cr} in the inter-cluster phase and the increasing of n_r in this simulation has no affect on the transmitting energy consumption under the approximation of $\bar{E}_b$ in (5.3).

When $\bar{E}_b$ is obtained from the bit-error-rate performance by using a numerical method such as Monte Carlo simulation, the calculated total energy consumption per bit would have a relationship with n_r because more receivers can improve the BER performance and consume less transmitting power to meet the BER requirement. In this situation, the curves of Co-MIMO may fall below those of Co-MISO when the parameters of circuit power are properly chosen. However, as discussed in chapter 3 (figure 3.4), there is a cluster head selection procedure between the n_r receivers for the next hop when $n_r > 1$, which will increase energy consumption. So, for the simplicity in practical use, it is reasonable to assume that only the cluster head of the next cluster with the most remaining energy is chosen as the receiver for the MISO link of this hop. In the remaining part of this thesis, we consider cooperative MISO instead of Co-MIMO.

It can be seen that the minimum curves across the different number of transmitters in figure 5-1 and 5-2 represents the minimum value that the total energy consumption per bit can reach. This lower bound can be achieved by switching transmission modes from SISO to cooperative 2x1 MISO along d_{ITE}, and continuing to 3x1 Co-MISO, 4x1 Co-MISO , and so on. The approximate sections of transmission distance (d_{ITE}) for each mode can also be obtained in the figures above.

As discussed in former chapters, the total energy for one bit transmission can be divided into the transmitting energy and the circuit energy, or the intra-cluster energy consumption and the inter-cluster energy consumption. To analyze the relationship between these components, firstly, we plot the energy lower bound divided into its transmitting energy and circuit energy for one-hop transmission in figure 5-3.

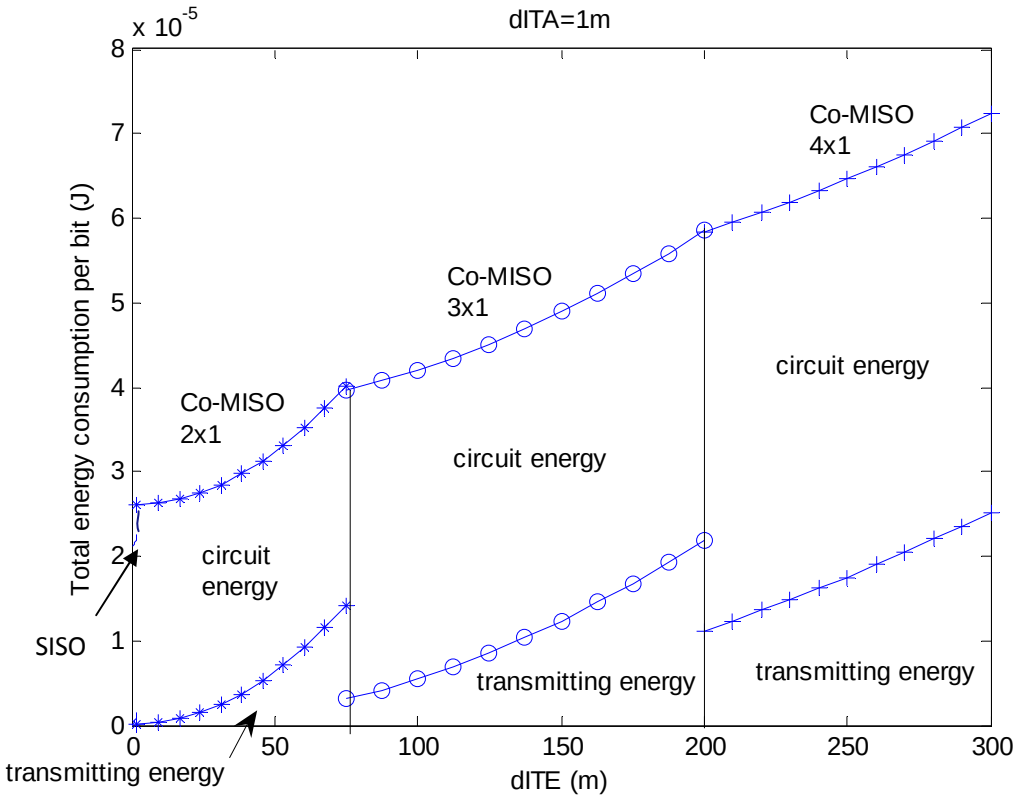

Figure 5-3 Minimum energy divided into transmitting and circuit energy consumption

In figure 5-3, SISO mode exists as the transmission distance is small enough. The circuit energy consumption grows by a fixed value as the number of n_t increases but stays as a constant in each mode, regardless the change of d_{ITE}. For each additional transmitter added as the mode switches, the circuit energy increases by $P_{cr} + P_{ct}$, as the additional cooperative node works as both a receiver in the intra-cluster phase and a transmitter in the inter-cluster phase.

It can also be seen that the transmission energy grows in each mode as d_{ITE} increases but experiences a sudden drop at the switching point, which is caused by the power gain obtained in the inter-cluster cooperative MISO transmission with an additional transmitter. The size of this drop equals to the increment of the circuit energy. For a fixed d_{ITA}, energy used for transmitting in the intra-cluster phases stays as a constant for all the range of d_{ITE}.

Another thing that needs to be stated is that with the present choice of circuit parameters, adopted from other publications, the circuit energy consumption is of the

same order or even bigger than the transmitting energy consumption. This confirms that it is necessary to consider both transmission and circuit energy when deriving the energy equations in Section 5.2.

The minimum energy value of the simulations for one-hop transmission with its energy divided into the intra-cluster and inter-cluster phases is shown in figure 5-4.

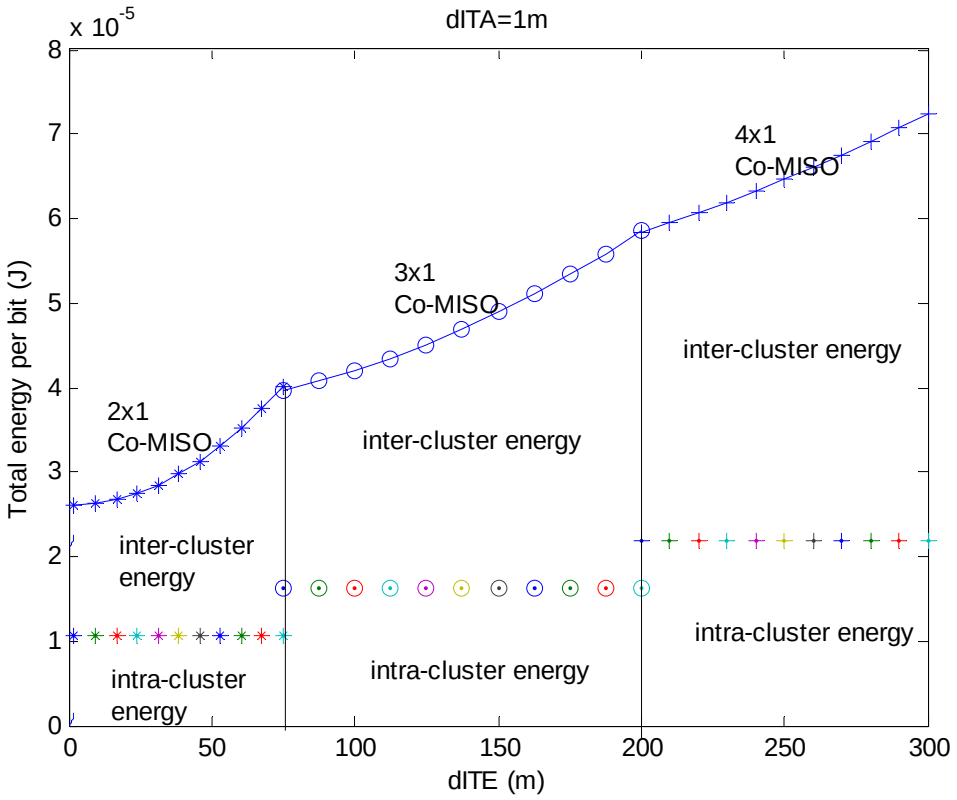

Figure 5-4 Energy lower bound divided into intra-cluster and inter-cluster energy consumption

It can be seen in figure 5-4 that the intra-cluster energy consumption increases by one P_{cr} at each mode switching point and remains constant in each mode due to no changes of d_{ITA}. At each mode switching point, the power gain obtained by adding one transmitter antenna in inter-cluster cooperative MISO transmission offsets the extra circuit energy consumption brought by it. As the inter-cluster transmission distance increases, the energy consumed in inter-cluster phase becomes a more significant part of the total consumption. This is because for a fixed d_{ITA}, the intra-cluster energy increases linearly between different modes, while the transmitting energy consumption in the inter-cluster phase grows exponentially with d_{ITE}.

Therefore, in a large area, methods used to dramatically cut down the inter-cluster transmitting energy can also efficiently decrease the total energy consumption.

From the discussions above, there are advantages in devising a mode switching framework in single-hop transmission in the wireless sensor network that makes the total system energy consumption follow the minimum in figure 5-4 as a function of distance. Details about this framework and its practical mode switching thresholds are discussed in the following section.

5.2 Path-Loss Based Single-hop Mode Switching Framework

5.2.1 Single-hop BER performance for different modes

Energy comparisons for different transmission modes in the last section are all based on (5.4) which is an idealisation of reality, thus cannot determine the exact switching points for practical use. When factors of fading, path loss, STBCs, and different power level allocations for ITA and ITE slots are taken into consideration, $\overline{E}_b$, $\overline{E}_{b-ITA}$, and $\overline{E}_{b-ITE}$ are different for the same BER requirement, so bit-error-rate performances generated by Monte Carlo simulation for these modes are needed, which are shown in figure 5-5.

Figure 5-5 shows the single-hop BER performances of SISO, 2x1 Co-MISO, and 3x1 Co-MISO, for which the bit-error rates for cluster-based cooperative transmissions are calculated over both phases (ITA and ITE) without error correction at the cooperative nodes within the cluster. The abscissa of E_b / N_0 is calculated at the receiver. BER performance of 2x1 Co-MISO using the Alamouti scheme in the ITE phase is also plotted in the same picture. Fading and path loss are both considered here. Rician fading is assumed in ITA broadcasting channels with a path-loss exponent of 1.6 and Rayleigh fading is assumed in ITE cooperative MISO channels with a path-loss exponent of 1.8. A different path loss will lead to different numerical answers, but does not alter the basic principles of your analysis. For simplicity, the time slot allocation parameter is set as $\alpha = 0.5$ for all these transmission modes. The power

allocation parameter β is set as 0.1, so the power level in the ITE phase is 9 times that in ITA phase. The noise levels for the two phases are set equal.

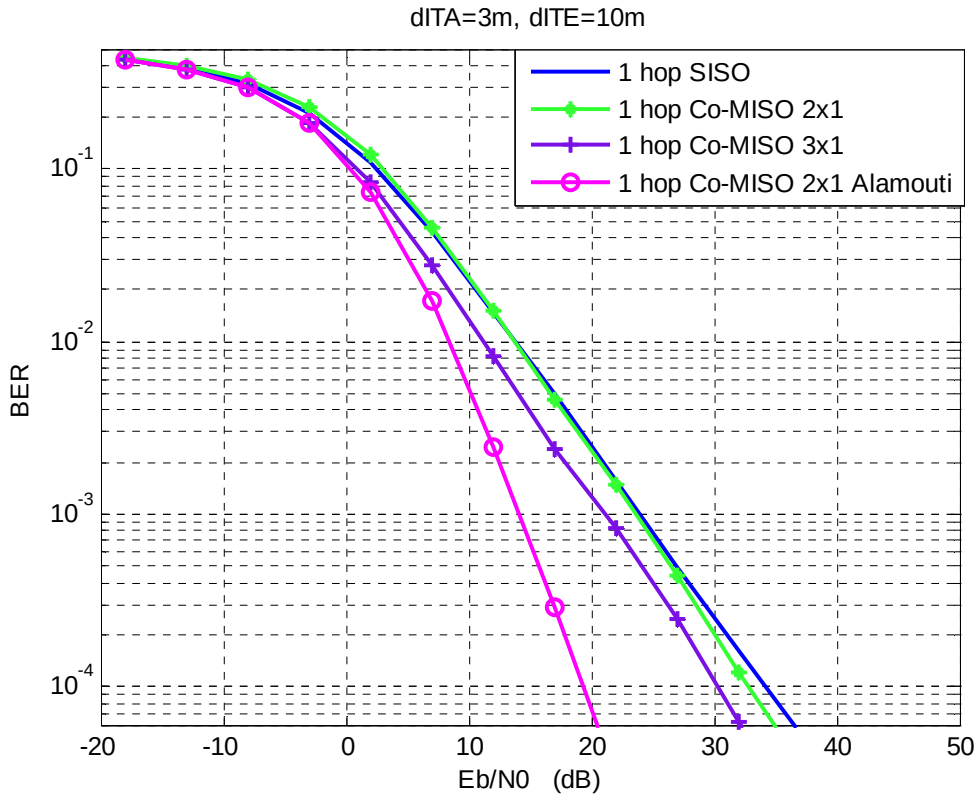

Figure 5-5 BER performance for each mode in single-hop transmission

It can be seen that the BER performance of 2x1 Co-MISO differs little from that of SISO. This is because the diversity gain generated by two repeated data streams is undermined by the extra intra-cluster broadcasting phase. The communication reliability in the ITA phase depends on the allocated power level and the errored data received in this slot is then passed to the ITE phase and cuts down the reliability of cooperative MISO communication. Only when the number of transmitters in cooperative transmission increases to 3 or bigger does the merit of MISO transmission in the ITE phase become clear, and the overall BER performance is better than in the SISO mode. However, more cooperative nodes increases the circuit energy consumption. When the total energy consumptions are compared, it is hard to say if the transmitting energy saved by more cooperative nodes at a fixed BER requirement can offset the extra circuit energy consumption. So, the ideal mode should be one that differs as much as possible from SISO in BER performance but contains as few cooperative nodes as possible. The 2x1 Co-MISO mode, using the Alamouti scheme,

in figure 5-5, balances these two requirements. Although 3x1 or 4x1 Co-MISO with STBCs adopted may get an even better BER performance, considering the system complexity and the loss of data throughput brought by these STBCs, only the 2x1 Co-MISO mode is considered in this section for mode switching from SISO in single-hop transmission. The detailed switching conditions will be discussed next.

5.2.2 Mode switching conditions

When we talk about the data transmission in wireless sensor networks, the first parameter the source node should know is the path-loss to the destination. This parameter can be found by sending an enquiry message before the data transmission or from a memory for a transmitter in a fixed network. In this section we assume that the environment has a path loss exponent of δ, not the ideal square one. Because the path-loss is related to the transmission distance, we use $d_{ITA}^{-\delta}$ and $d_{ITE}^{-\delta}$ to approximate the path-loss for ITA and ITE transmissions.

The total energy equation for the SISO mode in (5.1) can be rewritten as follows.

$$E_{bt\_SISO} = (1+\varepsilon)\cdot \bar{E}_b \times \frac{(4\pi)^2}{G_t G_R \lambda^2 d_{ITE}^{-\delta}} M_l N_f + (P_{ct} + P_{cr}) / R_b \qquad (5.5)$$

For 2x1 Co-MISO mode with Alamouti, the geometry positions of the sensor nodes involved are investigated, and shown in figure 5-6.

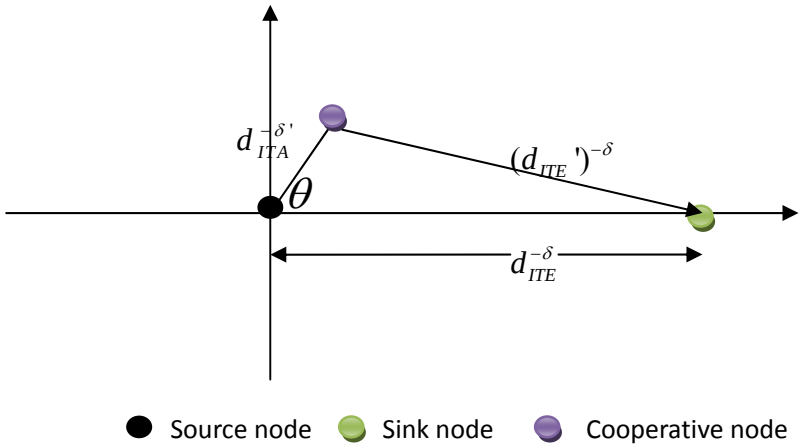

Figure 5-6 Geometry sketch for single-hop Co-MISO (Alamouti)

In figure 5-6, δ and δ' represent the path-loss exponents for intra-cluster and inter-cluster transmissions respectively. θ denotes the angle of the path to the cluster node, with respect to the direct source to destination path. d_{ITE} and d_{ITE}' represent the distances from the source node and from the cooperative node to the destination respectively. For the inter-cluster transmission, the energy received at the receiver for each link should be the direct ratio to the path loss. So, $\bar{E}_{b-ITE}$ obtained by the BER performance at the sink node needs to be divided proportionally into the two links from the source node and the cooperative one to calculate the transmitting power for each link. Under these parameters, the total energy equation for 2x1 Co-MISO (Alamouti) mode can be rewritten as:

$$E_{bt\_Co-MISO} = (1+\varepsilon)\frac{\bar{E}_{b\_ITE}\cdot d_{ITE}^{\ -\delta}}{d_{ITE}^{\ -\delta}+(d_{ITE}')^{-\delta}}\times\frac{(4\pi)^2}{G_tG_R\lambda^2 d_{ITE}^{\ -\delta}}M_lN_f$$

$$+(1+\varepsilon)\frac{\bar{E}_{b\_ITE}\cdot(d_{ITE}')^{-\delta}}{d_{ITE}^{\ -\delta}+(d_{ITE}')^{-\delta}}\times\frac{(4\pi)^2}{G_tG_R\lambda^2(d_{ITE}')^{-\delta}}M_lN_f+(1+\varepsilon)\frac{\bar{E}_{b\_ITA}\cdot(4\pi)^2}{G_tG_R\lambda^2 d_{ITA}^{-\delta'}}M_lN_f$$

$$+(P_{ct}+P_{cr})\cdot\alpha/R_b+(2P_{ct}+P_{cr})\cdot(1-\alpha)/R_b$$

$$=(1+\varepsilon)\frac{2\bar{E}_{b\_ITE}}{(d_{ITE})^{-\delta}+(d_{ITE}')^{-\delta}}\times\frac{(4\pi)^2}{G_tG_R\lambda^2}M_lN_f+(1+\varepsilon)\frac{\bar{E}_{b\_ITA}\cdot(4\pi)^2}{G_tG_R\lambda^2 d_{ITA}^{-\delta'}}M_lN_f$$

$$+(P_{ct}+P_{cr})\cdot\alpha/R_b+(2P_{ct}+P_{cr})\cdot(1-\alpha)/R_b \qquad (5.6)$$

To compare SISO and 2x1 Co-MISO (Alamouti) modes, an extreme situation is

investigated first. Let d_{ITA} equal zero, i.e. the location of the source node and the cooperative node overlap. d_{ITE} equals to d_{ITE}' at this time. There would be no transmitting power consumption in the broadcasting phase. Then the energy equation (5.6) for 2x1 Co-MISO (Alamouti) mode reaches the minimum value for a fixed destination path-loss $d_{ITE}^{-\delta}$.

$$\min(E_{bt\_Co-MISO}) = \lim_{d\to 0} E_{bt\_Co-MISO}$$

$$= (1+\varepsilon)\bar{E}_{b\_ITE} \times \frac{(4\pi)^2}{G_t G_R \lambda^2 d_{ITE}^{-\delta}} M_l N_f + (P_{ct} + P_{cr}) \cdot \alpha / R_b + (2P_{ct} + P_{cr}) \cdot (1-\alpha) / R_b \quad (5.7)$$

When the destination path-loss $d_{ITE}^{-\delta}$ changes, by comparing (5.5) and (5.7), we can get a critical point of $d_{ITE}^{-\delta}$ which sets the values of these two equations equal. This critical destination path-loss is shown in figure 5-7.

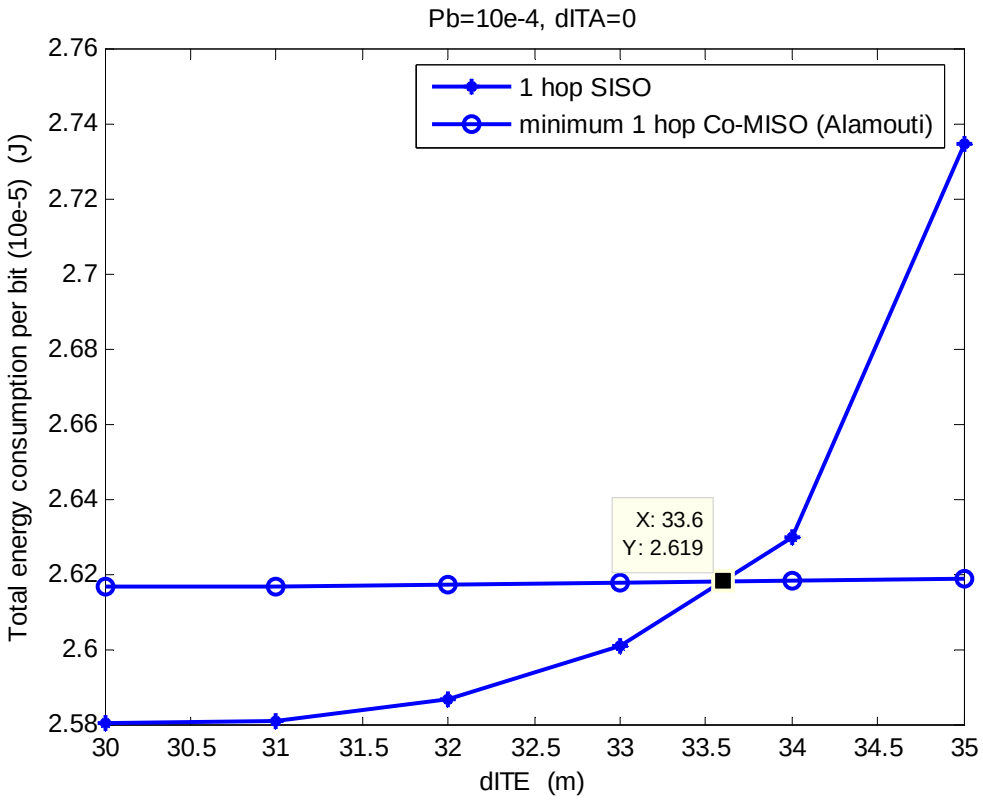

Figure 5-7 Energy consumption for single-hop SISO and Co-MISO with $d_{ITA} = 0$

It can be seen in figure 5-7 that under the parameters of this simulation, the critical point of destination path-loss is $33.6^{-\delta}$ ($\delta = 1.9$). When the transmission distance is smaller than 33.6m, the total energy consumption per bit of single-hop SISO mode is

smaller than the minimum value of Co-MISO (Alamouti) mode. If the destination path-loss falls into this range, SISO mode is more energy-efficient than Co-MISO (Alamouti) mode in single-hop transmission. The value of this critical path-loss depends on the system parameters, especially the circuit energy. When more energy-efficient circuits are adopted in sensor nodes, the advantage of Co-MISO in saving transmitting energy will be more pronounced, which makes the critical path-loss even smaller.

When the transmission distance is bigger than 33.6m, the energy curve of the single-hop SISO mode crosses over the minimum one of the Alamouti Co-MISO mode. In this situation, d_{ITA} needn't be zero to maintain the energy equation of these two modes. So, for the large destination path-loss in this situation, there exists a threshold for the cooperative node selection to make the Alamouti Co-MISO mode consume less energy than SISO. This threshold can be obtained as follows.

In figure 5-6, by the law of cosines, the geometry distances of all the signal paths can be expressed as:

$$(d_{ITE}')^2 = {d_{ITA}}^2 + {d_{ITE}}^2 - 2d_{ITA}d_{ITE}\cos\theta, \qquad \theta \in [0, 2\pi) \tag{5.8}$$

Then we get

$$(d_{ITE} - d_{ITA})^2 \le d_{ITE}' = ({d_{ITA}}^2 + {d_{ITE}}^2 - 2d_{ITA}d_{ITE}\cos\theta) \le (d_{ITE} + d_{ITA})^2, \theta \in [0, 2\pi) \tag{5.9}$$

Equality of the first condition in (5.9) is established only when $\theta = 0$, and the second when $\theta = \pi$, corresponding to the minimum and the maximum values of d_{ITE}' for a fixed d_{ITA}. A sketch of the area prescribed by this threshold is plotted in figure 5-8.

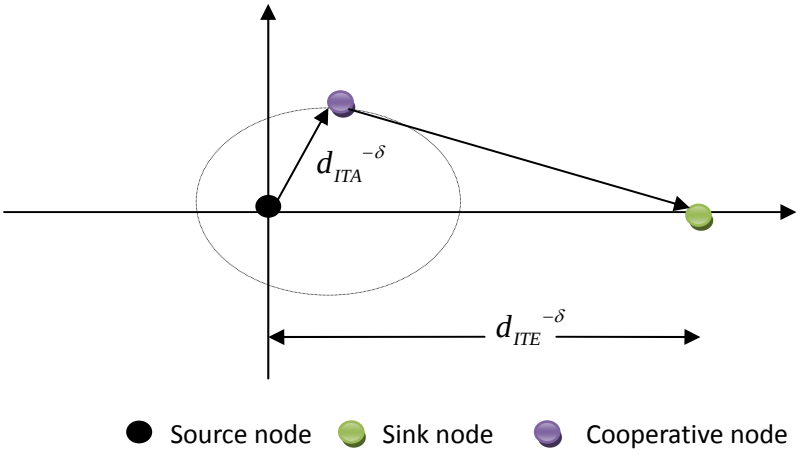

Figure 5-8 Sketch of the threshold area for Co-MISO (Alamouti)

Based on (5.5), (5.6), (5.8), the simulated threshold area for the destination path-loss of $35^{-\delta}$ is shown in figure 5-9.

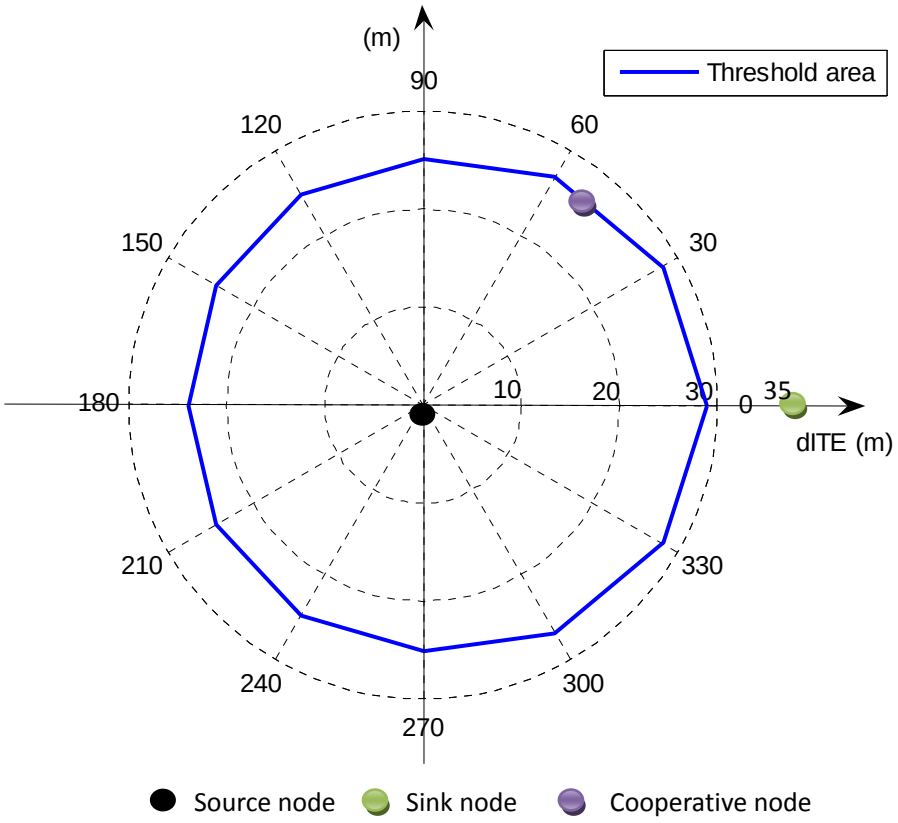

Figure 5-9 Simulated threshold area

In figure 5-9, the threshold distance area is plotted as θ increases by a increment of $\pi/6$. This area corresponds to a path-loss area for the intra-cluster phase. With a fixed destination pass loss of $35^{-\delta}$ ($\delta = 2.7$), single-hop Co-MISO (Alamouti) mode

is better than single-hop SISO mode in energy saving only when the local path-loss falls within this area. In another words, if the neighbor node with the smallest path-loss falls outside this area, no cooperative node can make the Co-MISO (Alamouti) mode more energy-efficient than the one-hop SISO mode and the latter one will always be chosen in this situation. Figure 5-9 also provides a criterion for cooperative node selection and the local cluster size. When the cluster-based Co-MISO (Alamouti) mode is to be adopted in a wireless sensor network, sensors within the path-loss threshold area should be formed into one cluster. Each cluster should involve at least one node within the path-loss threshold area of the cluster-head. The size of this threshold area depends on both the system parameters and the destination path-loss.

When the destination path-loss continues to increase, both single-hop SISO and single-hop Co-MISO (Alamouti) mode may not be energy-efficient for this long distance transmission. Multi-hop methods will then be adopted. The detailed mode switching framework for multi-hop transmission will be discussed in next chapter.

5.3 Conclusions

To achieve energy-efficient transmission in wireless sensor networks, energy evaluations for different transmission modes need to be made.

In this chapter, an approximate comparison of different single-hop transmission modes are made firstly based on the total energy equations. By adopting an estimated parameter of $\bar{E}_b$ ($\bar{E}_{b-ITA}$ and $\bar{E}_{b-ITE}$) in (5.4), the relationship of these transmission modes and their energy consumption components (transmitting and circuit, intra-cluster and inter-cluster) are illustrated in simulations. The simulation results indicate that when circuit energy is considered, there exists a mode switching framework for single-hop transmission based on the transmission distance or the path-loss, which can achieve the minimum total energy consumption of the whole system. The detailed operations for this framework and ways to get the mode switching thresholds are then discussed in Section 5.2.

In Section 5.2, BER performances of different transmission modes are first

investigated to calculate a more accurate $\overline{E}_b$ ($\overline{E}_{b-ITA}$ and $\overline{E}_{b-ITE}$). Taking into consideration of factors such as fading, path-loss, and power and time slot allocation, 2x1 Alamouti cooperative MISO mode can get a sufficient saving of transmitting energy compared with SISO and a relative lighter load compared to other cooperative MISO modes. So the mode switching framework in single-hop is constrained between SISO and Co-MISO (Alamouti).

With measures of destination path-loss, it is revealed in the simulation that there exists a critical path-loss (distance) from the source to the destination, below which the SISO mode will definitely better than the Co-MISO mode in energy saving. When the destination path-loss continues growing, there is a threshold area for the selection of cooperative node to make the Co-MISO (Alamouti) mode more energy-efficient than SISO. This area corresponds to the path-loss limitation within the cluster. Co-MISO mode is only switched to when there is at least one member node around the cluster-head satisfying the intra-cluster path-loss limitation. If no neighbor nodes fall into this area around the cluster-head, SISO mode will continue being used. However, multi-hop transmission is proved to be another effective method for energy-efficient transmission, so with the continuously growing destination path-loss (transmission distance), there should also be a mode switching framework between the single-hop and the multi-hop transmissions. This multi-hop mode switching framework will be discussed in Chapter 6.

Chapter 6
Multi-hop Mode Switching Framework for Wireless Sensor Networks

Besides MIMO techniques, multi-hop frameworks are also proved an effective way for energy-efficient transmission. Because the transmitted power usually decreases exponentially along the signal path, dividing the long transmission distance into several small pieces, which is called multi-hop, can effectively reduce the transmitting energy for the whole communication system. However, when circuit energy consumption is considered in wireless sensor networks, multi-hop will arouse more energy consumed within the sensor node circuits and may counteract the merit brought in transmitting energy saving. So similar to the single-hop transmission discussed in Chapter 5, there should also be a mode switching framework in multi-hop transmission to minimize the system energy consumption as little as possible.

The structure of this chapter is organized as follows. In Section 6.1, an approximated comparison of different modes in multi-hop transmission with equal-division relaying nodes is made. The energy lower bound for multi-hop modes versus transmission distance is also plotted and is used to compare with the lower bound for single-hop

modes. In Section 6.2, the BER performance for different transmission modes in multi-hop transmission is investigated. Then according to the geometry position relationship of the source node, cooperative nodes, relaying nodes (cluster), and the sink node, a path-loss based multi-hop mode switching framework is proposed. This framework investigates the critical condition when the single-hop mode switches to the multi-hop mode. Then, the operation of this framework in practical use with equal-division and unequal-division relaying nodes (cluster) is stated. The available existing area for the relaying node (cluster) is obtained by simulations. Finally, Section 6.3 gives the conclusions of this chapter.

6.1 Energy Comparison for Different Modes in Multi-hop transmission

Similar to the single-hop situation, the energy comparison for different modes in multi-hop transmission is firstly made based on the Chernoff bound estimation of $\overline{E}_b$ ($\overline{E}_{b-ITA}$ and $\overline{E}_{b-ITE}$). To make a fair comparison, the transmission distance of the whole multi-hop system is set the same as the single-hop one. The relaying nodes or clusters are assumed to be at the equal-division points along the signal path for the time being. So, the transmission distance for each hop is d_{ITE}/m, where m is the number of hops. The intra-cluster transmission distance for all the hops are set the same and equal to d_{ITA}. On a fixed end-to-end bit-error-rate P_e, the BER for each hop is calculated as $1-(1-P_e)^{1/m}$ in multi-hop transmission. The total energy consumption equations for multi-hop SISO and multi-hop Co-MISO can be written as follows.

- Multi-hop SISO

$$E_{bt\_multi\_SISO} = m \cdot \frac{P_{PA} + P_{ct} + P_{cr}}{R_b}$$

$$= (1+\varepsilon) \cdot m \cdot \overline{E}_b \times \frac{(4\pi d_{ITE}/m)^2}{G_t G_R \lambda^2} M_l N_f + m \cdot \frac{P_{DAC} + P_{mix} + P_{fil} + P_{syn}}{R_b}$$

$$+m\cdot\frac{P_{LNA}+P_{mix}+P_{IFA}+P_{fil}+P_{ADC}+P_{syn}}{R_b} \tag{6.1}$$

- Multi-hop Co-MISO

$$E_{bt\_multi\_Co-MISO}=m\cdot\frac{P_{PA\_ITA}+P_{PA\_ITE}+\alpha\cdot[P_{ct}+(n_t-1)P_{cr}]+(1-\alpha)\cdot(n_t\cdot P_{ct}+P_{cr})}{R_b}$$

$$=(1+\varepsilon)\cdot m\cdot\bar{E}_{b\_ITA}\times\frac{(4\pi d_{ITA})^2}{G_tG_R\lambda^2}M_lN_f+(1+\varepsilon)\cdot m\cdot\bar{E}_{b\_ITE}\times\frac{(4\pi d_{ITE}/m)^2}{G_tG_R\lambda^2}M_lN_f$$

$$+m\cdot[\alpha+(1-\alpha)\cdot n_t]\cdot\frac{P_{DAC}+P_{mix}+P_{fil}+P_{syn}}{R_b}$$

$$+m\cdot[\alpha\cdot(n_t-1)+(1-\alpha)]\cdot\frac{P_{LNA}+P_{mix}+P_{IFA}+P_{fil}+P_{ADC}+P_{syn}}{R_b} \tag{6.2}$$

$\bar{E}_{b-ITA}$ and $\bar{E}_{b-ITE}$ in (6.2) are estimated as the expression of $n_tN_0/[1-(1-P_b)^{1/m}]^{1/n_t}$. The total energy consumption per bit for multi-hop transmissions versus the transmission distance are plotted in the following figures.

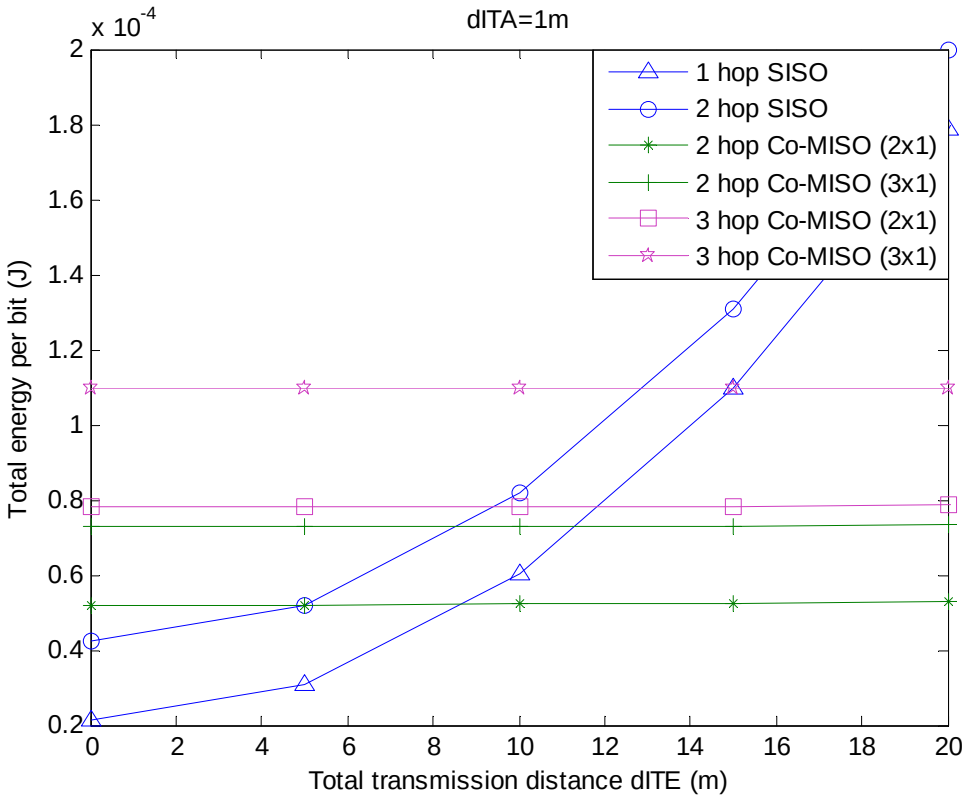

Figure 6-1 Multi-hop energy consumption in short range of distance

The total energy curve of the one-hop SISO mode in figure 6-1 is the same as that in figure 5-1. It can be seen that the two-hop SISO mode consumes more energy than the one-hop SISO because in the small range of d_{ITE}, the circuit energy generated by adding relaying nodes for multi-hop is the dominant part in the total energy consumption.

As d_{ITE} increases, the benefit of transmitting energy saving by dividing a large distance into short pieces for multi-hop transmission will stand out. The curves of one-hop SISO and two-hop SISO modes should intersect at a certain distance and after that the latter should be more energy efficient than the former. The reason that these two curves in figure 6-1 go close slowly lies on the evaluation of E_b again. E_b evaluated in (6.1) is only decided by P_b but takes no consideration of the path loss and fading. The larger of the difference in transmission distances, the bigger of the difference in E_b for a fixed BER.

Compared to figure 5-1, more hops make the energy curves in figure 6-1 higher. With the same explanation of single-hop situation, curves with more transmitters in cooperative MISO transmission all flow over those with the same number of hops but fewer transmitters. The energy curve of two-hop 3x1 Co-MISO is lower than that of three-hop 2x1 Co-MISO. This is because in short distance transmission with the preset parameters, the benefit gained by adding more cooperative transmitters for each hop is bigger than that caused by increasing the number of hops.

The total energy curves for multi-hop transmissions in large range of distance are plotted in figure 6-2.

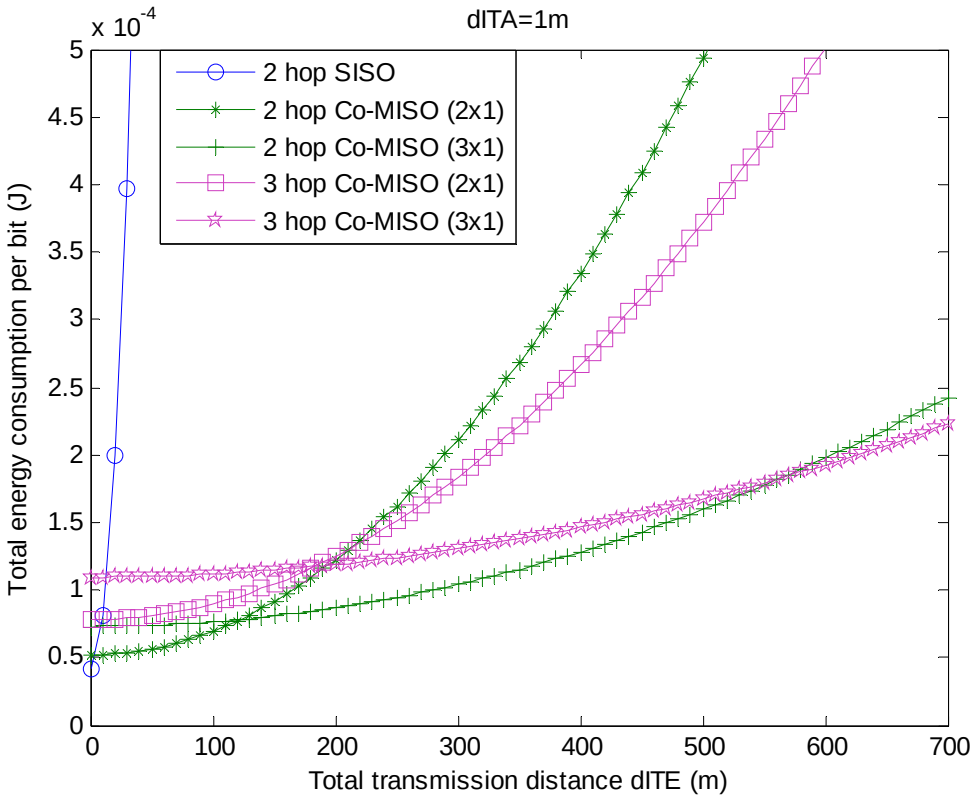

Figure 6-2 Multi-hop energy consumption in large range of distance

In figure 6-2, it can be seen that more hops and more cooperative transmitters with the same number of hops can save more energy for the whole system in large distance communication, despite of the extra circuit energy consumed. The curve of two-hop 3x1 Co-MISO always goes under that of three-hop 2x1 Co-MISO and there is no intersection between them under the chosen parameters. So, in conditions of this simulation, increasing of cooperative transmitters, not the number of hops, should be considered first to improve the energy efficiency of the communication system. The abscissa in figure 6-2 is only used to show the long trend of energy consumption over dITE. In practice use, there should be a range of reasonable ratio of dITA and dITE.

Similar to the single-hop situation, the minimum simulated bound of the total energy consumption per bit for multi-hop systems can also be obtained from figure 6-2, which is composed of sections such as 2-hop SISO, 2-hop 2x1 Co-MISO, 2-hop 3x1 Co-MISO, and 3-hop 3x1 Co-MISO. The energy lower bounds of multi-hop and single-hop transmissions are both plotted in figure 6-3.

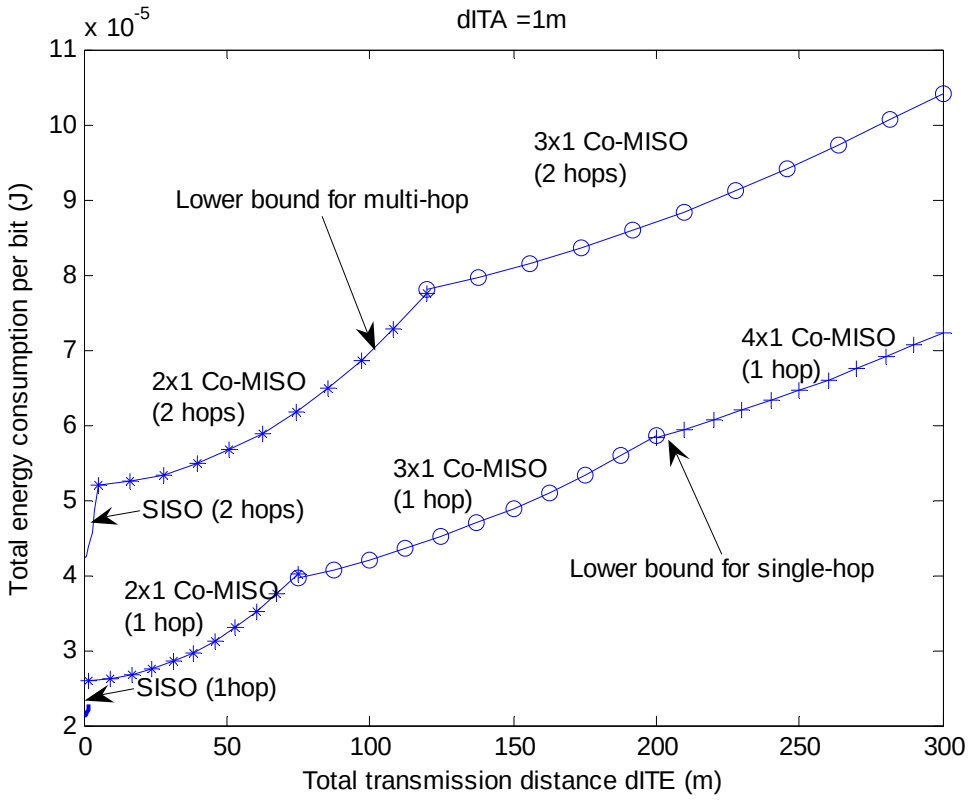

Figure 6-3 Energy lower bound of multi-hop and single-hop transmissions

From figure 6-3, it can be seen that the energy lower bound for single-hop transmission goes below that of multi-hop transmission, because the extra energy brought by adding more hops is bigger than that brought by adding more cooperative transmitters in short range based on the parameters of the circuit energy and the estimated E_b. In large distance, the energy benefit of multi-hop transmission will stand out and these two curves have the trend to get close but it is hard to say if they will intersect or not when both the number of hops and the number of cooperative antennas (n_t) are freely chosen. However, what we can got from this figure is that for an upper limit of n_t, these two curves will definitely cross at a certain transmission distance, which represents the switching threshold from single-hop to multi-hop transmission. The detailed mode switching framework in multi-hop transmission will be discussed in next section.

6.2 Path-loss Based Mode Switching Framework for Multi-hop Transmission

6.2.1 Multi-hop BER performance for different modes

Similar to the single-hop situation, the multi-hop mode switching framework is also based on the calculation of $\overline{E}_b$, $\overline{E}_{b-ITA}$, and $\overline{E}_{b-ITE}$ first. So, the BER performances for different modes in multi-hop transmission are plotted in figure 6-4.

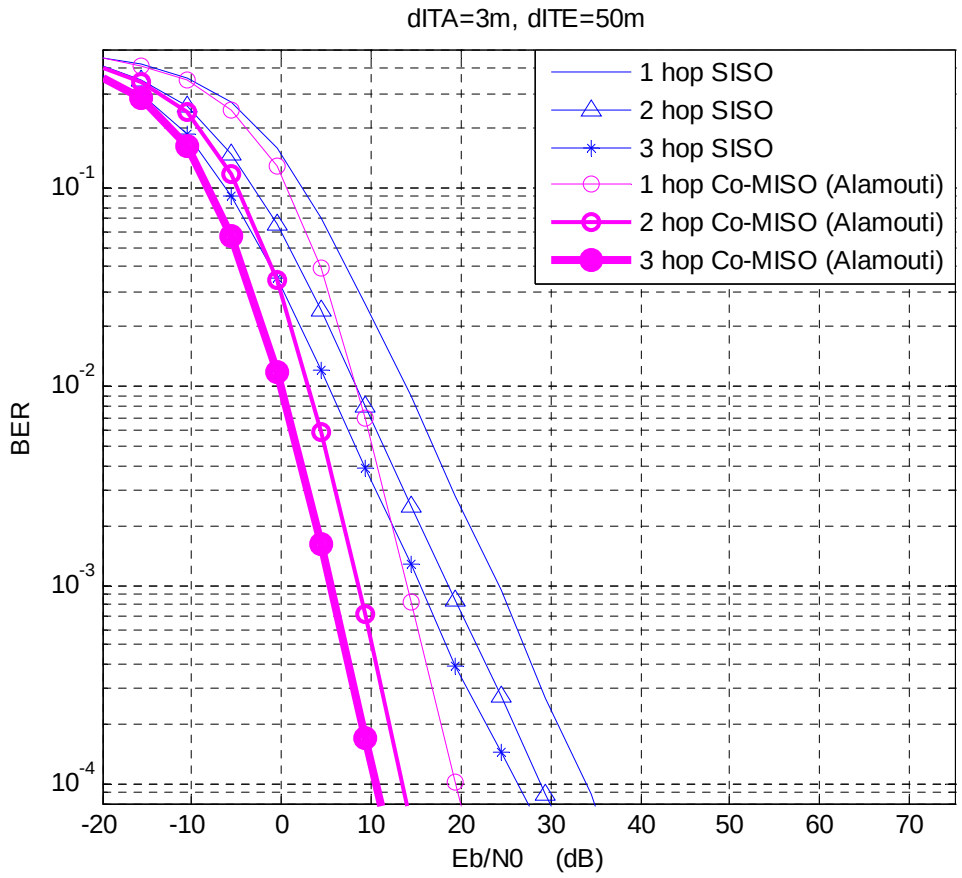

Figure 6.4 BER performances in multi-hop transmission

Figure 6.4 shows the BER performances of 1-hop, 2-hop, 3-hop transmission for SISO and cooperative MISO (Alamouti) modes under the condition of $d_{ITA} = 3\,\mathrm{m}$, $d_{ITE} = 50\,\mathrm{m}$. E_b / N_0 is calculated at the destination receiver. Rician fading is assumed in intra-cluster phase with the path-loss exponent of 2.7 and Rayleigh fading is assumed in inter-cluster phase with 3 as the path-loss exponent. The parameter for power level allocation between intra-cluster and inter-cluster phases is also set as

$\beta = 0.1$. Time slot allocation is set as $\alpha = 0.5$.

In figure 6.4, it can be seen that for the same number of hops, the BER performance of Co-MISO (Alamouti) mode is better than that of SISO. This improvement is caused mainly by the MISO link in ITE phase for Co-MISO mode.

It can also be seen that with the number of hops increasing, the BER performance has a diminishing improvement. This is because dividing longer distance into small pieces does reduce the bit-error-rate caused by fading or path-loss along the channel but for a fixed total transmission distance, this improvement caused by distance division is limited. Considering more hops will cause more extra circuit energy, a tradeoff between the number of hops and the BER improvement need to be made. In this chapter, only two-hop transmission modes are considered in the multi-hop mode switching framework. Three and more hops transmission can be composed of two and single hop mode. The switching threshold from single-hop to two-hop transmission modes including SISO and Co-MISO (Alamouti) will be discussed in the following section.

6.2.2 Mode switching conditions for two-hop SISO

According to the discussion in Chapter 5, the transmission mode in single-hop will switch from SISO to Co-MISO as the destination path-loss or distance increases. When the destination path-loss grows further, multi-hop may be adopted. However, it is not clear which multi-hop mode should be adopted first, two-hop SISO or two-hop Co-MISO (Alamouti). The former one is discussed first here.

Before comparing one-hop Co-MISO (Alamouti) with two-hop SISO, the most energy efficient situation for the latter mode should be found first. Because the transmitting energy consumed in this two-hop system is related to the distance sum of the two hops, to save more energy, the relay node (cluster) should be on the line of the sight signal. Assuming the transmission distances for these two hops are d_{ITE1} and d_{ITE2} ($d_{ITE1} + d_{ITE2} = d_{ITE}$), figure 6.5 shows the transmission sketches of the single-hop Co-MISO (Alamouti) and the two-hop SISO modes.

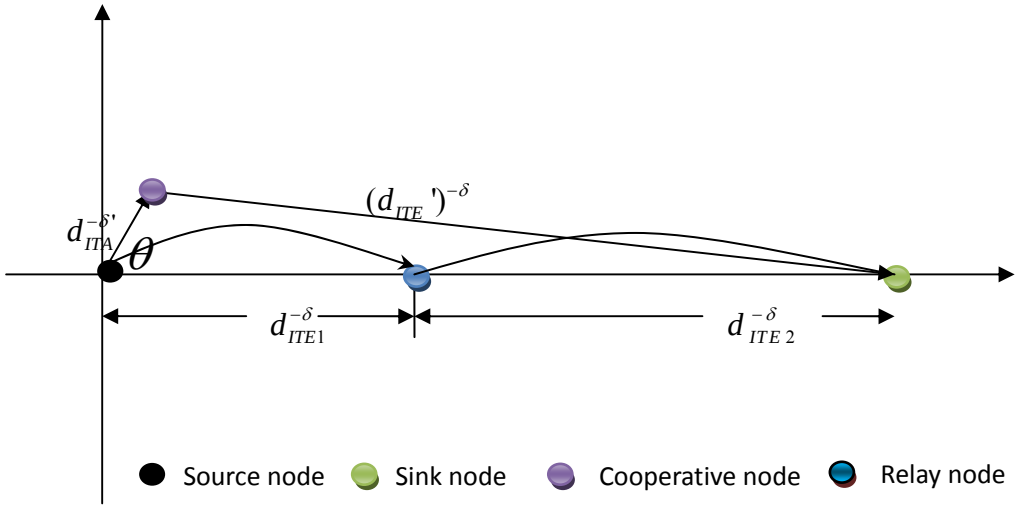

Figure 6.5 Sketches of one-hop Co-MISO (Alamouti) and two-hop SISO

In the figure above, the path-loss exponents for inter-cluster transmission in the two hops are set the same as δ. Based on (6.1), the total energy equation of the two-hop SISO mode can be written as

$$E_{bt\_2hop\_SISO} = (1+\varepsilon)\cdot \bar{E}_{b\_ITE1} \times \frac{(4\pi)^2}{G_t G_R \lambda^2 d_{ITE1}^{-\delta}} M_l N_f$$

$$+(1+\varepsilon)\cdot \bar{E}_{b\_ITE2} \times \frac{(4\pi)^2}{G_t G_R \lambda^2 d_{ITE2}^{-\delta}} M_l N_f + 2(P_{ct}+P_{cr})/R_b \quad (6.3)$$

$\bar{E}_{b-ITE1}$ and $\bar{E}_{b-ITE2}$ are the received energy per bit in these two hops respectively. By Hölder Mean (or Generalized Power Mean) Inequality, the distances of d_{ITE1}, d_{ITE2} and d_{ITE} satisfy an inequation as:

$$\left(\frac{1/d_{ITE1}^{-\delta} + 1/d_{ITE2}^{-\delta}}{2}\right)^{\frac{1}{\delta}} = \left(\frac{d_{ITE1}^{\delta} + d_{ITE2}^{\delta}}{2}\right)^{\frac{1}{\delta}} \geq \frac{d_{ITE1}+d_{ITE2}}{2} = \frac{d_{ITE}}{2} \quad (6.4)$$

The equation of (6.4) establishes only when $d_{ITE1} = d_{ITE2}$. So the equation (6.3) reaches the minimum value when the relay node (cluster) is right at the center point of the signal line. The minimum value of (6.3) can be expressed as:

$$\mathbf{min}(E_{bt\_2hop\_SISO}) = 2\cdot(1+\varepsilon)\cdot \bar{E}_{b\_ITE1} \times \frac{(4\pi)^2}{G_t G_R \lambda^2 (\frac{d_{ITE}}{2})^{-\delta}} M_l N_f + 2(P_{ct}+P_{cr})/R_b \quad (6.5)$$

In one-hop Co-MISO (Alamouti) transmission, the intra-cluster transmission distance d_{ITA} has a natural limit, which is $d_{ITA} \le d_{ITE}$. The total energy consumption of this mode in (5.6) reaches the maximum value when we set $d_{ITA} = d_{ITE}$ and $\theta = \pi$. By comparing this maximum energy consumption of one-hop Co-MISO (Alamouti) mode with the minimum value of two-hop SISO mode in (6.5), we can find if there exists a threshold point for mode switching. These two curves of total energy versus destination distance are plotted in figure 6.6.

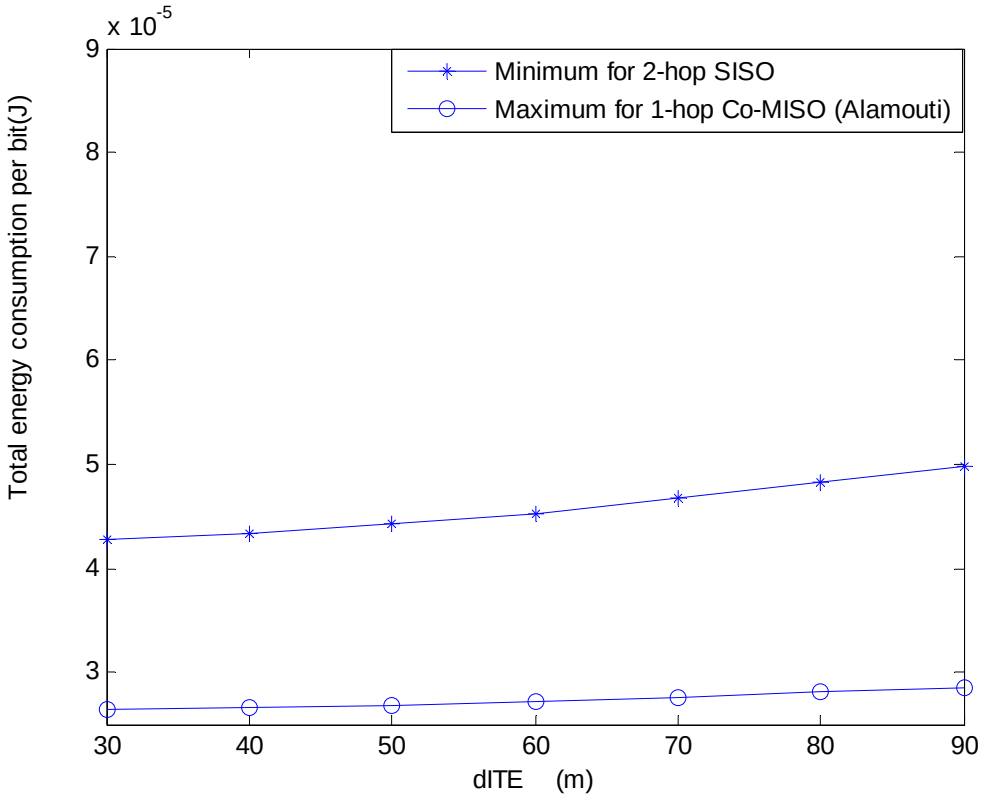

Figure 6.6 Energy consumption of two-hop SISO and one-hop Co-MISO modes

It can be seen that the maximum energy curve of the one-hop Co-MISO (Alamouti) mode is always below the minimum one of the two-hop SISO mode. As the transmission distance increases, these two curves diverge and there is no intersection， This is because in short distance transmission, the circuit energy consumption caused by adding a relaying node is more than that brought by a cooperative one under the time division scheme, while in long distance transmission, the transmitting energy consumption grows faster in SISO link than in MISO link, which makes the one-hop Co-MISO (Alamout) mode even better in total energy saving.

Figure 6.6 reveals that along the whole range of transmission distance , one-hop Co-MISO (Alamouti) is better than two-hop SISO mode under the simulation parameters of circuit energy. When the location of the relay node is not so ideal (at the middle point of the line of sight), the energy situation of the latter one will be even worse. The transmission power gain obtained by multi-hop is not obvious in this situation. So, multi-hop SISO is not fit for this mode switching framework.

6.2.3 Mode switching conditions for two-hop Co-MISO (Alamouti)

In this section, we will investigate mode switching from one-hop Co-MISO (Alamouti) to two-hop Co-MISO (Alamouti). Firstly, we consider the situation that the relaying node (cluster) is along the line of sight signal, shown in figure 6.7.

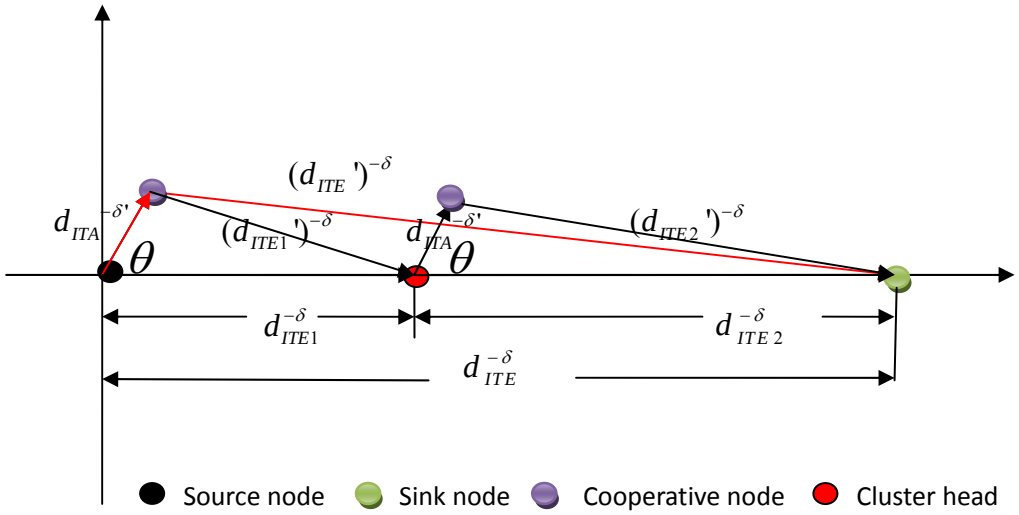

Figure 6.7 Sketches of one-hop and two-hop Co-MISO (Alamouti)

In figure 6.7, let the angle θ and d_{ITA} in each cluster are the same. $(d_{ITE1}')^{-\delta}$ and $(d_{ITE2}')^{-\delta}$ represent the inter-cluster path-loss for the cooperative node in each hop. Based on (5.6), the energy equation for two-hop Co-MISO (Alamouti) mode can be expressed as:

$$E_{bt\_2hop\_Co-MISO} = (1+\varepsilon)\frac{\overline{E}_{b\_ITE1}\cdot d_{ITE1}{}^{-\delta}}{d_{ITE1}{}^{-\delta}+(d_{ITE1}')^{-\delta}}\times\frac{(4\pi)^2}{G_tG_R\lambda^2 d_{ITE1}{}^{-\delta}}M_lN_f$$

$$+(1+\varepsilon)\frac{\overline{E}_{b\_ITE1}\cdot (d_{ITE1}')^{-\delta}}{d_{ITE1}{}^{-\delta}+(d_{ITE1}')^{-\delta}}\times\frac{(4\pi)^2}{G_tG_R\lambda^2 (d_{ITE1}')^{-\delta}}M_lN_f$$

$$+(1+\varepsilon)\frac{\overline{E}_{b\_ITE2}\cdot d_{ITE2}{}^{-\delta}}{d_{ITE2}{}^{-\delta}+(d_{ITE2}')^{-\delta}}\times\frac{(4\pi)^2}{G_tG_R\lambda^2 d_{ITE2}{}^{-\delta}}M_lN_f$$

$$+(1+\varepsilon)\frac{\overline{E}_{b\_ITE2}\cdot (d_{ITE2}')^{-\delta}}{d_{ITE2}{}^{-\delta}+(d_{ITE2}')^{-\delta}}\times\frac{(4\pi)^2}{G_tG_R\lambda^2 (d_{ITE2}')^{-\delta}}M_lN_f$$

$$+2\cdot(1+\varepsilon)\frac{\overline{E}_{d\_ITA}\cdot(4\pi)^2}{G_tG_R\lambda^2 d_{ITA}{}^{-\delta'}}M_lN_f$$

$$+2\cdot(P_{ct}+P_{cr})\cdot\alpha/R_b+2\cdot(2P_{ct}+P_{cr})\cdot(1-\alpha)/R_b \qquad (6.6)$$

Similar to the two-hop SISO mode, (6.6) reaches the minimum value when the relaying cluster-head is at the center point of the sight signal ($d_{ITE1}=d_{ITE2}$), which can be written as:

$$\min(E_{bt\_2hop\_Co-MISO}) = (1+\varepsilon)\frac{2\overline{E}_{b\_ITE1}+2\overline{E}_{b\_ITE2}}{(d_{ITE}/2)^{-\delta}+(d_{ITE}'/2)^{-\delta}}\times\frac{(4\pi)^2}{G_tG_R\lambda^2}M_lN_f$$

$$+2(1+\varepsilon)\frac{\overline{E}_{b\_ITA}\cdot(4\pi)^2}{G_tG_R\lambda^2 d_{ITA}{}^{-\delta'}}M_lN_f+2(P_{ct}+P_{cr})\cdot\alpha/R_b$$

$$+2(2P_{ct}+P_{cr})\cdot(1-\alpha)/R_b \qquad (6.7)$$

By comparing (5.6) and (6.7), we hope to find a critical $d_{ITE}{}^{-\delta}$, which sets the energy consumption of the one-hop Co-MISO mode equals the minimum value of the two-hop Co-MISO mode. These two energy curves versus the transmission distance are shown in figure 6.8.

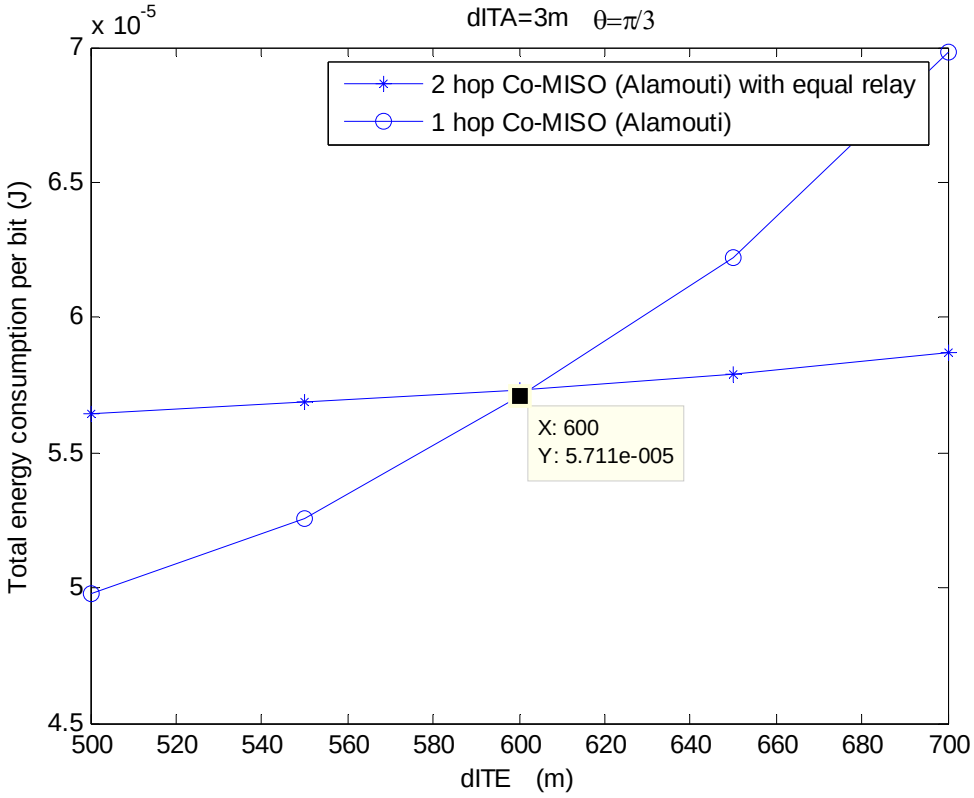

Figure 6.8 Energy consumption of one-hop and two-hop Co-MISO modes

The intersection in figure 6.8 represents the destination path-loss threshold. When the destination distance is smaller than 600m, one-hop Co-MISO mode is more energy-efficient than two-hop Co-MISO mode. When the path-loss is bigger than $600^{-\delta}$, the energy curve of the single-hop mode crosses over that of the two-hop mode with equal relay. In this situation, transmitting power gain obtained in two-hop transmission overcomes the extra circuit energy caused by relaying node (cluster). One-hop Co-MISO (Alamouti) mode should switch to the two-hop Co-MISO (Alamouti) mode for energy saving. This critical destination path-loss largely depends on the parameters of circuit energy. Diminished circuit energy makes the mode switch in smaller path-loss (shorter distance).

When the destination path-loss is bigger than this threshold, the location limitation of the relaying node (cluster) is loosened. The relaying node can move within an area (not only along the line of sight signal) and maintain the total energy consumption less than that of single-hop. A sketch of this two-hop transmission without middle point relaying node (cluster) is shown in figure 6.9.

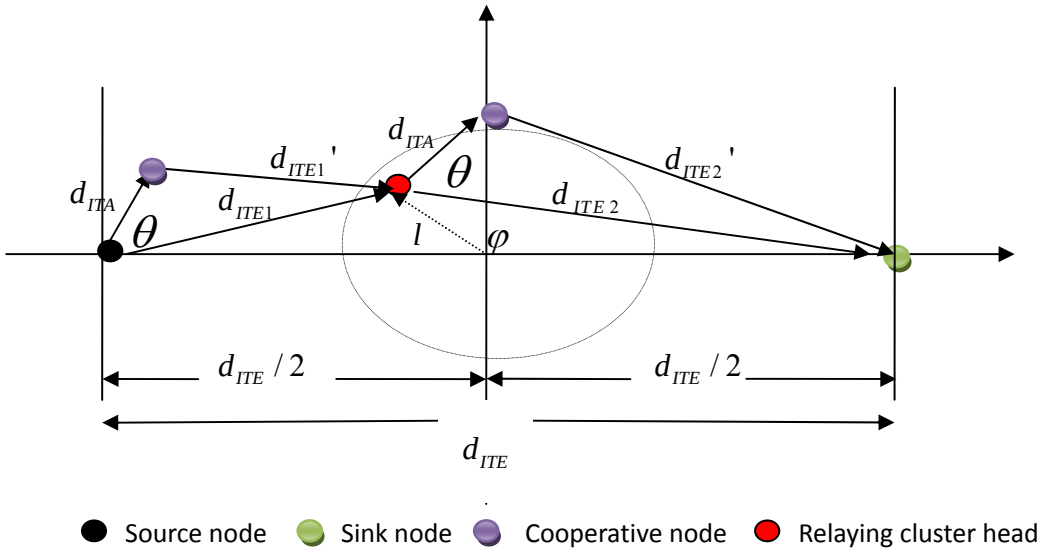

Figure 6.9 Sketch of the area for relaying node (cluster)

In the figure above, $d_{ITE1}+d_{ITE2}\geq d_{ITE}$. (l,φ) is the polar coordinate from the middle point of the sight signal with l as the radius and φ as the angle. In this non-ideal situation, the energy equation has the same expression of (6.6) but with additional limitations.

$$\begin{cases} d_{ITE1}^2=\left(\frac{d_{ITE}}{2}\right)^2+l^2-2\cdot\frac{d_{ITE}}{2}\cdot l\cdot\cos(\pi-\varphi) \\ d_{ITE2}^2=\left(\frac{d_{ITE}}{2}\right)^2+l^2-2\cdot\frac{d_{ITE}}{2}\cdot l\cdot\cos\varphi \\ (d_{ITE1}')^2={d_{ITE1}}^2+{d_{ITA}}^2-2\cdot d_{ITE1}\cdot d_{ITA}\cdot\cos\theta \\ (d_{ITE2}')^2={d_{ITE2}}^2+{d_{ITA}}^2-2\cdot d_{ITE2}\cdot d_{ITA}\cdot\cos\theta \\ (\varphi\in[0,2\pi)) \end{cases} \tag{6.8}$$

For a fixed destination path-loss ($700^{-\delta}$), by comparing the energy consumption of single-hop Alamouti Co-MISO in (5.6) with that of two-hop Alamouti Co-MISO in (6.6) and (6.8), the possible existing area for relaying node (cluster) can be obtained and shown in figure 6.10.

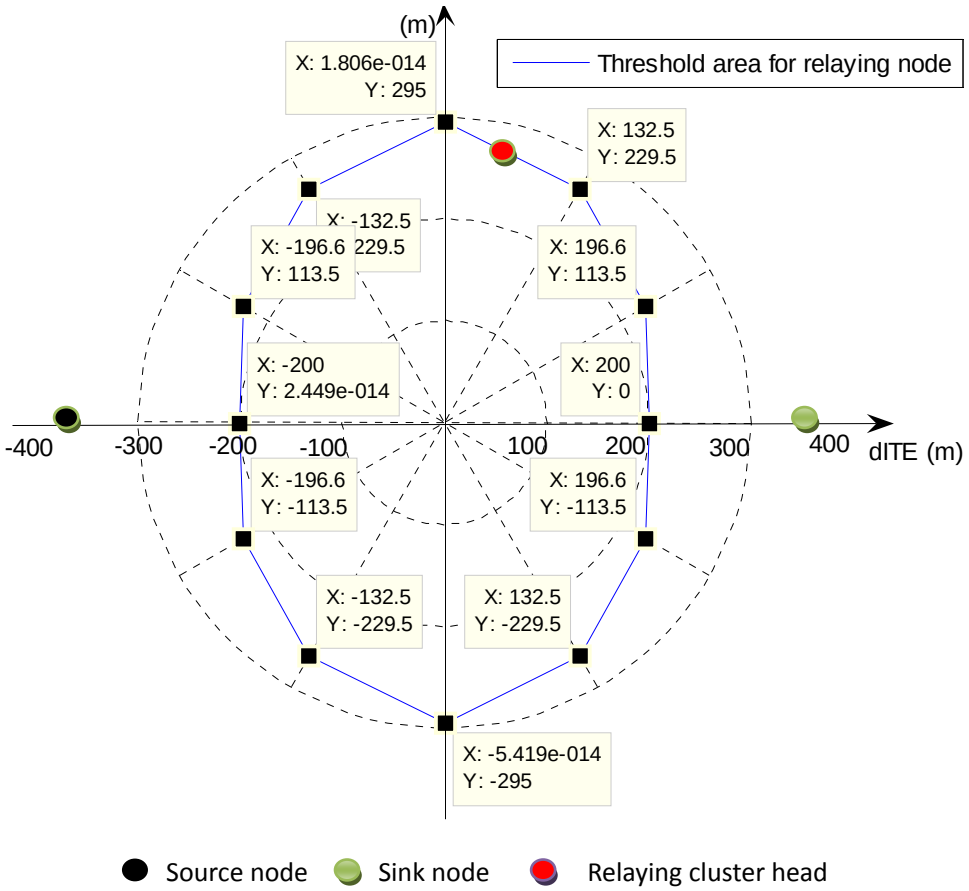

Figure 6.10 Threshold area for relaying node (cluster)

In the figure above, the threshold area for relaying node (cluster) is plotted by increasing φ with the increment of $\pi/6$ (A more smoother curve could be obtained with less φ intervals. The interval of $\pi/6$ here is set for simulation simplicity). d_{ITA} is kept as 3m and θ is kept as $\pi/6$. The nodes or cluster falls into this area can be used for data relaying. If there is no node within this area, one-hop Co-MISO (Alamouti) mode will be adopted continuously.

Based on the mode switching framework discussed in Chapter 5 and 6, the path-loss mode switching framework can be summarized in the figure below.

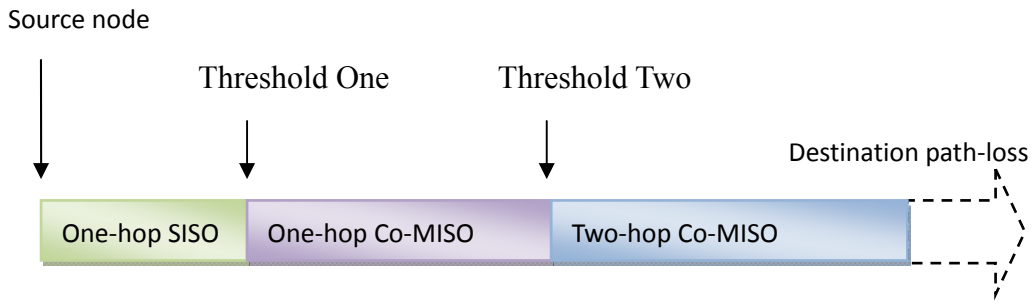

Figure 6.11 Path-loss based mode switching framework.

The thresholds in the figure above are decided by the parameters of circuit energy. Sensor nodes with more energy-efficient circuit models can reduce these thresholds. The single-hop and two-hop mode switching frameworks can be concatenated to form multi-hop transmission.

6.3 Conclusions

In this chapter, the path-loss based multi-hop mode switching framework in wireless sensor network is investigated. By simulation, it can be seen that there is no such a threshold point for mode switching from one-hop Co-MISO (Alamouti) mode to two-hop SISO mode. This is because the former one consumes less energy not only in data transmission but also in signal processing within the circuits under the cluster-based time-division framework.

When comparing the one-hop Co-MISO (Alamouti) transmission with the two-hop Co-MISO (Alamouti) mode, there does exist a threshold destination path-loss that the extra circuit energy caused by relaying cluster can be offset by the transmitting power gain from the multi-hop.

When a sensor node has data to transmit to the sink, it can first send an enquiry message to the network and gather the necessary path-loss information from the backhaul signal. Then, based on the destination path-loss, the source node will choose a mode for data transmission. If the destination path-loss is bigger than the multi-hop threshold, relaying node (cluster) is needed. The relaying node (cluster) should be within the path-loss area between the source and the destination. Combination of the

single-hop and the two-hop mode switching framework can be used for even larger distance transmission.

Chapter 7
Conclusions

Distributed MIMO in wireless sensor networks is one of the hot topics in research. This thesis investigates different transmission modes in wireless sensor networks and provides a profound understanding of cooperative MIMO technology compared with SISO in respect of energy measurement. The contributions can be used as a good starting point for follow-up research work. In this concluding chapter, all the key findings from each chapter are summarized. Several possible areas for future research are suggested as well.

7.1 Conclusions Summary

To compare the different transmission modes in wireless sensor networks, a total energy consumption model for each mode needs to be set up. The total energy consumption of a wireless communication system is revealed to be made up of two parts: the transmitting energy consumption and the circuit energy consumption. It is reasonable to omit the latter one in higher-power or large distance communication where the transmitting power is the dominant part of the total power consumption. However, when it come to wireless sensor networks, where the transmission distance is relatively short and the transmitting power for lower data streams is comparable to the power of circuit modules, the circuit energy consumption needs to be counted. In addition, due to the time division scheme adopted in the cluster-based cooperative MIMO mode, the total energy consumption model for this mode should involve two phases: intra-cluster and inter-cluster phases. The energy equations derived in Chapter 3 consider all the factors above and serve as the theoretical basis for the whole thesis.

To calculate the total energy consumption of cluster-based cooperative MIMO transmission mode, the energy used for signal transmitting and data processing within

the circuits need to be calculated respectively. Because the transmitting power levels in intra-cluster and inter-cluster phases depend on the transmission distance, communication reliability requirement, and the time slot allocated for each phase, there should be a resource allocation framework in this mode. Chapter 4 proposed such a resource allocation framework to maximize the data throughput of the whole system and simultaneously maintain within the tolerance of the outage probability requirement. The time slots allocation depends on the modulation code rate during the intra-cluster broadcasting and the STBC code rate in inter-cluster transmission. Due to the time division scheme, there is a loss of the data throughput in the cluster-based cooperative MIMO mode compared to SISO mode. Two transmitters with Alamouti scheme in ITE phase can reach the possible maximum data throughput of the cooperative MIMO mode. In transmitting power allocation, the circuit energy should be considered in this algorism, because without doing this, the results can be overly optimistic about the benefits of the cooperative MIMO over SISO mode.

Based on the total energy equations and the resource allocation framework, Chapter 5 made a comparison of different transmission modes and proposed a mode switching framework in single-hop communication. According to the path-loss from the destination and the neighboring node, the source node can choose a most energy-efficient single-hop mode for data transmission. When the destination path-loss is below a threshold, SISO mode is selected and no neighboring nodes need to be awakened for collaboration. When the destination path-loss is above this threshold, which mode should be adopted depends on the path-loss from the neighboring nodes. If there exists a neighboring node within a certain area, which can be calculated by the total energy equations, cooperative MISO mode will be chosen. If there is no such a neighboring node, SISO mode will continue to be used.

This mode switching framework for multi-hop transmission is proposed in Chapter 6. Because of the time-division method and the transmitting power gain, single-hop Co-MISO mode is more energy-efficient than two-hop SISO in both circuit energy and transmitting energy. The multi-hop mode switching framework only applies when the one-hop Co-MISO mode switches to the two-hop Co-MISO mode. Similar to the mode switching in single-hop, there is a threshold point in multi-hop mode switching. When the destination path-loss is below this threshold, single-hop Co-MISO is chosen

and no relaying node (cluster) is needed. When the destination path-loss is above this threshold, which mode should be adopted depends on the path-loss from the nodes or clusters along the signal paths. If a node (cluster) falls within a calculated area between the source node and the sink node, it can be selected as the relaying node (cluster) for two-hop cooperative MISO transmission. Otherwise, single-hop Co-MISO continues to be used.

7.2 Future Research Areas

There are several areas of this thesis that can be expanded at a future stage, which are listed below.

- The cooperative MIMO transmission mode considered in the mode switching framework is mainly 2x1 Co-MISO (Alamouti). When considering more antennas at both Tx and Rx, more problems will be brought forward, such as the selection of more corporative nodes in transmitting cluster, the information exchange phase in the relaying cluster and its cluster-head selection mechanism. In addition, the differences of energy consumption of relaying nodes working in AF and DF ways need to be investigated clearly.
- In higher layers, more energy-efficient radio resource management and routing protocols need to be discussed. The problems like routing expense, enquiry cost, as well as transmission delay are all need to be considered.

Appendix A
Original Publications

[1] Xiaojun Wen, D. I. Laurenson, “A Resource Allocation Algorithm for Cluster-based Cooperative MIMO in Wireless Sensor Networks”, Proceedings of 17 Software, Telecommunications & Computer Networks (SoftCOM 2009), 2009, pp. 211-215.

[2] Xiaojun Wen, D. I. Laurenson, “An Energy-Efficient Mode Switch Scheme for Cooperative Transmission in Wireless Sensor Networks ”, submitted to the Journal of Wireless Sensor Networks.

A Resource Allocation Algorithm for Cluster-based Cooperative MIMO In Wireless Sensor Networks

Xiaojun Wen, D.I. Laurenson
Institute for Digital Communications
Joint Research Institute for Signal and Image Processing
School of Engineering and Electronics
The University of Edinburgh
Edinburgh, EH9 3JE, UK
Email: {X.Wen, Dave.Laurenson}@ed.ac.uk

Abstract: **Energy efficiency is a considerable criterion in design of Wireless Sensor Networks. MIMO technology has the potential of supporting a higher data rate under a lower power budget and bit-error-rate, which makes cooperative MIMO in WSNs a popular research topic. This paper investigates a cluster-based time division cooperative MIMO communication system for WSNs. An optimum algorithm for the power and time allocation for an intra-cluster and inter-cluster slot has been proposed. By introducing two adjusting parameters, alpha and beta, for the energy and the time slot respectively, this algorithm is designed to achieve the maximum data throughput for one single-hop and at the same time remain within the tolerance of the outage probability requirement. Performance of different STBC schemes using such an optimum algorithm and the SISO transmission method are compared by simulation. The simulation results show that this algorithm is more energy efficient than SISO and the Alamouti scheme can best balance the trade off between the outage performance and the data rate compared with other STBCs.**

1. INTRODUCTION

Wireless Sensor Networks (WSNs) have received more and more research attention in recent years. Within a sensor network, information gathered from the collector node can be delivered node by node to the target one, or, by applying some selection strategies, these nodes can also form several clusters to do the same job, termed cluster-based communication. Like other wireless networks, the communication capacity and reliability are also required in WSNs. Besides, however, due to the battery capacity and difficulty of recharging a large number of sensors[1], a more important criterion in the design of WSN is energy efficiency.

MIMO (Multiple-Input Multiple-Output) technology is a significant breakthrough in wireless communication and intelligent antenna research. It has proved to be an effective method of dramatically increasing the channel capacity in fading channels, consequently supporting higher data rates under the same power budget and bit-error-rate requirements of a SISO system [2-3], which raises the potential applying of MIMO to WSNs. However, direct application of multiple antennas on a sensor node is impractical due to the limited physical size of a sensor node [4-6]. Consequently, a popular research topic named cooperative, or virtual, MIMO has recently been proposed [7-9], which uses cooperation between individual single-antenna nodes to form an energy-efficient distributed MIMO system.

There are two approaches to achieve cooperative diversity in WSNs. The first is based on the multi-hop structure which contains source-relay, relay-relay and relay-target communication channels [10]. The second is a cluster-based approach presented in [11-12]. The sensor nodes are grouped into so-called cooperative clusters and all clusters transmit and receive information from other cooperative clusters. This cluster-based scheme has become the focus in cooperative communication research. However, there is not an explicit energy evaluation for this scheme in wireless sensor networks and the allocation of other resources such as the time slot in a time division mode is not quite clear. Reference [13] proposes a so-called optimum resource allocation scheme to obtain the minimum outage probability but does not consider about the data through-put for the system. In this paper, a new resource allocation algorithm for cluster-based WSNs is proposed. By taking care of the energy and the time slot allocations together, the maximum data throughput for one single-hop is achieved and at the same time the outage probability remains within the tolerance of requirement.

The remainder of this paper is organized as follows. In Section 2, we describe a cluster-based cooperative MIMO system. Theoretical analysis of the system is given in Section 3. Section 4 presents the optimum scheme for the resource allocation, and simulation results are shown in Section 5. Finally, Section 6 concludes the paper.

2. CLUSTER-BASED COOPERATIVE MIMO

A multi-hop cluster-based virtual MIMO communication is shown in Fig.1.

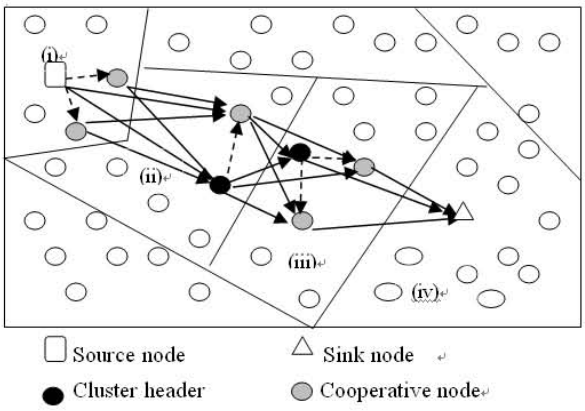

Figure 1 - Cluster-based Cooperative MIMO Multi-hop

For analysis purposes, all the sensors with the same structure are grouped by a distributed clustering algorithm [14-16], and LEACH is chosen as the routing protocol [6]. When a sensor (source node) is ready to transmit data to the sink node, it first broadcasts the information with power P_1 within cluster (i) during an Intra-cluster (ITA) time slot. A set of nodes in cluster (i) are chosen as the cooperative sensors. They decode data and jointly together with the source node communicate with cluster (ii) with power P_2 during an Inter-cluster (ITE) time slot so that a cooperative MIMO transmission scheme is established. The receiver node in cluster (ii) with the highest SNR is chosen as the cluster header and repeats this in the direction of the sink node via cluster (iii) and (iv). We assume that for the broadcast channel during an ITA slot, every node has full and updated transmit and receive channel statement information (CSI), while for the MIMO channels in an ITE slot, there is no such transmit CSI among nodes in two independent clusters [13]. As the local distance within the cluster is much shorter than the distance between two clusters, the power needed to maintain a level of communication reliability in these two cases should not be the same. In addition, the data throughput of the whole scheme has a strong relationship with the duration of ITA and ITE time slots. Allocation of P_1, P_2 and ITA/ITE slots is an interesting topic and thus becomes the aim of this paper.

3. MATHEMATICAL PREPARITION

Let a transmitter cluster (TxC) composed of N_t nodes communicate with an N_r-node-receiver cluster (RxC). n_t, and n_r are the active cooperative sensors in TxC and RxC respectively, where $n_t \le N_t$, $n_r \le N_r$.

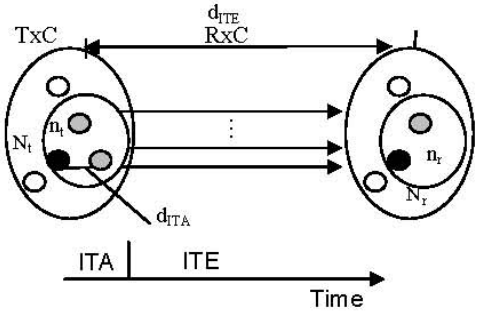

Figure 2 - Single-hop Cooperative MIMO Communication

As shown in Fig.2, d_{ITE} and d_{ITA} are the distances for the inter-cluster transmission and intra-cluster transmission. As $d_{ITE} >> d_{ITA}$ and the sensor nodes during the ITA slot know full CSI within the cluster while in an ITE slot there is no such CSI between two clusters, we can assume the intra-cluster broadcasting is a SIMO transmission over ergodic Rayleigh fading channels and the inter-cluster communication as cooperative MIMO over non-ergodic Rayleigh fading channels. All the channels are flat in frequency.

As for the SIMO situation, the capacity of ergodic Rayleigh fading channels is given in [17],

$$C_{1\times r} = \hat{C}_{r-1}\left(\frac{S}{N}\right)/\Gamma(r) \tag{1}$$

where r is the number of receivers. $\hat{C}_{r-1}$ is referred as the Capacity Integral with a closed form derived in [17]:

$$\hat{C}_{\zeta}(a) = \sum_{\mu=0}^{\zeta}\frac{\zeta!}{(\zeta-\mu)!}\left[(-1)^{\zeta-\mu-1}\left(\frac{1}{a}\right)^{\zeta-\mu}e^{1/a}Ei\left(\frac{-1}{a}\right) + \sum_{k=1}^{\zeta-\mu}(k-1)!\left(\frac{-1}{a}\right)^{\zeta-\mu-k}\right] \tag{2}$$

S/N is the signal-to-noise ratio. $\Gamma(n)$ is the Gamma Function: $\Gamma(n) = (n-1)!$.

For the cooperative MIMO situation over non-ergodic fading channels, since the channel realization $\mathbf{H}$ is chosen randomly and kept constant over the codeword transmission, there is a non-zero outage probability, that a given transmission rate Φ cannot be supported by the channel. The outage probability for one sensor node at the receiver side can be derived as follows [18].

$$P_{out}(\Phi) = \Pr\left(\log_2(1+\frac{\lambda}{n_t}\cdot\frac{S}{N}) < \Phi\right) \tag{3}$$

where λ is the eigenvalues of $\mathbf{HH}^H$. With some changes in variables, (3) can be written as

$$P_{out}(\Phi) = \int_0^{(2^{\Phi}-1)\cdot\frac{n_t}{S/N}} pdf_{\lambda}(\lambda)d\lambda \quad (4)$$

When Rayleigh fading is considered and assuming all sub-channel gains are equal, $\gamma_1 = \cdots = \gamma_{n_t}$, the $pdf_{\lambda}(\lambda)$ is derived in [19].

$$pdf_{\lambda}(\lambda) = \frac{1}{\Gamma(n_t)}\frac{\lambda^{n_t-1}}{\gamma^{n_t}}e^{-\lambda/\gamma} \quad (5)$$

Computing (4) with the pdf given by (5), one obtains

$$P_{out}(\Phi) = \int_0^{(2^{\Phi}-1)\frac{n_t/\gamma}{S/N}} \frac{1}{\Gamma(n_t)}\lambda^{n_t-1}e^{-\lambda}d\lambda$$

$$= \frac{1}{\Gamma(n_t)}\Upsilon\left(n_t, \left(2^{\Phi}-1\right)\cdot\frac{n_t/\gamma}{S/N}\right) \quad (6)$$

where $\Upsilon(\cdot)$ is the lower incomplete Gamma function.

$$\Upsilon(s,x) = \int_0^x t^{s-1}e^{-t}dt \quad (7)$$

When a Space-Time Block Code (STBC) with data rate R is applied, (6) can be rewritten as

$$P_{out}(\Phi) = \frac{1}{\Gamma(n_t)}\Upsilon\left(n_t, \left(2^{\Phi/R}-1\right)\cdot\frac{n_t/\gamma}{S/N}\cdot R\right) \quad (8)$$

Based on the mathematics above, a power and time slot allocation scheme is given in the following section.

4. RESOURCE ALLOCATION

We assume that the energy consumption in single cluster-to-cluster hop is limited to E, thus $E = E_s + E_l$, where E_s and E_l are the energy spent in the ITA slot and ITE slot respectively. E can be viewed as the energy consumption in a point-to-point transmission without such a cooperative MIMO scheme for comparison. By introducing an energy allocation parameter $\alpha(0 \le \alpha \le 1)$, and a uniform time slot allocation parameter $\beta(0 \le \beta \le 1)$, the power allocated for intra-cluster broadcasting and inter-cluster cooperative MIMO transmission is as shown in table 1.

In order to compare the performance of the proposed Algorithm with the SISO situation, the parameters in table 1 are set to satisfy that the energy spent in a point-to-point SISO transmission is equal to that in a cluster-based cooperative MIMO scheme. In table 1, δ is the path loss exponent. Let the maximum data rate of a sensor node be Φ (bit/s), the maximum data throughput of the ITA slot is $\Phi\cdot\beta$. Given the STBC with data rate R used in cooperative MIMO communication, the data throughput of the ITE slot is $R(1-\beta)\Phi$. So the overall data throughput for the single-hop can be written as

Table 1- Parameters expression with α and β

	ITA	ITE	SISO mode
Energy	$E_s = \alpha E$	$E_l = (1-\alpha)E$	E
Time slot	β	$1-\beta$	1
Power	$\frac{\alpha E}{\beta}$	$\frac{(1-\alpha)E}{1-\beta}$	$P = E/1$
S/N	$\frac{\alpha E}{\beta N}d_{ITA}^{-\delta}$	$\frac{(1-\alpha)E}{(1-\beta)N}d_{ITE}^{-\delta}$	$\frac{P}{N}d_{ITE}^{-\delta}$
Data rate	Φ	$R\Phi$	Φ
Throughput	$\Phi\cdot\beta$	$R(1-\beta)\Phi$	Φ

$$\Phi' = R\cdot\Phi\cdot(1-\beta) \le \Phi\cdot\beta \quad (9)$$

By using the parameters given in table 1, one can derive the capacity limit in an ITA slot

$$\hat{C}_{r-1}\left(\frac{\alpha E}{\beta N}d_{ITA}^{-\delta}\right)/\Gamma(r) \ge \Phi \quad (10)$$

From (8), the outage probability for ITE slot can be rewritten as

$$P_{out}(R\Phi) = \frac{1}{\Gamma(n_t)}\Upsilon\left(n_t, \left(2^{\Phi}-1\right)\cdot\frac{n_t}{\gamma}\cdot\frac{(1-\beta)N}{(1-\alpha)E}\cdot d_{ITE}^{\delta}\cdot R\right) \quad (11)$$

The aim of the resource allocation algorithm is to obtain the $\max(\Phi')$ and at the same time keep $P_{out}(R\Phi)$ as small as possible. The $\max(\Phi')$ can be obtained when (9) becomes an equality. As the Capacity Integral in (10) and the outage probability in (11) are both increasing functions with α, when the equality of (10) established, (11) will reach the minimum value. So the optimum values of α and β can be calculated by a combination of (9), (10), (11).

5. SIMULATION RESULTS

Firstly, the Alamouti scheme is investigated ($r=1, R=1$). Let $\Phi = 1(\text{bit/s})$, $\delta = 1.7$, $d_{ITA}/d_{ITE} = 0.3$, $n_t = r+1$. The sub-channel gain γ is set equal, $\gamma = 1$. β can be obtained from (9) as $\beta = 0.5$. The SISO transmission SNR is set as

$$SNR_{SISO} = 10\log\left(\frac{P}{N}d_{ITE}^{-\delta}\right) = -2(\text{dB})$$

Then the channel capacity for the ITA slot and the outage probability for the ITE slot versus the time allocation parameter α can be plotted in one figure, as in Fig.3.

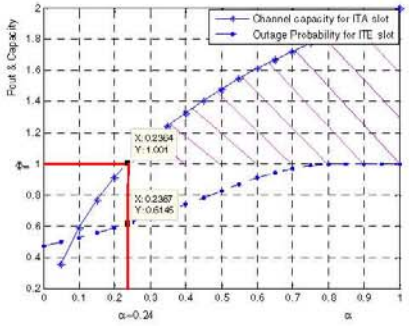

Figure 3 - Resource allocation for Alamouti scheme

Based on (10), the ever changing capacity related to α should be bigger than Φ. Due to $P_{out}(\alpha)$ being an increasing function, the optimum α is the abscissa of the intersection point of the capacity function and $C = \Phi$. So the optimum value of α is obtained as $\alpha = 0.24$, and the corresponding outage probability is 61%.

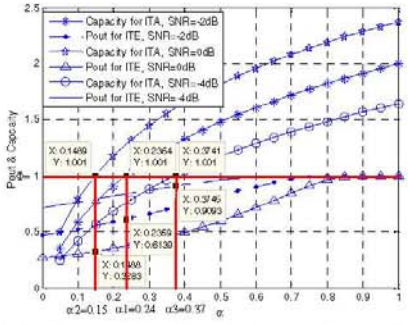

Figure 4 - Optimum algorithm for Alamouti in different SNR

The algorithm to obtain the optimum α when SNR_{SISO} is changing is shown in figure 4. The optimum α reduces as SNR_{SISO} grows, which means the capacity in the broadcasting channel is increased and less energy is need to maintain reliable communication. Clearly, the performance of outage probability in MIMO transmission will improve with increasing the energy allocation in an ITE slot.

Fig. 5 gives the trend of α versus SNR_{SISO} using different STBC schemes with R as the data rate. It can be seen that the energy spent on MIMO transmission using STBCs becomes the dominant consumption under lower noise conditions. And the Alamouti scheme is more sensitive to SNR_{SISO} on energy allocation than other STBCs.

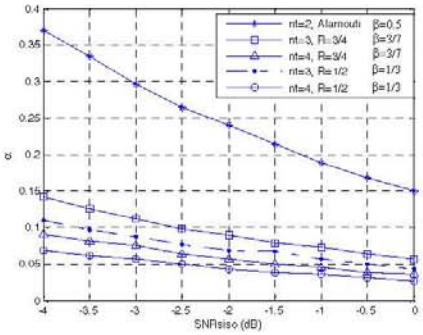

Figure 5 - α versus SNR_{SISO} in different STBCs, $d_{ITA} / d_{ITB} = 0.3$

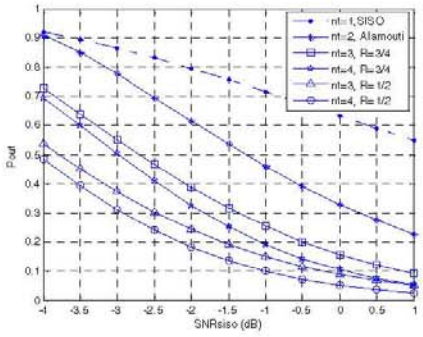

Figure 6 - Outage probability versus SNR_{SISO} for different methods of transmission $d_{ITA} / d_{ITE} = 0.3$

Fig. 6 shows the performance of outage probability in SISO transmission and in cooperative MIMO transmission after choosing the optimum α and β. Different STBCs with data rate R are compared. Note that SNR_{SISO} indicates the energy expended in SISO and the proposed algorithm. It can be seen that by energy allocation, the cluster-based scheme can get a better performance of outage probability than SISO with the same energy budget. The more transmitting nodes, the better performance is obtained. However, considering the time division system and the data rate R of STBCs used is less than 1 (except for Alamouti), the performance improvement can be seen as a sacrifice of data rate. From (9), the maximum overall data throughput for the single-hop can be reached only if $\beta = R/(1+R) \le 0.5$. The equation is satisfied when R=1, i.e. the Alamouti scheme. So the Alamouti scheme can best balance the trade off between the outage performance and the data rate.

Fig. 7 shows the outage probability performance for different d_{ITA} / d_{ITE} ratios. The results indicate that the performance improvement of the proposed scheme over SISO

transmission is obvious when d_{ITE} is much bigger than d_{ITA}. This is understandable because more energy can be allocated to ITE slot when d_{ITA} is shorter, which will benefit the outage performance for MIMO communication.

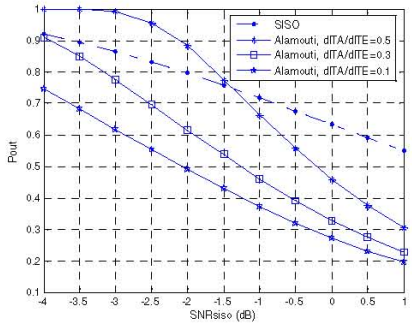

Figure 7 - Outage probability versus SNR_{SISO} for different d_{ITA} / d_{ITE} ratios

5. CONCLUSIONS

This paper investigated a cluster-based time division cooperative MIMO communication system. Compared to SISO transmission, an optimum algorithm for the power and time allocation between intra-cluster and inter-cluster communication has been proposed. By introducing two adjusting parameters for the energy and the time slot respectively, the maximum data throughput is achieved whilst maintaining an acceptable outage probability. The performance of different STBC schemes using the optimum algorithm and point-to-point SISO transmission are compared in this paper. The simulation results show that this algorithm is more energy efficient than SISO and the Alamouti scheme can best balance the trade off between the outage performance and the data rate compared with other STBCs.

REFERENCES

[1] I.F. Akyildiz, W. Su, Y. Sankarasubramaniam, E. Cayirci, "A survey on sensor networks", IEEE Communications Magazine, vol. 40, no.8, Aug. 2002. pp:102-114

[2] Gerard J. Foschini, Michael. J. Gans. "On limits of wireless communications in a fading environment when using multiple antennas". Wireless Personal Communications. vol. 6, no. 3, Jan. 1998. pp: 311–335.

[3] S. Cui, A. J. Goldsmith, A. Bahai. "Energy-efficiency of MIMO and Cooperative MIMO in Sensor Networks". IEEE J. Select. Areas of Commun. Vol. 22, no. 6, Aug. 2004. pp: 1089–1098.

[4] Jayaweera, S.K.; "Energy-efficient Virtual MIMO-based Cooperative Communications for Wireless Sensor Networks" Intelligent Sensing and Information Processing, 2005. Proceedings of 2005 International Conference, Jan. 2005. pp:1 - 6

[5] J.N. Laneman and G. Wornell, "Distributed space-time coded protocols for exploiting cooperative diversity in wireless networks," IEEE Trans. on Information Theory, vol. 49, no. 10, Oct. 2003. pp. 2415–2425

[6] Yong Yuan, Min Chen, and Taekyoung Kwon. "A Novel Cluster-Based Cooperative MIMO Scheme for Multi-Hop Wireless Sensor Networks" EURASIP Journal on Wireless Communications and Networking, 2006 , pp: 1-9

[7] E. Zimermann, P. Herhold, and G. Fettweis, "On the performance of cooperative relaying protocols in wireless networks," European Trans. on Telecommunications, vol. 16, no. 1, Jan. 2005.pp. 5–16,

[8] Baccarelli, E.; Biagi, M.; Pelizzoni, C. "On the information throughput and optimized power allocation for MIMO wireless systems with imperfect channel estimation" IEEE Trans. on Signal Processing, vol. 53, no. 7, Jul. 2005 pp:2335 – 2347

[9] Islam, M.R., Jinsang Kim. "Energy efficient cooperative MIMO in wireless sensor network". Intelligent Sensors, Sensor Networks and Information Processing, Dec. 2008. pp:505 – 510

[10] O. Simeone, U. Spagnolini, "Capacity region of wireless ad hoc networks using opportunistic collaborative communications," in Proc. International Conference on Communications (ICC), Istanbul, Turkey, May. 2006.

[11] Mischa Dohler, Yonghui Li, Branka Vucetic, A. Hamid aghvami, Marylin Arndt, Dominique Barthel. "Performance Analysis of Distributed Space-Time Block-encoded Sensor Networks". IEEE Trans. on Vechnology, vol.55, no.6, Nov. 2006, pp:1776-1789

[12] Mischa Dohler, Athanasios Gkelias, A. Hamid Aghvami. "Capacity of Distributed PHY-Layer Sensor Networks". IEEE Transactions on Vehicular Technology, vol.55, No.2, March 2006, pp:622-639

[13] Del Coso, A. Spagnolini, U. Ibars, C.; "Cooperative Distributed MIMO Channels in Wireless Sensor Networks" IEEE Jour. Selected Areas in Comms., vol 25, no. 2, Feb. 2007 pp:402 – 414

[14] S. Bandyopadhyay and E. Coyle, "An energy-efficient hierarchical clustering algorithm for wireless sensor networks," in Proc. IEEE Conference on Computer Communications (INFOCOM), San Francisco, CA, USA, Apr. 2003, pp. 1713–1723.

[15] A.D. Amis, R. Prakash, T.H.P. Voung, and D.T. Huynh, "Max-min d-cluster formation in wireless ad hoc networks," in Proc. IEEE Conference on Computer Communications (INFOCOM), Tel-Aviv, Israel, Mar. 2000, pp. 32–41.

[16] E.G. Larsson and Y. Cao, "Collaborative transmit diversity with adaptive radio resource and power allocation," IEEE Communications Letters, vol. 9, no. 6, pp. 511–513, Jun. 2005.

[17] Mischa Dohler. "Virtual Antenna Arrays", PhD dissertation, King's Colledge London, UK, Nov. 2003

[18] E. Telater, "Capacity of multi-antenna Gaussian channels", European Trans. On Telecomm., vol. 10, no. 6, Dec. 1999 pp:585-595

[19] J. Proakis, "Digital Communication", McGraw Hill, 3rd Ed, 1995

An Energy-Efficient Mode Switch Scheme for Cooperative Transmission in Wireless Sensor Networks

Xiaojun Wen, D.I. Laurenson
Institute for Digital Communications
Joint Research Institute for Signal and Image Processing
School of Engineering and Electronics
The University of Edinburgh
Edinburgh, EH9 3JE, UK
Email: {X.Wen, Dave.Laurenson}@ed.ac.uk

ABSTRACT

A new path-loss based mode switch scheme is proposed according to the total energy equation model in wireless sensor networks. Based on the geometry positions of the cooperative nodes and the relaying nodes, the transmission system can switch among SISO, cooperative MISO, single-hop, and multi-hop modes. The switching thresholds can be obtained from this scheme and in return used as the existing area to choose the proper cooperative nodes or relaying nodes.

Index Terms* — *cooperative MISO, transmission energy, circuit energy, mode decision

I. INTRODUCTION

Cooperative MIMO (Co-MIMO), involving the concepts of Co-MIMO, Co-MISO, Co-SIMO, has gained more and more research attention in recent years and becomes one of the hottest topics in wireless communication society. Different from the conventional MIMO, i.e., single-user MIMO, Co-MIMO utilizes distributed antennas which belong to different users to improve the performance of a wireless network.[1] Compared with SISO, it can also obtain the multiple-antenna advantages, such as diversity, multiplexing and beamforming, which make it properly useful for wireless Ad-hoc networks especially wireless sensor networks.[2-4]

A wireless sensor network (WSN) is composed of a large number of single-antenna sensor nodes that are densely and randomly deployed in specific terrains, like battlefields or some inaccessible environment, for monitoring.[5] Information gathered from the collector node can be delivered to the target one by a cluster-based multi-hop communication strategy. To optimize the channel capacity, Co-MIMO concepts and techniques can be applied to multiple links between the transmitting and receiving clusters.[6-9] However, due to the rigid energy restriction of sensor batteries, energy-efficiency is a key criterion in design of WSNs.

Studies of cooperative MIMO in WSNs have been done intensively by researchers. References [10] and [11] propose a cluster-based cooperative MIMO scheme in WSNs and present the derivation of the Shannon capacity for ergodic flat-fading Rayleigh channels as well as the communication-rate outage without considering the energy restriction of the sensor nodes. A resource allocation scheme is proposed in [12] to obtain the optimum power distribution and time slot allocation for a one-hop cluster-based cooperative MIMO in WSNs. But it focuses on minimizing the transmission energy only, which is reasonable in long-range applications where the transmission energy is dominant in the total energy consumption [13]. When the transmission distance is short enough, the energy consumed in circuit blocks within each sensor node is comparable to or even dominates the transmission energy and can not be omitted. By comparing the total energy consumption for each transmission mode under a fixed bit-error-rate requirement, researchers have found that there is not a single unique optimum transmission mode for all wireless sensor networks. Based on different conditions, such as the transmission distance, the optimum energy-efficient transmission mode changes from SISO to cooperative MIMO/MISO, and from single-hop to multi-hop, namely mode switch scheme. However, all the mode switching schemes proposed by other researchers perform the mode switching only based on the destination transmission distance, but do not explain how the distance information in a densely deployed wireless sensor network can be determined. A more practical parameter fit for mode switching should be path-loss, which is easy to measure in distributed nodes. No angle position relationship of the sensor nodes is taken into account on choosing of transmission mode. The affect caused by the location of the cooperative nodes within the cluster is not stated. When it comes to the multi-hop situation, all the published schemes made an assumption that the relaying nodes (clusters) are all at equally spaced points along the signal path. However, how this scheme works when the relaying nodes (clusters) are not ideally situated like this is still not clear.

So, to solve the problems above, an improved path-loss based mode switching scheme for wireless sensor networks is proposed in this paper.

The remainder of this paper is organized as follows. In Section 2, the transmission and energy consumption models are proposed. The path-loss based mode switch scheme in single-hop transmission is proposed in Section 3. This scheme in multi-hop transmission is proposed in Section 4. Finally, Section 5 concludes the paper.

II. Transmission and Energy Consumption Model

In this paper, all the sensor nodes in the network are assumed of the same physical structure. These nodes can be grouped by any cluster forming algorithms [14-16] to carry out cluster-based communication. In each cluster, the node with the most energy left is chosen as the cluster head. We assume that each cluster head has full and updated routing table for all other cluster heads in this network. The structure of this cluster-based multi-hop transmission scheme is shown in Figure 1.

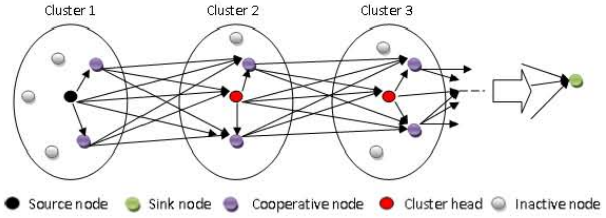

Figure 1 Cluster-based multi-hop transmission scheme

Information collected by the source node is firstly broadcasted within the cluster. Then the information is relayed cluster by cluster to the final cluster head by cooperative transmission and then to the sink node. For each cluster-to-cluster single-hop communication during the whole course, a cooperative MIMO mode of transmission is adopted, shown in Figure 2.

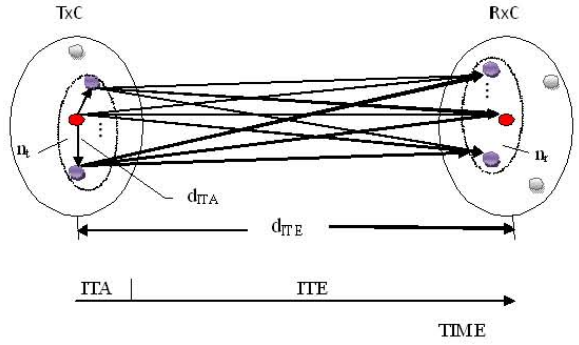

Figure 2 Cooperative MIMO transmission for single-hop

For a typical $n_t \times n_r$ MIMO link, the total energy consumed per bit can be expressed as [17-18]:

$$E_{bt} = P_{PA} + (n_t \cdot P_{ct} + n_r \cdot P_{cr}) / R_b \quad (1)$$

$$P_{PA} = (1+\varepsilon) \cdot \bar{E}_b \times \frac{(4\pi d)^2}{G_t G_R \lambda^2} M_l N_f \quad (2)$$

$$P_{ct} = P_{DAC} + P_{mix} + P_{fil} + P_{syn} \quad (3)$$

$$P_{cr} = P_{LNA} + P_{mix} + P_{IFA} + P_{fil} + P_{ADC} + P_{syn} \quad (4)$$

where $\varepsilon = \xi / \eta - 1$ with η the drain efficiency of the RF power amplifier [19] and ξ the Peak-to-Average Ratio which depends on the modulation scheme and the associated constellation size [20]. $\bar{E}_b$ is the mean required energy per bit at the receiver for a given BER requirement. R_b is the bit rate of the RF system. d is the transmitting distance. G_t and G_R are the antenna gain of the transmitter and the receiver respectively. λ is the wavelength of the signal. M_l is the link margin compensating the hardware process variations and other additive background noise or interference. N_f is the receiver noise figure defined as $N_f = (N_s / N_0)$ with N_s as the power spectral density of the total effective noise at input of the receiver and N_0 as the power spectral density of the single-sided thermal noise. P_{PA} represents the power consumed in all the amplifier. P_{ct} and P_{cr} represent all the other circuit power consumption in Tx and Rx. P_{DAC}, P_{mix}, P_{fil}, P_{syn}, P_{LNA}, P_{IFA}, P_{ADC} represent the power consumption for each functional circuit blocks respectively.

Because the circuit energy is considerable in this topic, the number of both transmitters and receivers to form cooperative transmission shouldn't be large. So instead of Co-MIMO, Co-MISO is adopted in this paper.

III. Single-hop Mode Switch Scheme

In this section, the comparison of SISO mode and Co-MISO scheme in one single-hop is concerned. We assume BPSK signal is used in this simulation and all the wireless channels obey Rayleigh fading. The system parameters are set in table 1.

Table 1 System Parameters

$P_e = 10^{-5}$	$P_{IFA} = 3$ mW
$N_0 / 2 = -174$ dBm/Hz	$P_{syn} = 50$ mW
$\xi = 1$	$P_{LNA} = 20$ mW
$\eta = 0.35$	$P_{DAC} = 15.5$ mW
$R_b = 10$ Kbit/s	$P_{ADC} = 6.7$ mW
$P_{mix} = 30$ mW	
$P_{fil} = 2.5$ mW	

The total energy equation for the SISO mode can be rewritten as follows.

$$E_{bt\_SISO} = (1+\varepsilon) \cdot \bar{E}_b \times \frac{(4\pi)^2}{G_t G_R \lambda^2 d_{ITE}^{-5}} M_l N_f + (P_{ct} + P_{cr}) / R_b \quad (5)$$

For 2x1 Co-MISO mode with Alamouti, the geometry positions of the sensor nodes involved are investigated, and shown in figure 3

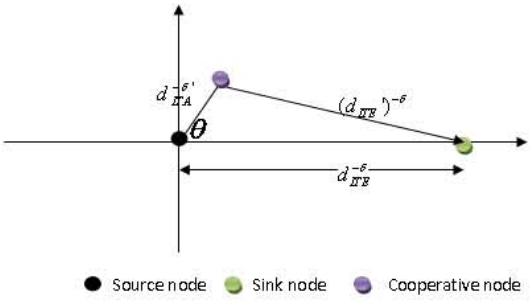

Figure 3 Geometry sketch for single-hop Co-MISO (Alamouti)

the total energy equation for 2x1 Co-MISO (Alamouti) mode can be rewritten as:

$$E_{bt\_Co\text{-}MISO} = (1+\varepsilon)\frac{\overline{E}_{b\_ITE}\cdot d_{ITE}^{-\delta}}{d_{ITE}^{-\delta}+(d_{ITE}')^{-\delta}}\times\frac{(4\pi)^2}{G_tG_R\lambda^2 d_{ITE}^{-\delta}}M_lN_f$$

$$+(1+\varepsilon)\frac{\overline{E}_{b\_ITE}\cdot(d_{ITE}')^{-\delta}}{d_{ITE}^{-\delta}+(d_{ITE}')^{-\delta}}\times\frac{(4\pi)^2}{G_tG_R\lambda^2(d_{ITE}')^{-\delta}}M_lN_f+(1+\varepsilon)\frac{\overline{E}_{b\_ITA}\cdot(4\pi)^2}{G_tG_R\lambda^2 d_{ITA}^{-\delta'}}M_lN_f$$

$$+(P_{ct}+P_{cr})\cdot\alpha/R_b+(2P_{ct}+P_{cr})\cdot(1-\alpha)/R_b$$

$$=(1+\varepsilon)\frac{2\overline{E}_{b\_ITE}}{(d_{ITE})^{-\delta}+(d_{ITE}')^{-\delta}}\times\frac{(4\pi)^2}{G_tG_R\lambda^2}M_lN_f+(1+\varepsilon)\frac{\overline{E}_{b\_ITA}\cdot(4\pi)^2}{G_tG_R\lambda^2 d_{ITA}^{-\delta'}}M_lN_f$$

$$+(P_{ct}+P_{cr})\cdot\alpha/R_b+(2P_{ct}+P_{cr})\cdot(1-\alpha)/R_b \qquad (6)$$

where α is the time slot allocation parameter.

To compare SISO and 2x1 Co-MISO (Alamouti) modes, an extreme situation is investigated first. Let d_{ITA} equal zero, i.e. the location of the source node and the cooperative node overlap. d_{ITE} equals to d_{ITE}' at this time. There would be no transmitting power consumption in the broadcasting phase. Then the energy equation (5.6) for 2x1 Co-MISO (Alamouti) mode reaches the minimum value for a fixed destination path-loss $d_{ITE}^{-\delta}$.

$$\min(E_{bt\_Co\text{-}MISO})=\lim_{d\to 0}E_{bt\_Co\text{-}MISO}$$

$$=(1+\varepsilon)\overline{E}_{b\_ITE}\times\frac{(4\pi)^2}{G_tG_R\lambda^2 d_{ITE}^{-\delta}}M_lN_f+(P_{ct}+P_{cr})\cdot\alpha/R_b+(2P_{ct}+P_{cr})\cdot(1-\alpha)/R_b \qquad (7)$$

When the destination path-loss $d_{ITE}^{-\delta}$ changes, by comparing (5) and (7), we can get a critical point of $d_{ITE}^{-\delta}$ which sets the values of these two equations equal. This critical destination path-loss is shown in figure 4.

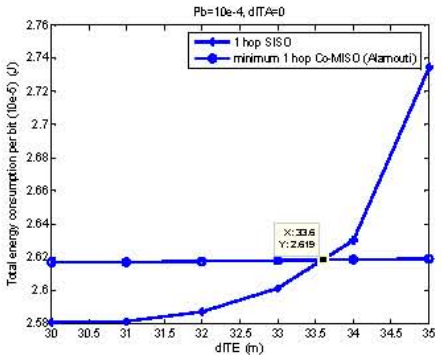

Figure 4 Energy consumption for single-hop SISO and Co-MISO with $d_{ITA}=0$

It can be seen in figure 5-7 that under the parameters of this simulation, the critical point of destination path-loss is $33.6^{-\delta}$ (δ=1.9). When the transmission distance is smaller than 33.6m, the total energy consumption per bit of single-hop SISO mode is smaller than the minimum value of Co-MISO (Alamouti) mode. If the destination path-loss falls into this range, SISO mode is more energy-efficient than Co-MISO (Alamouti) mode in single-hop transmission. The value of this critical path-loss depends on the system parameters, especially the circuit energy. When more energy-efficient circuits are adopted in sensor nodes, the advantage of Co-MISO in saving transmitting energy will be more pronounced, which makes the critical path-loss even smaller.

When the transmission distance is bigger than 33.6m, the energy curve of the single-hop SISO mode crosses over the minimum one of the Alamouti Co-MISO mode. In this situation, d_{ITA} needn't be zero to maintain the energy equation of these two modes. So, for the large destination path-loss in this situation, there exists a threshold for the cooperative node selection to make the Alamouti Co-MISO mode consume less energy than SISO. This threshold for the destination path-loss of $35^{-\delta}$ can be obtained as follows.

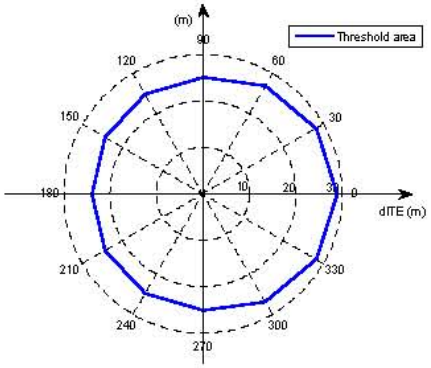

Figure 5 Simulation threshold area

In figure 5, the threshold distance area is plotted as θ increases by a increcent of $\pi/6$. This area corresponds to a path-loss area for the intra-cluster phase. With a fixed destination pass loss of $35^{-\delta}$ ($\delta=1.9$), single-hop Co-MISO (Alamouti) mode is better than single-hop SISO mode in energy saving only when the local path-loss falls within this area. In another words, if the neighbor node with the smallest path-loss falls outside this area, no cooperative node can make the Co-MISO (Alamouti) mode more energy-efficient than the one-hop SISO mode and the latter one will always be chosen in this situation. Figure 5 also provides a criterion for cooperative node selection and the local cluster size. When the cluster-based Co-MISO (Alamouti) mode is to be adopted in a wireless sensor network, sensors within the path-loss threshold area should be formed into one cluster. Each cluster should involve at least one node within the path-loss threshold area of the cluster-head. The size of this threshold area depends on both the system parameters and the destination path-loss.

When the destination path-loss continues to increase, both single-hop SISO and single-hop Co-MISO (Alamouti) mode may not be optimum for this long distance transmission. Multi-hop methods will then be adopted.

IV. Multi-hop Mode Switch Scheme

Firstly, the mode switching conditions for two-hop SISO are discussed. Before comparing one-hop Co-MISO (Alamouti) with two-hop SISO, the most energy efficient situation for the latter mode should be found first. Because the transmitting energy consumed in this two-hop system is related to the distance sum of the two hops, to save more energy, the relay node (cluster) should be on the line of the sight signal. Assuming the transmission distances for these two hops are d_{ITE1} and d_{ITE2} ($d_{ITE1}+d_{ITE2}=d_{ITE}$), figure 6 shows the transmission sketches of the single-hop Co-MISO (Alamouti) and the two-hop SISO modes.

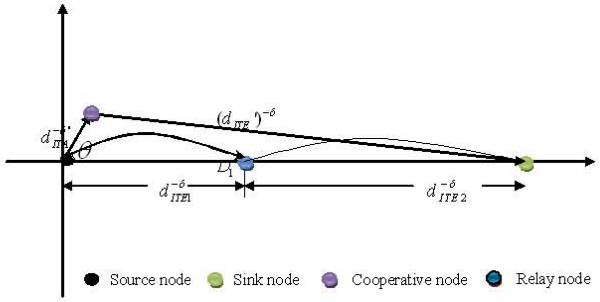

Figure 6 Sketches of one-hop Co-MISO (Alamouti) and two-hop SISO

In the figure above, the path-loss exponents for inter-cluster transmission in the two hops are set the same as δ. The total energy equation of the two-hop SISO mode can be written as:

$$E_{bt\_2hop\_SISO}=(1+\varepsilon)\cdot\bar{E}_{b\_ITE1}\times\frac{(4\pi)^2}{G_tG_R\lambda^2 d_{ITE1}^{-\delta}}M_lN_f$$
$$+(1+\varepsilon)\cdot\bar{E}_{b\_ITE2}\times\frac{(4\pi)^2}{G_tG_R\lambda^2 d_{ITE2}^{-\delta}}M_lN_f+2(P_{ct}+P_{cr})/R_b \quad (8)$$

$\bar{E}_{b-ITE1}$ and $\bar{E}_{b-ITE2}$ are the received energy per bit in these two hops respectively. the equation (8) reaches the minimum value when the relay node (cluster) is right at the center point of the signal line.

$$\min(E_{bt\_2hop\_SISO})=2\cdot(1+\varepsilon)\cdot\bar{E}_{b\_ITE1}\times\frac{(4\pi)^2}{G_tG_R\lambda^2(\frac{d_{ITE}}{2})^{-\delta}}M_lN_f+2(P_{ct}+P_{cr})/R_b \quad (9)$$

In one-hop Co-MISO (Alamouti) transmission, the intra-cluster transmission distance d_{ITA} should have a nature limitation, which is $d_{ITA}\le d_{ITE}$. The total energy consumption of this mode reaches the maximum value when we set $d_{ITA}=d_{ITE}$ and $\theta=\pi$. By comparing this maximum energy consumption of one-hop Co-MISO (Alamouti) mode with the minimum value of two-hop SISO mode in (9), we can find if there exists a threshold point for mode switching. These two curves of total energy versus destination distance are plotted in figure 7.

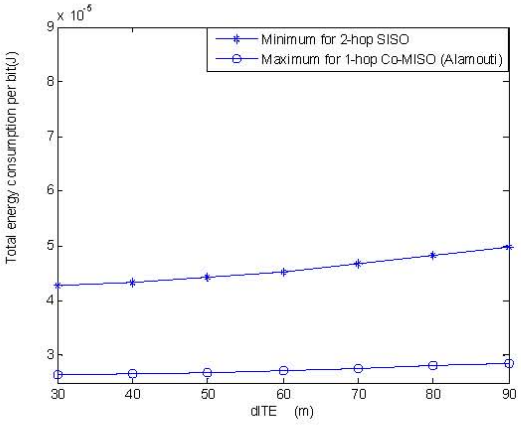

Figure 7 Energy consumption of two-hop SISO and one-hop Co-MISO modes

It can be seen that the maximum energy curve of the one-hop Co-MISO (Alamouti) mode is always below the minimum one of the two-hop SISO mode. As the transmission distance increases, these two curves diverge and there is no intersection，This is because in short distance transmission, the circuit energy consumption caused by adding a relaying node is more than that brought by a cooperative one under the time division scheme, while in long distance transmission, the transmitting energy consumption grows faster in SISO link than in MISO link, which makes the one-hop Co-MISO (Alamout) mode even better in total energy saving.

Figure 7 reveals that along the whole range of transmission distance , one-hop Co-MISO (Alamouti) is better than two-hop SISO mode under the simulation parameters of circuit energy. When the location of the relay node is not so ideal (at the middle point of the line of sight), the energy situation of the latter one will be even worse. The transmission power gain obtained by multi-hop is not obvious in this situation. So, multi-hop SISO is not fit for this mode switching scheme.

Then the mode switching conditions for two-hop Co-MISO is investigated. The situation that the relaying node (cluster) is along the line of sight signal is discussed first, shown in figure 8.

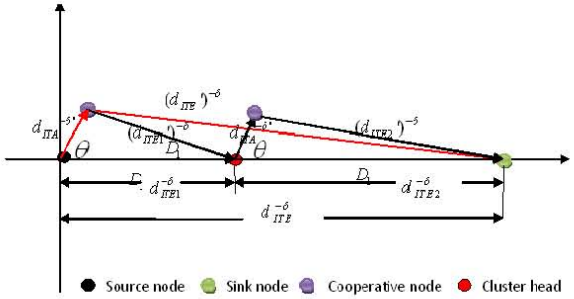

Figure 8 Sketches of one-hop and two-hop Co-MISO (Alamouti)

In figure 8, let the angle θ and d_{ITA} in each cluster are the same. $(d_{ITE1}')^{-\delta}$ and $(d_{ITE2}')^{-\delta}$ represent the inter-cluster path-loss for the cooperative node in each hop. The energy equation for two-hop Co-MISO (Alamouti) mode can be expressed as:

$$E_{bt\_2hop\_Co-MISO} = (1+\varepsilon)\frac{\overline{E}_{b\_ITE1}\cdot d_{ITE1}{}^{-\delta}}{d_{ITE1}{}^{-\delta}+(d_{ITE1}')^{-\delta}}\times\frac{(4\pi)^2}{G_tG_R\lambda^2 d_{ITE1}{}^{-\delta}}M_lN_f$$

$$+(1+\varepsilon)\frac{\overline{E}_{b\_ITE1}\cdot (d_{ITE1}')^{-\delta}}{d_{ITE1}{}^{-\delta}+(d_{ITE1}')^{-\delta}}\times\frac{(4\pi)^2}{G_tG_R\lambda^2 (d_{ITE1}')^{-\delta}}M_lN_f$$

$$+(1+\varepsilon)\frac{\overline{E}_{b\_ITE2}\cdot d_{ITE2}{}^{-\delta}}{d_{ITE2}{}^{-\delta}+(d_{ITE2}')^{-\delta}}\times\frac{(4\pi)^2}{G_tG_R\lambda^2 d_{ITE2}{}^{-\delta}}M_lN_f$$

$$+(1+\varepsilon)\frac{\overline{E}_{b\_ITE2}\cdot (d_{ITE2}')^{-\delta}}{d_{ITE2}{}^{-\delta}+(d_{ITE2}')^{-\delta}}\times\frac{(4\pi)^2}{G_tG_R\lambda^2 (d_{ITE2}')^{-\delta}}M_lN_f$$

$$+2\cdot(1+\varepsilon)\frac{\overline{E}_{d\_ITA}\cdot(4\pi)^2}{G_tG_R\lambda^2 d_{ITA}{}^{-\delta}}M_lN_f$$

$$+2\cdot(P_{ct}+P_{cr})\cdot\alpha/R_b+2\cdot(2P_{ct}+P_{cr})\cdot(1-\alpha)/R_b \quad (10)$$

Similar to the two-hop SISO mode, (10) reaches the minimum value when the relaying cluster-head is at the center point of the sight signal ($d_{ITE1}=d_{ITE2}$), which can be written as:

$$\min(E_{bt\_2hop\_Co-MISO}) = (1+\varepsilon)\frac{2\overline{E}_{b\_ITE1}+2\overline{E}_{b\_ITE2}}{(d_{ITE}/2)^{-\delta}+(d_{ITE}'/2)^{-\delta}}\times\frac{(4\pi)^2}{G_tG_R\lambda^2}M_lN_f$$

$$+2(1+\varepsilon)\frac{\overline{E}_{b\_ITA}\cdot(4\pi)^2}{G_tG_R\lambda^2 d_{ITA}{}^{-\delta}}M_lN_f+2(P_{ct}+P_{cr})\cdot\alpha/R_b$$

$$+2(2P_{ct}+P_{cr})\cdot(1-\alpha)/R_b \quad (11)$$

By comparing (6) and (11), a critical $d_{ITE}{}^{-\delta}$ is expected, which sets the energy consumption of the one-hop Co-MISO mode equals the minimum value of the two-hop Co-MISO mode. These two energy curves versus the transmission distance are shown in figure 9.

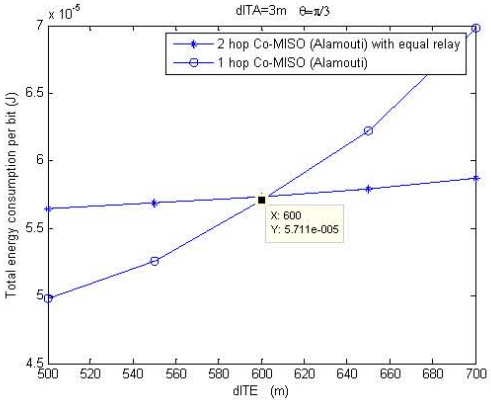

Figure 9 Energy consumption of one-hop and two-hop Co-MISO modes

The intersection in figure 9 represents the destination path-loss threshold. When the destination distance is smaller than 600m, one-hop Co-MISO mode is more energy-efficient than two-hop Co-MISO mode. When the path-loss is bigger than $600^{-\delta}$, the energy curve of the single-hop mode crosses over that of the two-hop mode with equal relay. In this situation, transmitting power gain obtained in two-hop transmission overcomes the extra circuit energy caused by relaying node (cluster). One-hop Co-MISO (Alamouti) mode should switch to the two-hop Co-MISO (Alamouti) mode for energy saving. This critical destination path-loss largely depends on the parameters of circuit energy. Diminished circuit energy makes the mode switch in smaller path-loss (shorter distance).

When the destination path-loss is bigger than this threshold, the location limitation of the relaying node (cluster) is loosened. The relaying node can move within an area (not only along the line of sight signal) and maintain the total energy consumption less than that of single-hop. A sketch of this two-hop transmission without middle point relaying node (cluster) is shown in figure 10.

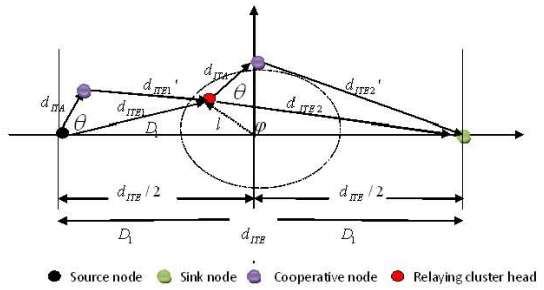

Figure 10 Sketch of the area for relaying node (cluster)

In the figure above, $d_{ITE1} + d_{ITE2} \geq d_{ITE}$. (l, φ) is the polar coordinate from the middle point of the sight signal with l as the radius and φ as the angle. In this non-ideal situation, the energy equation has the same expression of (10) but with additional limitations.

$$\begin{cases} d_{ITE1}^2 = \left(\frac{d_{ITE}}{2}\right)^2 + l^2 - 2 \cdot \frac{d_{ITE}}{2} \cdot l \cdot \cos(\pi - \varphi) \\ d_{ITE2}^2 = \left(\frac{d_{ITE}}{2}\right)^2 + l^2 - 2 \cdot \frac{d_{ITE}}{2} \cdot l \cdot \cos\varphi \\ (d_{ITE1}')^2 = d_{ITE1}^2 + d_{ITA}^2 - 2 \cdot d_{ITE1} \cdot d_{ITA} \cdot \cos\theta \\ (d_{ITE2}')^2 = d_{ITE2}^2 + d_{ITA}^2 - 2 \cdot d_{ITE2} \cdot d_{ITA} \cdot \cos\theta \\ (\varphi \in [0, 2\pi)) \end{cases} \quad (12)$$

For a fixed destination path-loss ($700^{-\delta}$), by comparing the energy consumption of single-hop Alamouti Co-MISO with that of two-hop Alamouti Co-MISO, the possible existing area for relaying node (cluster) can be obtained and shown in figure 11.

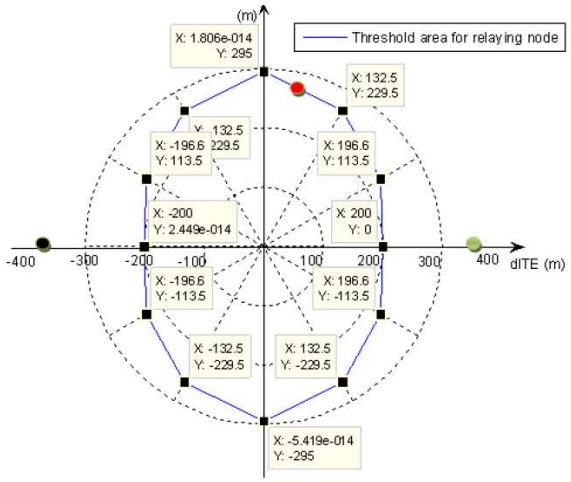

Figure 6.10 Threshold area for relaying node (cluster)

In the figure above, the threshold area for relaying node (cluster) is plotted by increasing φ with the increment of $\pi/3$. d_{ITA} is kept as 3m and θ is kept as $\pi/3$. The nodes or cluster falls into this area can be used for data relaying. If there is no node within this area, one-hop Co-MISO (Alamouti) mode will be adopted continuously.

V. CONCLUSIONS

This paper proposed an improved energy-efficient mode switch scheme for cooperative transmission in wireless sensor networks, based on the total energy equations. According to the path-loss from the destination and the neighboring node, the source node can choose a most energy-efficient single-hop mode for data transmission. In single-hop communication, when the destination path-loss is below a threshold, SISO mode is selected and no neighboring nodes need to be awaked for collaboration. When the destination path-loss is above this threshold, which mode should be adopted depends on the path-loss from the neighboring nodes. If there exists a neighboring node within a certain area, which can be calculated by the total energy equations, cooperative MISO mode will be chosen. If there is no such a neighboring node, SISO mode will continue to be used.

In multi-hop transmission, because of the time-division method and the transmitting power gain, single-hop Co-MISO mode is more energy-efficient than two-hop SISO in both circuit energy and transmitting energy, and there is no mode switching scheme between these two transmission modes. The multi-hop mode switching scheme only applies when the one-hop Co-MISO mode switches to the two-hop Co-MISO mode. Similar to the mode switching in single-hop, there is a threshold point in multi-hop mode switching. When the destination path-loss is below this threshold, single-hop Co-MISO is chosen and no relaying node (cluster) is needed. When the destination path-loss is above this threshold, which mode should be adopted depends on the path-loss from the nodes or clusters along the signal paths. If a node (cluster) falls within a calculated area between the source node and the sink node, it can be selected as the relaying node (cluster) for two-hop cooperative MISO transmission. Otherwise, single-hop Co-MISO continues to be used.

The thresholds in the scheme are decided by the parameters of circuit energy. Sensor nodes with more energy-efficient circuit models can make these thresholds move smaller. The single-hop and two-hop mode switching schemes can be concatenated to form even more hops' transmission.

ACKNOWLEDGEMENTS

The authors would like to thank the supports from the Wolfson Microelectronics Scholarship and the funding from the School of Engineering & Electronics and the Joint Research Institute of Signal and Image Processing.

REFERENCES

[1]C. B. Chae, D. Mazzarese, N. Jindal, and R. W. Heath, Jr., "Coordinated Beamforming with Limited Feedback in the MIMO Broadcast Channel", IEEE Jour. on Selected Topics in Communication, 2008.

[2]E. Zimermann, P. Herhold, and G. Fettweis, "On the performance of cooperative relaying protocols in wireless networks," European Trans. on Telecommunications, vol. 16, no. 1, Jan. 2005.pp. 5–16,

[3]Baccarelli, E.; Biagi, M.; Pelizzoni, C. "On the information throughput and optimized power allocation for MIMO wireless systems with imperfect channel estimation" IEEE Trans. on Signal Processing, vol. 53, no. 7, Jul. 2005 pp:2335 – 2347

[4]Islam, M.R., Jinsang Kim. **"**Energy efficient cooperative MIMO in wireless sensor network**"**. Intelligent Sensors, Sensor Networks and Information Processing, Dec. 2008. pp:505 – 510

[5] Akyildiz, I.F., Weilian Su, Sankarasubramaniam, Y., Cayirci, E.. "A Survey on Sensor Networks", Communications Magazine, IEEE, Vol 40, Issue 8, Aug. 2002, pp:102 – 114

[6] Yong Yuan, Min Chen, Taekyoung Kwon. "A novel Cluster-Based Cooperative MIMO Scheme for Multi-Hop Wireless Sensor Networks", EURASIP Journal on Wireless Communications and Networking. 2006, pp:1-9

[7] X. Li, "Energy efficient wireless sensor networks with transmission diversity", IEE Electronics Letters, vol. 39, no.24, pp:1753-1755, 2003

[8] X. Li, M. Chen, W. Liu, "Application of STBC-encoded cooperative transmissions in wireless sensor networks", IEEE Signal Processing Letters, vol. 12, no.2, pp:134-137, 2005.

[9]S. K. Jayaweera, "Energy analysis of MIMO techniques in wireless sensor networks", Proceedings of 38th Annual Conference on Information Sciences and Systems (CISS '04), Princeton, NJ, USA, March 2004.

[10]Mischa Dohler, Y. Li, Branka Vucetic, A. Hamid aghvami, Marylin Arndt, Dominique Barthel. "Performance Analysis of Distributed Space-Time Block-encoded Sensor Networks". IEEE Trans. on Vechnology, vol.55, no.6, Nov. 2006, pp:1776-1789

[11] Mischa Dohler, Athanasios Gkelias, A. Hamid Aghvami. "Capacity of Distributed PHY-Layer Sensor Networks". IEEE Transactions on Vehicular Technology, vol.55, No.2, March 2006, pp:622-639

[12] Del Coso, A. Spagnolini, U. Ibars, C.; "Cooperative Distributed MIMO Channels in Wireless Sensor Networks" IEEE Jour. Selected Areas in Comms., vol 25, no. 2, Feb. 2007 pp:402 – 414S.

[13]S. Cui, A. J. Goldsmith, A. Bahai, "Energy-efficiency of MIMO and cooperative MIMO techniques in sensor networks", IEEE Journal on Selected Areas in Communications, vol.22, no.6, pp:1089-1098, 2004.

[14]S. Bandyopadhyay and E. Coyle, "An energy-efficient hierarchical clustering algorithm for wireless sensor networks," in Proc. IEEE Conference on Computer Communications (INFOCOM), San Francisco, CA, USA, Apr. 2003, pp. 1713–1723.

[15]A.D. Amis, R. Prakash, T.H.P. Voung, and D.T. Huynh, "Max-min d-cluster formation in wireless ad hoc networks," in Proc. IEEE Conference on Computer Communications (INFOCOM), Tel-Aviv, Israel, Mar. 2000, pp. 32–41.

[16]M. Gustavsson, J. J.Wikner, N. N. Tan, "CMOS Data Converters for Communications", Boston, MA: Kluwer, 2000.

[17]E. Lauwers, G. Gielen, "Power Estimation Methods for Analog Circuits for Architectual Exploration of Integrated Systems", IEEE Trans. Very Large Scale Integer. (VLSI) Syst., vol. 10, no.2, pp. 155-162, Apr. 2002.

[18]M. R. Islam, Jinsang Kim, "Energy efficient cooperative MIMO in wireless sensor network," Intelligent Sensors, Sensor Networks and Information Processing, 2008. ISSNIP 2008. International Conference on , pp.505-510, 15-18 Dec. 2008

[19]S. K. Jayaweera, "Energy efficient virtual MIMO-based cooperative communications for wireless sensor networks," Intelligent Sensing and Information Processing, 2005. Proceedings of 2005 International Conference on , vol., no., pp. 1- 6, 4-7 Jan. 2005

[20]Wenqing Cheng, Kanru Xu, Wei Liu, Zongkai Yang, Zheng Feng, "An Energy-Efficient Cooperative MIMO Transmission Scheme for Wireless Sensor Networks," Wireless Communications, Networking and Mobile Computing, 2006. WiCOM 2006.International Conference on , pp.1-4, 22-24 Sept. 2006

References

[1] T. S. Rappaport, “Wireless Communications: Principles and Practice”, Second Edition, Prentice Hall, 2002, pp. 23-40.

[2] G. L. Stuber, J. R. Barry, S. W. McLaughlin, Ye Li, M. A. Ingram, T. G. Pratt, “Broadband MIMO-OFDM Wireless Communications”, Proceedings of the IEEE, 2004, vol. 92, no. 2, pp. 271-294.

[3] E. H. Gallaway, “Wireless Sensor Network: Architecture and Protocols”, CRC Press LLC, 2004, pp. 41-62.

[4] J. Burdin, J. Dunyak, “Enhancing the Performance of Wireless Sensor Networks with MIMO Communications”, IEEE Military Communications Conference, 2005, vol. 4, pp. 2321-2326.

[5] David Tse, Pramod Viswanath, “Fundamentals of Wireless Communication”, Cambridge University Press, 2005, pp. 10-25.

[6] A. J. Coulson, G. Williamson, R. G. Vaughan, “A statistical basis for lognormal shadowing effects in multipath fading channels”. IEEE Transactions on Communications, 1998, vol. 46, pp. 494-502.

[7] Guoqiang Mao, D. O. Brian, Anderson, Barış Fidan, “Path Loss Exponent Estimation for Wireless Sensor Network Localization”, Computer Networks, 2007, vol. 51, pp. 2467-2483.

[8] John G. Proakis. “Digital Communications”, 3rd edition, Singapore: McGraw-Hill Book Co., 1995, pp. 767–768.

[9] Bernard Sklar, “Rayleigh Fading Channels in Mobile Digital Communication Systems Part I: Characterization”. IEEE Communications Magazine, July 1997, vol. 35, no. 7, pp. 90–100.

[10] Yijia Fan, “MIMO Communications Over Relay Channels”. PhD thesis of the University of Edinburgh, December, 2006, pp. 10-15.

[11] Nikolay Kostov, “Mobile Radio Channels Modeling in Matlab”, Radio Engineering, December 2003, vol. 12, no. 4, pp. 38-45.

[12] A. Abdi, C. Tepedelenlioglu, M. Kaveh, G. Giannakis, “On the Estimation of the K Parameter for the Rice Fading Distribution”, IEEE Communications Letters,

March 2001, pp. 92 -94.

[13] M. A. Richards, “Rician Distribution for RCS”, Georgia Institute of Technology, September 2006, pp.130-140.

[14] D. Laurenson, “Nakagami Distribution”, Indoor Radio Channel Propagation Modelling by Ray Tracing Techniques, 2007, pp. 1-5.

[15] Michail Matthaiou, “Characterization and Modeling of Indoor and Short-Range MIMO Communications”, PhD dissertation of the university of Edinburgh, November 2008, pp. 5-20.

[16] J. Salz, “Digital Transmission Over Cross-coupled Linear Channels,” At&T Technical Journal, July-August 1985, vol. 64, no. 6, pp. 1147-1159.

[17] A. J. Paulraj, D. Gore, R. Nabar and H. Bolcskei, “An Overview of MIMO Communications – A Key to Gigabit Wireless,” Proc. IEEE, February 2004, vol. 92, no. 2, pp. 198-218.

[18] G. J. Foschini, M. J. Gans, “On Limits of Wireless Communications in a Fading Environment when Using Multiple Antennas”, Wireless Personal Communications, 1998, vol. 6, no. 3, pp. 311–335.

[19] E. Telatar, “Capacity of Multiantenna Gaussian Channels”, European Transactions on Telecommunications, 1999, vol. 10, no. 6, pp. 585-595.

[20] E. Björnson, R. Zakhour, D. Gesbert, B. Ottersten, “Cooperative Multicell Precoding: Rate Region Characterization and Distributed Strategies with Instantaneous and Statistical CSI”, IEEE Transactions on Signal Processing, 2010, vol. 58, no. 8, pp. 4298-4310.

[21] M. A. Louay Jalloul, Sam. P. Alex, “Evaluation Methodology and Performance of an IEEE 802.16e System”, Presented to the IEEE Communications and Signal Processing Society, Orange County Joint Chapter (ComSig), December 7, 2006

[22] Gerard J. Foschini. “Layered Space-time Architecture for Wireless Communications in a Fading Environment When Using Multi-element Antennas”. Bell Labs Technical Journal, Autumn 1996, pp. 41–59.

[23] L. Zheng and D. Tse . “Diversity and Multiplexing: A Fundamental Tradeoff in Multiple-Antenna Channels”. IEEE Transaction on Inf. Th. May 2003, vol. 49, no. 5, pp. 1073–1096

[24] Claude Oestges, Bruno Clerckx, “MIMO Wireless Communications : From Real-world Propagation to Space-time Code Design”, Academic, 2007, pp.

78-90.

[25] C. E. Shannon, “A mathematical Theory of Communication,” Bell Syst. Tech. J., July-Oct. 1948, vol.27, pp. 379-423, 623-656.

[26] I. E. Telatar, “Capacity of Multi-antenna Gaussian Channels”, ATT-Bell LabsInternal Technical Memorandum, June 1995, pp. 227-250.

[27] D. Love, R. Heath, V. Lau, D. Gesbert, B. Rao and M. Andrews, “An Overview of Limited Feedback in Wireless Communication Systems”, IEEE Journal on Selected Areas Communications, 2008, vol 26, pp. 1341-1365.

[28] A. Del Coso, U. Spagnolini, C. Ibars, “Cooperative Distributed MIMO Channels in Wireless Sensor Networks”, Selected Areas in Communications, IEEE Journal on, February 2007, vol. 25, no. 2, pp. 402 – 414.

[29] Vahid Tarokh, Hamid Jafarkhani, A. R. Calderbank, “Space–time Block Codes from Orthogonal Designs”, IEEE Transactions on Information Theory, July 1999, vol. 45, no. 5, pp. 744–765.

[30] Vahid Tarokh, Nambi Seshadri, A. R. Calderbank, “Space–time Codes for High Data Rate Wireless Communication: Performance Analysis and Code Construction”, IEEE Transactions on Information Theory, March 1998, vol. 44, no. 2, pp. 744–765.

[31] S. M. Alamouti. “A Simple Transmit Diversity Technique for Wireless Communications”, IEEE Journal on Selected Areas in Communications, October 1998, vol. 16, no. 8, pp. 1451–1458.

[32] Vahid Tarokh, Hamid Jafarkhani, and A. R. Calderbank, “Space–time Block Codes from Orthogonal Designs”, IEEE Transactions on Information Theory, July 1999, vol. 45, no. 5, pp. 744–765.

[33] Vahid Tarokh, Hamid Jafarkhani, and A. Robert Calderbank, “Space–time Block Coding for Wireless Communications: Performance Results”, IEEE Journal on Selected Areas in Communications, March 1999, vol. 17, no. 3, pp. 451–460.

[34] I. F. Akyildiz, Weilian Su, Y. Sankarasubramaniam, E. Cayirci, “A Survey on Sensor Networks”, Communications Magazine, IEEE, Aug. 2002, vol. 40, no. 8, pp. 102 – 114.

[35] Haibin Yu, Peng Zeng, Wei Liang. “Intelligent Wireless Sensor Networks”. Science Publication in Beijing, 2006, pp. 6-9.

[36] I. P. Kaminow, “Channel Access Technologies: State of the Art”, Conference Digest of Optical Multiple Access Networks, 1990, pp. 35-36.

[37] Zhifeng Zhao, Shaoren Zheng, “Dual Channel Based Ad hoc Network Channel Access Protocol”, Proceedings of 5th Eutopean Personal Mobile Communications Conference, 2003, pp. 32-36.

[38] Zhifeng Zhao, Shaoren Zheng, “Research about Ad hoc Network Channel Access Technology”, Journal of PLA University of Science and Technology, 2001, pp. 147-152.

[39] N. Abramson, “The ALOHA System - Another Alternative for Computer Communications”, Proceeding of Joint Computer Conference. AFIPS Press, 1970, pp. 1047-1072.

[40] Andrew S. Tanenbaum, “Computer Networks”, US patent 5761431, Prentice Hall, Upper Saddle River, NJ 2003, pp. 892.

[41] Zygmunt J. Haas, “Dual Busy Tone Multiple Access (DBTMA)-A Multiple Access Control Scheme for Ad hoc Networks”, IEEE Transactions on communications, vol. 50, no. 6, June 2002, pp. 975-985.

[42] F. Tobagi, L. Kleinrock, “Packet Switching in Radio Channels: Part III--Polling and (Dynamic) Split-Channel Reservation Multiple Access”, IEEE Transactions on Communications, Aug 1976, vol. 24, no. 8, pp. 832-845.

[43] H. Peyravi, “Medium Access Control Protocols Performance in Satellite Communications”, Communications Magazine, IEEE, Mar 1999, vol. 37, no. 3, pp. 62-71.

[44] Shiangrung Ye, Yuchee Tseng, “A Multichain Backoff Mechanism for IEEE 802.11 WLANs”, IEEE Transactions on Vehicular Technology , September 2006, vol. 55, no. 5, pp. 1613-1620.

[45] T. Sugimoto, N. Komuro, H. Sekiya, S. Sakata, K. Yagyu, “Maximum Throughput Analysis for RTS/CTS-used IEEE 802.11 DCF in Wireless Multi-hop Networks”, International Conference on Computer and Communication Engineering (ICCCE), May 2010, pp. 1-6, 11-12.

[46] Benny B. Kluwer, “Broadband Wireless Access”, International Series in Engineering and Computer Science, 2002, vol. 578, pp. 61-75.

[47] J. Olenewa, M. Ciampa, “Wireless Guide to Wireless Communications”, 2nd edition, Boston, United States, 2007, pp. 290-310.

[48] S. Gobriel, D. Mosse, R. Cleric, “TDMA-ASAP: Sensor Network TDMA Scheduling with Adaptive Slot-Stealing and Parallelism”, 29th IEEE International Conference on Distributed Computing Systems, 2009, pp.

458-465.

[49] Siyang Liu, Zhendong Luo, Yuanan Liu, Jinchun Gao, “Spreading Code Design for Downlink Space-Time-Frequency Spreading CDMA”, IEEE Transactions on Vehicular Technology, 2008, vol. 57, no. 5, pp. 2933-2946.

[50] T. F. Maciel, A. Klein, “A Convex Quadratic SDMA Grouping Algorithm Based on Spatial Correlation”, IEEE International Conference on Communications, 2007, pp. 5342-5347.

[51] Yiwen Lan, Jyhcheng Chen, “Asymptotic Weighted Fair Queuing (AWFQ) for IEEE 802.11 Point Coordination Function (PCF)”, 3rd IEEE Consumer Communications and Networking Conference, 2006, vol. 2, pp. 823-827.

[52] M. Ergen, Duke Lee, Raja Sengupta, P. Varaiya, “WTRP - Wireless Token Ring Protocol”, IEEE Transactions on Vehicular Technology, 2004, vol. 53, no. 6, pp. 1863-1881.

[53] Quan Zhou, Yongjun Xu, Xiaowei Li, “HTSMAC: High Throughput Sensor MAC for Wireless Video Networks”, International Conference on Wireless Communications, Networking and Mobile Computing, 2007, pp. 2428-2431.

[54] P. C. Nar, E. Cayirci, “PCSMAC: A Power Controlled Sensor-MAC Protocol for Wireless Sensor Networks”, Proceedings of the Second European Workshop on Wireless Sensor Networks, 2005, pp. 81-92.

[55] Afshin Fallahi, Ekram Hossain, “Distributed and Energy-Aware MAC for Differentiated Services Wireless Packet Networks: A General Queuing Analytical Framework”, IEEE Transactions on Mobile Computing, vol. 6, no. 4, pp. 381-394.

[56] V. Shahmansouri, M. G. Rezaie, H. R. Pakravan, “Modified Distributed Mediation Device for Low Power Consumption in Large Scale Sensor Networks”, Proceedings of 2005 International Conference on intelligent Sensing and Information Processing, 2005, pp. 7-12.

[57] Joanna Kulik, Wendi Heinzelman Hari ,Balakrishnan, “Negotiation-based Protocols for Disseminating Information in Wireless Sensor Networks”, Journal of Wireless Networks - Selected Papers from Mobicom'99 archive, March-May 2002, vol. 8, no.2, pp.169-185.

[58] Chalermek Intanagonwiwat, Ramesh Govindan and Deborah Estrin, “Directed Diffusion: A Scalable and Robust Communication Paradigm for Sensor Networks”, Proceedings of the Sixth Annual International Conference on

Mobile Computing and Networking (MobiCOM '00), August 2000, Boston, Massachussetts. pp.80-93.

[59] Deepak Ganesan, Ramesh Govindan, Scott Shenker, Deborah Estrin, "Highly-Resilient, Energy-Ef_cient Multipath Routing in Wireless Sensor Networks", Mobile Computing and Communications Review, vol. 1, no.2, pp.1-13.

[60] Yanjun Li, Jiming Chen, Ruizhong Lin, Zhi Wang, "A Reliable Routing Protocol Design for Wireless Sensor Networks", Mobile Adhoc and Sensor Systems Conference, 2005. IEEE International Conference on, Nov. 2005, pp.61- 77.

[61] M. J. Handy, M. Haase, D. Timmermann, "Low Energy Adaptive Clustering Hierarchy with Deterministic Cluster-head Selection", 4th International Workshop on Mobile and Wireless Communications Network, 2002, pp. 368-372.

[62] S. Lindsey, C. S. Raghavendra, "PEGASIS: Power-efficient Gathering in Sensor Information Systems", Aerospace Conference Proceedings, IEEE, 2002, vol.3, pp. 1125- 11350.

[63] Qiangfeng Jiang; D. Manivannan, "Routing Protocols for Sensor Networks," IEEE Consumer Communications and Networking Conference, Jan. 2004, pp. 93- 98, 5-8.

[64] F. Ian, Akyildiz, S. Weilian, S. Yogesh, C. Erdal, "A Survey on Routing Protocols for Wireless Sensor Networks", IEEE Communication Magzine, 2002, vol. 40, no. 8, pp. 102-114.

[65] J. N. Al-Karaki, A. E. Kamal. "Routing Techniques in Wireless Sensor Networks: A Survey", IEEE Personal Communication, 2004, vol. 11, no. 6, pp. 6-28.

[66] W. Heizelman, A. Chandrakasan, H. Balakrishnan, "Energy-efficient Communication Protocols for Wireless Sensor Networks", IEEE Proceedings of the Hawaii International Conference System Sciences, 2000, pp. 3005-3014.

[67] Y. Yu, D. Estrin, R. Govindan, "Geographical and Energy-aware Routing: A Recursive Data Dissemination Protocol for Wireless Sensor Networks", UCLA Computer Science Department Technical Report, 2001, pp. 130-150.

[68] T. Pering, T. Burd, R. Brodersen, "Dynamic Voltage Scaling and the Design of a Low-power Microprocessor System", Power Driven Microarchitecture Workshop, June 1998, pp. 1080-1100.

[69] A. Sinha, A. Chandrakasan, "Dynamic Power Management in Wireless Sensor

Networks", IEEE Desigh & Test of Computers, 2001, pp. 331-349.

[70] Yong Yuan, Min Chen, Taekyoung Kwon. "A Novel Cluster-Based Cooperative MIMO Scheme for Multi-Hop Wireless Sensor Networks", EURASIP Journal on Wireless Communications and Networking , 2006 , pp. 1-9.

[71] Shuguang Cui, Andrea J. Goldsmith, Ahmad Bahai, "Energy-efficiency of MIMO and Cooperative MIMO Techniques in Sensor Networks", IEEE Journal on Selected Areas in Communication, August 2004, Vol. 22, No. 6, pp. 1089-1098.

[72] J. N. Laneman and G. Wornell, "Distributed Space-time Coded Protocols for Exploiting Cooperative Diversity in Wireless Networks," IEEE Trans. on Information Theory, October 2003, vol. 49, no. 10, pp. 2415–2425.

[73] A. Sendonaris, E. Erkip, and B. Aazhang, "User Cooperation Diversity– part I: System Description," IEEE Trans. on Communications, November 2003, vol. 51, no. 11, pp. 1927–1938.

[74] E. Zimermann, P. Herhold, G. Fettweis, "On the Performance of Cooperative Relaying Protocols in Wireless Networks," European Trans. on Telecommunications, January 2005, vol. 16, no. 1, pp. 5–16.

[75] T. M. Cover, A. A. El Gamal, "Capacity Theorems for the Relay Channel," IEEE Trans. on Information Theory, September 1979, vol. 525, no. 5, pp. 572–584.

[76] E. Baccarelli, M. Biagi, C. Pelizzoni, "On the Information Throughput and Optimized Power Allocation for MIMO Wireless Systems With Imperfect Channel Estimation", IEEE Transactions on Signal Processing, July 2005, vol. 53, no. 7, pp. 2335 – 2347.

[77] G. Kramer, M. Gastpar, P. Gupta, "Cooperative Strategies and Capacity Theorems for Relay Networks," IEEE Transactions on Information Theory, September 2005, vol. 51, no. 9, pp. 3037–3063.

[78] P. Mitran, H. Ochiai, and V. Tarokh, "Space-time Diversity Enhancements Using Collaborative Communications," IEEE Transactions on Information Theory, June 2005, vol. 51, no. 6, pp. 2041–2057.

[79] O. Simeone and U. Spagnolini, "Capacity Region of Wireless Ad Hoc Networks Using Opportunistic Collaborative Communications," Proceeding of International Conference on Communications (ICC), Istanbul, Turkey, May 2006, pp. 526-544.

[80] P. Gupta, P. R. Kumar, “The Capacity of Wireless Networks,” IEEE Transactions on Information Theory, March 2000, vol. 46, no. 2, pp. 388–404.

[81] L. Pillutla, V. Krishnamurthy, “Joint Rate and Cluster Optimization in Cooperative MIMO Sensor Networks,” Proceeding of IEEE 6th Workshop on Signal Processing Advances in Wireless Communications, Philadelphia, USA, March 2005, pp. 265–269.

[82] L. Pillutla and V. Krishnamurthy, “Energy Efficiency of Cluster Based Cooperative MIMO Techniques in Sensor Networks,” IEEE Transactions on Signal Processing, 2005, pp. 34-40.

[83] M. Gastpar and M. Vetterli, “On the Capacity of Large Gaussian Relay Networks,” IEEE Transactions on Information Theory, March 2005, vol. 51, no. 3, pp. 765–779.

[84] J. Boyer, D. Falconer, and H. Yanikomeroglu, “Multihop Diversity in Wireless Relaying Channels,” IEEE Transactions on Communications, October 2004, vol. 52, no. 10, pp. 1820–1830.

[85] A. del Coso and C. Ibars, “Bounds on Ergodic Capacity of Multirelay Cooperative Links with Channel State Information,” Proceeding of IEEE Wireless Communications and Networking Conference, Las Vegas, NV, USA, April 2006, pp. 337-350.

[86] Zheng Huang, Takaya Yamazato, “Energy Efficiency of Cooperative MISO Technique in Multi-hop Wireless Sensor Networks”, IEEE 2008, pp. 511-515

[87] S. Cui, A. J. Goldsmith, A. Bahai, “Energy-Constrained Modulation Optimization”, IEEE Transactions on Wireless Communications, September 2005, vol 4, no. 5, pp. 2349 – 2360.

[88] Tuan-Duc Nguyen, Olovier Berder and Olivier Sentieys, “Cooperative MIMO Schemes Optimal Selection for Wireless Sensor Networks”, IEEE 2007, pp. 85-89.

[89] N. Eshghi, A. T. Haghighat, “Energy Conservation Strategy in Cluster-Based Wireless Sensor Networks”, International Conference on Advanced Computer Theory and Engineering, 2008, pp. 1015-1019.

[90] Li Fei, Qiang Gao, Xu Zhang, “Energy Efficient Cooperative MIMO with Idle Nodes in Cluster Based Wireless Sensor Networks”, 6th International Symposium on Wireless Communication Systems, 2009, pp. 448-452.

[91] H. Gharavi, K. Ban, “Master-slave Cluster-based Multihop Ad-hoc Networking”,

Electronics Letters, 2002, vol. 38, no. 25, pp. 1756-1757.

[92] C. Cano, B. Bellalta, P. Villalonga, J. Perello, “Multi-hop Cluster-based Architecture for Sparse Wireless Sensor Networks”, 14th European Wireless Conference, 2008, pp. 1-5.

[93] Nguyen, Tuanduc, Berder, Olivier, Sentieys, “Cooperative MISO and Relay Comparison in Energy Constrained WSNs”, IEEE 71st Vehicular Technology Conference, 2010, pp. 1-5.

[94] S. Cui; A. J. Goldsmith, A. Bahai, “Modulation Optimization Under Energy Constraints”, Proceeding of ICC’03, AK, May 2003, pp.2805-2811.

[95] T. H. Lee, “The Design of CMOS Radio-Frequency Integrated Circuits”, Cambridge, U.K., Cambridge Univ. Press, 1998, pp. 523-551.

[96] M. Gustavsson, J. J.Wikner, N. N. Tan, “CMOS Data Converters for Communications”, Boston, MA: Kluwer, 2000, pp. 582-601.

[97] E. Lauwers, G. Gielen, “Power Estimation Methods for Analog Circuits for Architectual Exploration of Integrated Systems”, IEEE Transactions on Very Large Scale Integer. (VLSI) System, April 2002, vol. 10, no.2, pp. 155-162.

[98] M. R. Islam, Jinsang Kim, "Energy Efficient Cooperative MIMO in Wireless Sensor Network," International Conference on Intelligent Sensors, Sensor Networks and Information Processing, December 2008, pp.505-510, 15-18.

[99] S. K. Jayaweera, "Energy Efficient Virtual MIMO-based Cooperative Communications for Wireless Sensor Networks," Proceedings of 2005 International Conference on Intelligent Sensing and Information Processing, January 2005, pp. 1- 6, 4-7.

[100] Wenqing Cheng, Kanru Xu, Wei Liu, Zongkai Yang, Zheng Feng, "An Energy-Efficient Cooperative MIMO Transmission Scheme for Wireless Sensor Networks," International Conference on Wireless Communications, Networking and Mobile Computing, September 2006, pp.1-4, 22-24.

[101] Islam, Mohammad Rakibul, Kim, Jinsang, “Energy Efficient Cooperative MIMO Communication for Uncorrelated Data Transmission at Wireless Sensor Network,” 2nd International Conference on Computer Science and its Applications, December 2009, pp.1-6, 10-12.

[102] Liang, Ying, Feng, Yongxin, “An Energy-Efficient Routing Protocol Based Dynamic Cooperative MIMO for Wireless Sensor Network,” 3rd International Conference on Intelligent Networks and Intelligent Systems (ICINIS),

November 2010 , pp. 610-613, 1-3.

[103] Tiankui Zhang, Song Zhao, L. Cuthbert, Yue Chen, "Energy-efficient Cooperative Relay Selection Scheme in MIMO Relay Cellular Networks", 2010 IEEE International Conference on Communication Systems (ICCS), 2010, pp. 269-273.

[104] Kanru Xu, Wei Yuan, Wenqing Cheng, Yi Ding, Zongkai Yang, "An Energy-Efficient V-BLAST Based Cooperative MIMO Transmission Scheme for Wireless Sensor Networks," Wireless Communications and Networking Conference, IEEE, 2008, pp.688-693.

[105] I. Ahmed, Mugen Peng, Wenbo Wang, "Uniform Energy Consumption through Adaptive Optimal Selection of Cooperative MIMO Schemes in Wireless Sensor Networks", IEEE Vehicular Technology Conference, 2008, pp.198-202.

[106] N. Jindal, A. J. Goldsmith, "Capacity and Optimal Power Allocation for Fading Broadcast Channels with Minimum Rates", IEEE Transactions on Information Theory, September 2001, pp. 253-261.

[107] L. Li, A. J. Goldsmith, "Capacity and Optimal Resource Allocation for Fading Broadcast Channels- Part I: Ergodic Capacity", IEEE Transactions on Information Theory, March 2001, vol. 47, no. 3, pp. 1083-1102.

[108] L. Li, A.J. Goldsmith, "Capacity and Optimal Resource Allocation for Fading Broadcast Channels- Part II: Outage Capacity", IEEE Transactions on Information Theory, March 2001, vol. 47, no. 3, pp. 1083-1102.

[109] Mischa Dohler, "Virtual Antenna Arrays", PhD thesis, November 2003, pp. 60-130.

[110] A. Edelman, "Eigenvalues and Condition Numbers of Random Matrices", PhD thesis, Department of Mathematics, MIT, Cambridge, MA, 1989, pp. 70-90.

[111] J. Proakis, "Digital Communication", McGraw Hill, 3rd Ed, 1995, pp. 310-330.

[112] E. G. Larsson, P. Stoica, "Space-Time Block Coding for Wireless Communications", Cambridge University Press, 2003, pp. 231-244.

[113] A. Paulraj, R. Nabar, D. Gore, "Introduction to Space-Time Wireless Communications", Cambridge, UK, Cambridgr Univ. Press, 2003, pp. 250-269.